ZmMADS1 is a positive flowering time regulator in *Zea mays* L.

DISSERTATION ZUR ERLANGUNG DES
DOKTORGRADES DER NATURWISSENSCHAFTEN (DR. RER. NAT.)
DER FAKULTÄT FÜR BIOLOGIE UND VORKLINISCHE MEDIZIN
DER UNIVERSITÄT REGENSBURG

vorgelegt von
Philipp Alter

aus
Brilon

im Jahr
2014

Das Promotionsgesuch wurde eingereicht am: 18.02.2014

Die Arbeit wurde angeleitet von: Dr. Manfred Gahrtz, Prof. Dr. Thomas Dresselhaus

Unterschrift:

(Philipp Alter)

TABLE OF CONTENT

1. SUMMARY

Flowering time is an important agronomical trait of relevance for harvest date, crop rotation schemes, biomass yield, and terminal drought avoidance. The regulation of flowering time and associated transition from vegetative to inflorescence meristems in the most important crop maize seems to be dominated by small additive QTLs with few genetic and/or environmental interactions. Mutants do not promise as much insight into the pathways regulating flowering time compared with *Arabidopsis thaliana* and rice, since only three late flowering mutants are known to date: *indeterminate1* (*id1*), *delayed flowering1* (*dlf1*) and *leafy*. *ID1* encodes a zinc-finger transcription factor absent in Arabidopsis and *DLF1* a bZIP transcription factor homologous to the Arabidopsis floral integrator *FLOWERING LOCUS D* (*FD*). *LEAFY* has not yet been cloned to date.

In order to gain new insights into the processes regulating flowering time in day-neutral maize the transcriptome of leaves was analyzed before, during and after the switch from vegetative to reproductive development of the shoot apical meristem (SAM). In the beginning of this work, two pairs of genetically related maize inbred lines were identified differing significantly in flowering time. By obtaining and analyzing transcriptome data from these four lines two genes were identified as putative components of the flowering time regulating machinery in maize, *ZmMADS1* and *ZmM26*. Both candidate genes encode MADS-box transcription factors. Homology analyses revealed that *ZmMADS1* is one of at least three *SOC1*-like genes in maize and *ZmM26* was identified as one of four maize *SVP*-like genes.

ZmMADS1 was expressed in a diurnal pattern over the day. This effect was stronger during short days compared with long days. A day time or day length specific expression of *ZmM26* could not be detected. The findings suggest that *ZmMADS1* might be involved in the photoperiodic flowering time regulation of maize. A complementation assay in Arabidopsis *soc1* mutants showed that *ZmMADS1* is able to rescue the late flowering phenotype. Functional characterization of *ZmMADS1* and *ZmM26* in transgenic maize plants indicated that *ZmM26* does not have an effect on flowering time under long day conditions, while *ZmMADS1* seems to be involved in the positive regulation of flowering time in a dosage dependent manner.

2. ZUSAMMENFASSUNG

Der Blühzeitpunkt ist ein wichtiges agronomisches Merkmal und von großer Relevanz für Erntezeit, Fruchtfolge, Biomasseproduktion und die Vermeidung von terminalem Trockenstress. In Mais scheint die Regulation des Blühzeitpunktes und der damit verknüpfte Übergang vom vegetativen Meristem zum Infloreszenzmeristem von kleinen, additiven QTL dominiert zu sein, die nur wenige genetische und/oder umweltbedingte Interaktionen aufweisen. Mutantenstudien versprechen bei Mais keine großen Erkenntnisse über blühzeitregulatorische Signalwege wie in *Arabidopsis thaliana* oder Reis, da bisher nur drei spät blühende Maismutanten bekannt sind: *indeterminate1* (*id1*), *delayed flowering1* (*dlf1*) und *leafy*. *ID1* kodiert einen in Arabidopsis nicht vorkommenden Zinkfingertranskriptionsfaktor und *DLF1* einen bZIP Transkriptionsfaktor der homolog zu *FLOWERING LOCUS D* (*FD*) ist, einem Blühsignalintegrator aus Arabidopsis. *LEAFY* wurde bis jetzt noch nicht kloniert.

Um neue Einblicke in den Prozess der Blühzeitregulation von tag-neutralem Mais zu erhalten, wurden Blatttranskriptomanalysen vor, während und nach dem Übergang vom vegetativen zum reproduktiven Entwicklungsstadium des Sprossapikalmeristems (SAM) durchgeführt. Zu Beginn der Arbeit wurden zwei Paare genetisch nah verwandter Mais-Inzuchtlinen identifiziert, die sich signifikant im Blühzeitpunkt unterschieden. Durch die Analyse der Transkriptomdaten dieser vier Linien wurden mit *ZmMADS1* und *ZmM26* zwei Gene identifiziert, die möglicherweise Bestandteile des blühzeitregulatorischen Mechanismus in Mais sind. Beide Gene kodieren MADS-Box Transkriptionsfaktoren. Homologieanalysen ergaben, dass *ZmMADS1* eines von mindestens drei *SOC1*-ähnlichen Genen ist, während *ZmM26* als eines von möglicherweise vier *SVP*-ähnlichen Genen identifiziert wurde.

Die Expression von *ZmMADS1* folgte einer Tagesrhythmik, die unter Kurztagbedingungen stärker ausgeprägt war als unter Langtagbedingungen. Ein ähnliches Ergebnis war für *ZmM26* nicht zu beobachten. Dies deutet darauf hin, dass *ZmMADS1* im Gegensatz **zu** *ZmM26* in der fotoperiodischen Blühzeitregulation beteiligt ist. Komplementationsstudien in Arabidopsis *soc1* Mutanten zeigten, dass *ZmMADS1* den spät blühenden Phänotyp komplementieren konnte. Die funktionelle Charakterisierung von *ZmMADS1* und *ZmM26* in transgenen Maispflanzen ergaben, dass *ZmM26* anscheinend

keine Rolle in der Regulation des Blühzeitpunktes unter Langtagbedingungen spielt, während *ZmMADS1* dosisabhängig eine Rolle in der positiven Blühzeitregulation bei Mais spielt.

3. INTRODUCTION

3.1. FLOWERING INDUCTION IN MAIZE

Zea mays also known as maize or corn is an annual monoecious plant with unisexual flowers. A solely male inflorescence, the tassel, is formed terminally at the apex of the shoot. The female inflorescence, the ear, is formed as a lateral branch in the axil of a leaf. The number of ears differs among maize lines. The ancestor of modern maize is teosinte, a sweet grass originally found in Mexico, Guatemala and Nicaragua. Teosinte is a short day plant, *i. e*. short days are required for flower initiation (Emerson, 1924). Maize is considered as a day-neutral plant due to the history in maize breeding, in which lines were selected with the ability to grow in much broader latitudes. Some tropical maize lines exist as well that still perceive short photoperiods (Colasanti & Coneva, 2009).

Flowering time is an important agronomical trait that is of relevance for harvest date, biomass yield, crop rotation schemes and terminal drought avoidance (Jung & Müller, 2009). The regulation of flowering time and the associated transition of the meristems from vegetative to reproductive or flower meristems, which is called floral transition, is a critical event in the life history of a plant. This event has to guarantee the maximal reproductive success under given environmental conditions.

While all root structures are formed by the root apical meristem (RAM), all shoot structures are formed by the shoot apical meristem (SAM). During the vegetative growth phase, the SAM produces phytomers, consisting of a leaf, an axillary meristem and an internode. At the beginning of the floral transition in maize, the SAM starts to elongate, which comes along with a repression of leaf initiation. Axillary meristems, so called branch meristems, are formed in files on the flanks of the elongated SAM. This marks the beginning of the development of the male inflorescence (*Figure 1*). The floral transition of maize may take place already when the SAM is just a few centimeters above the ground, however the mature maize plant can reach a height of several meters. Since a maize plant has only one SAM, it has to be ensured that all vegetative above ground parts of the plant body are installed at that time point of floral transition, because it is an irreversible process.

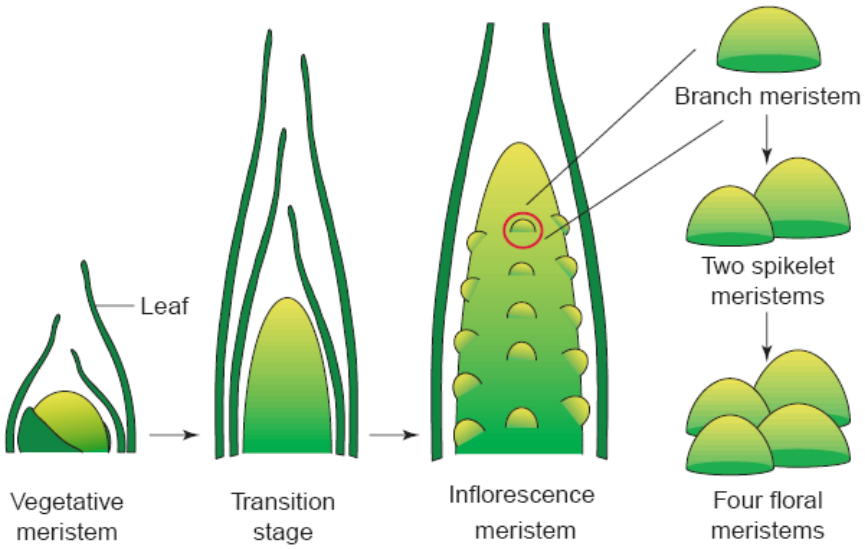

Figure 1. **Development of the shoot apical meristem (SAM) during floral transition.** The elongation of the vegetative SAM marks the beginning of the floral transition (transition stage). Branch meristems are produced at the flank of the inflorescence meristem in files, which give rise to two spikelet meristems each. Each spikelet meristem again gives rise to two floral meristems, which will form the floral organs (Image from McSteen *et al*., 2000).

Plants depend on internal and external signals to regulate the right time for flowering. The internal or endogenous signals are processed independently of the external or environmental signals.

The endogenous signals, which are related to the developmental state of the plant, are divided in three different flowering time inductive pathways: (i) the autonomous, (ii) the aging and (iii) the gibberellic acid pathway. The floral initiation of *Nicotiana tabacum* can be mentioned as an example for the result of the autonomous pathway. Floral transition occurs after the SAM has formed a fixed number of nodes, independent of environmental conditions (McDaniel & Hsu, 1976). The aging pathway is related to the age of the plant and depends on different phase transitions during the plant life cycle, like the transition from the juvenile to the adult phase. Such transitions can be necessary for the plant to become competent for flowering and reproduction (Strable *et al.,* 2008). The gibberellin pathway uses the information of growth and development, which are mediated by the endogenous plant growth regulator gibberellin.

Additionally, two major environmental signals have to be mentioned here: (iv) photoperiod or day length and (v) temperature. Some species like rye, wheat and barley need a period of cold temperatures for their winter genotypes to get primed for early flowering, which is called vernalization. However, vernalization does not play a role in flowering time regulation in maize.

These five floral inductive pathways do not regulate flowering time separately but there exists also crosstalk between the signaling pathways, for example, between the vernalization and the photoperiodic pathway (Searle *et al*., 2006) as well as the autonomous pathway and the photoperiodic pathway (Lazakis *et al*., 2011). An overall scheme of floral induction is depicted in *Figure 2*.

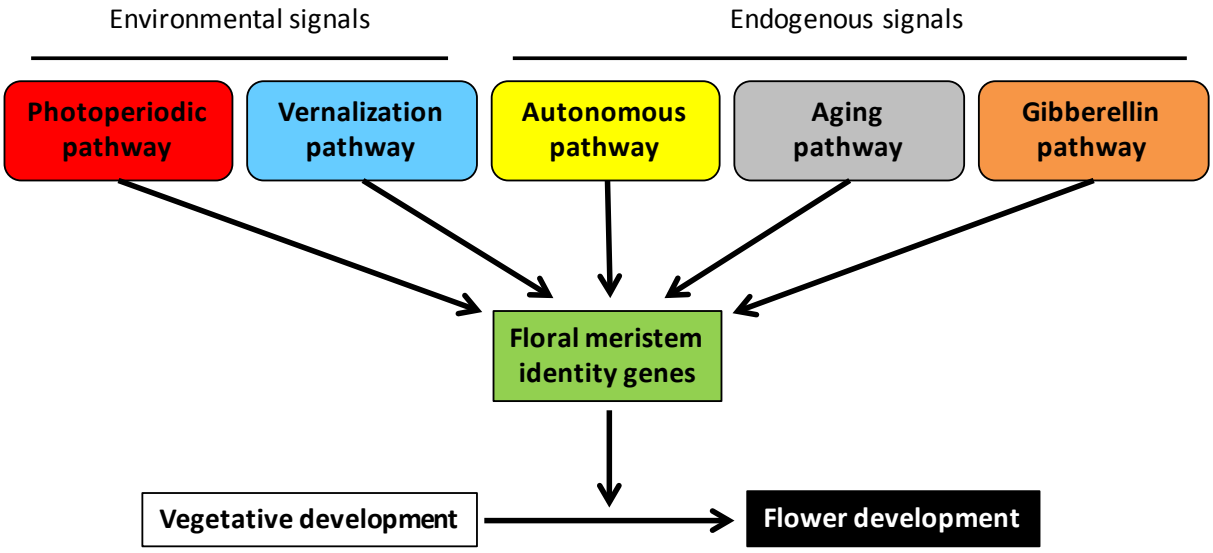

Figure 2. **Overview of the five different pathways that influence the transition to flowering.** The photoperiodic, the vernalization, the autonomous, the aging and the gibberellin pathway induce the expression of floral meristem identity genes. These genes promote transition from vegetative to flower development. Additionally there exist interactions between the different pathways (not depicted in the scheme).

The molecular mechanisms underlying these pathways are investigated in many plant species, but are largely unknown in maize. This is due to the fact that not many flowering time mutants are available to identify the affected genes. In general it has been shown that flowering time regulation in maize is dominated by small additive QTLs with few genetically or environmental interactions (Buckler *et al*., 2009). More is known about the molecular mechanism underlying the floral transition in the photoperiod-sensitive, facultative short day plant rice (*Oryza sativa*), but most progress about flowering time regulation has been achieved in the long day model plant *Arabidopsis thaliana*.

Since maize leaf derived flowering time regulators are investigated during this work, some general flowering time regulators from leaves and downstream targets will now be introduced. These genes will be mainly parts of the photoperiodic pathway.

3.2. LEAF-EXPRESSED FLOWERING TIME REGULATING GENES

3.2.1. *GIGANTEA*

Mutations in the *Arabidopsis thaliana GIGANTEA (AtGI)* gene cause photoperiod-insensitive flowering, leading to a late flowering phenotype under long day conditions. AtGI is a large plant-specific protein of 1173 amino acids, which is associated with the circadian clock. This association is based on the circadian expression of the gene, which peaks 8 to 10 hours after dawn, and on the altered expression pattern of two other clock-associated genes *LATE ELONGATED HYPOCOTYL* (*LHY*) and *CIRCADIAN CLOCK ASSOCIATED1* (*CCA1*) in the *gi* mutant background (Fowler *et al*., 1999; Park *et al*., 1999). The rice homolog of *GI*, *Oryza sativa GIGANTEA* (*OsGI*) shows a circadian expression pattern as well. Overexpression of *OsGI* results in late flowering under long and short day conditions (Hayama *et al*., 2003). Maize has two homologous genes to *AtGI* and *OsGI*: *GIGANTEA OF ZEA MAYS1a* (*GIGZ1a* also known as *ZmGI1*) and *GIGANTEA OF ZEA MAYS1b* (*GIGZ1b* also known as *ZmGI2*). Both genes are expressed in a circadian pattern similar to *AtGI* and *OsGI* (Miller et al., 2008; Bendix et al, 2013). It has been shown that loss of *GIGZ1a* activity causes early flowering under long day conditions. This is in contrast to Arabidopsis and rice *gi* mutants. Nevertheless, maize *GIGZ1a* is able to rescue Arabidopsis *gi* loss-of-function mutants (Bendix *et al*., 2013).

3.2.2. *CONSTANS*

The *CONSTANS* (*CO*) gene encodes a zinc finger protein (Putterill *et al.*, 1995) and serves as an integrator of circadian clock outputs and the flowering time regulatory network. This becomes visible when clock associated genes, like *GIGANTEA*, are mutated. *CO* is down-regulated when *GI* is mutated in *Arabidopsis* and the overexpression of *CO* can rescue the late flowering phenotype of circadian clock mutants (Suárez-López *et al*., 2001). In maize however, the overall expression of *CONSTANS OF ZEA MAYS1* (*CONZ1* also known as *ZmCO1*) is up-regulated, when *GIGZ1a* is down-regulated (Bendix et al, 2013). Taken together, it seems that GI regulates the expression of *CO* positively in Arabidopsis, but GIGZ1a of maize has a negative effect on the expression of *CONZ1*. In both species, Arabidopsis and maize, *CO* shows a circadian expression pattern with a single peak during the night in short days (SD), but with two peaks in long days (LD). The first peak appears shortly before sunset and the

second peak occurs during the night period, like in SD (Miller *et al*., 2008; Suárez-López *et al*., 2001). The expression of *GIGZ1a* and *GIGZ1b* peaks 6 h before the peak of *CONZ1* occurs in SD, but in LD it seems that only the second peak of *CONZ1* is regulated by GIGZ1a/b, because the first peak appears at the same time as the single *GIGZ1a/b* peak (Miller *et al*., 2008). As a prove that *CO* is involved in flowering time regulation, at least under long day conditions in Arabidopsis (Putterlin *et al*., 1995), it has been shown that overexpression of *CO* causes an early flowering phenotype in Arabidopsis (Onouchi *et al.*, 2000).

3.2.3. *FLOWERING LOCUS T*

Wigge *et al*. (2005) identified a downstream target of *CO* by microarray analyses. They compared gene expression pattern in Arabidopsis *co* mutant leaves and wild-type leaves after one day of floral inductive long day. The only gene that did not show a response to day length in the mutant was *FLOWERING LOCUS T* (*FT*). *FT* encodes a phosphatidylethanolamine binding protein (PEBP), which leads to an early flowering phenotype under overexpression (Kardailsky *et al.*, 1999; Kobayashi *et al.*, 1999). It could be shown that FT is a mobile signal that moves from the leaves to the SAM. In the SAM this leaf-derived protein induces flowering after interacting with FLOWERING LOCUS D (FD) (Abe *et al*., 2005; Corbesier *et al.*, 2007; Jaeger & Wigge, 2007; Wigge *et al.*, 2005). The identification of a mobile signal, which moves from the leaves to the shoot apex, was the confirmation of a hypothesis that was brought up for the first time already in 1865 by the famous botanist Julius Sachs. He concluded from his experiments that light produces flower-forming substances in leaves, which lead to flower formation at darkened shoots. However, the 'flowering time community' attributes the 'florigen' - hypotheses to Knott (1934) and Chailakhyan (1936). For a more complex picture of the regulation of the leaf derived florigen FT see *Figure 3*.

In rice, HD3a was identified as 'florigen' homolog of FT. The CO homolog HEADING DATE1 (HD1) of rice (Yano *et al*., 2000) activates *HD3a* under short day conditions, but is also repressed by HD1 under long day conditions (Tamaki *et al.*, 2007). *HD3a* is also activated under short day and long day conditions by EARLY HEADING DATE1 (EHD1), a b-type cytokinin response regulator. This activation is independent of HD1 (Itoh *et al*., 2010). In contrast to findings in Arabidopsis, rice contains a second florigen: *RICE FLOWERING LOCUS T1* (*RFT1*). Unlike *HD3a*, *RFT1* is only activated under long day conditions by EHD1 and

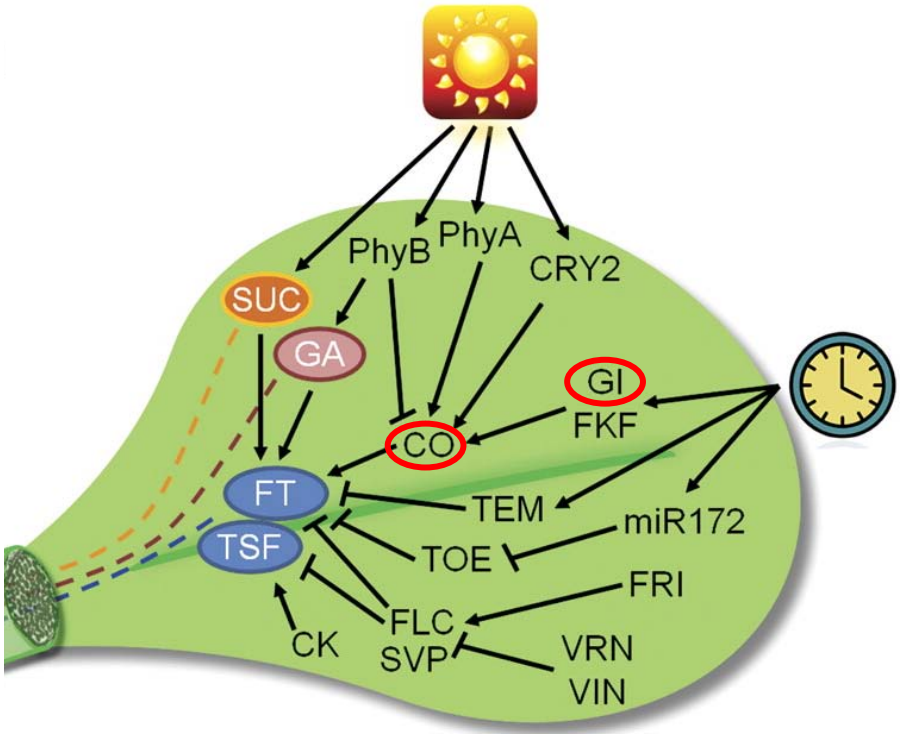

Figure 3. **Regulation of long-distance florigenic signals in Arabidopsis leaves.** The main regulators *FLOWERING LOCUS T* (*FT*) and *TWIN SISTER OF FT* (*TSF*) are depicted in blue. For visual clarity, not all known relationships are shown. CONSTANS (CO) and GIGANTEA (GI) are encircled in red. Arrows indicate positive regulation, T-arrows represent negative regulation. Mobile signals are outlined with ovals and dashed lines indicate movement of signals through the phloem towards the shoot apex. Abbreviations: CK (cytokinins), CRY2 (CRYPTOCHROME2), FKF1 (FLAVIN-BINDING KELCH DOMAIN F BOX1), FLC (FLOWERING LOCUS C), FRI (FRIGIDA), GA (gibberellic acid), miR172 (microRNA172), PhyA/B (Phytochrome A/B), SUC (sucrose), SVP (SHORT VEGETATIVE PHASE), TEM (TEMPRANILLO), TOE (TARGET OF EAT), VIN (VERNALIZATION INSENSITIVE), VRN (VERNALIZATION) (Image modified from Turnbull, 2011).

other factors (Komiya *et al*., 2009). *HD3a* RNAi lines do not show a flowering time phenotype under long day conditions, while under short day conditions *HD3a* RNAi plants flower after 90 days, which is about 30 days later then wild-type plants (Komiya *et al*., 2009). Unlike *HD3a* RNAi plants, *RFT1* RNAi plants do not show a flowering phenotype under short day conditions, but show a late flowering phenotype under long day conditions. Wild-type plants and *HD3a* RNAi plants flower after 120 days, while *RFT1* RNAi plants flower after 210 days (Komiya *et al*., 2009). *HD3a* and *RFT1* double knockout lines do not flower within 300 days of observation in SD (Komiya *et al*., 2008). Taken together, in rice there exist two separate photoperiod-sensing pathways.

In maize the PEBP gene family consists of 25 members, which are named as *Zea mays CENTRORADIALES* (*ZCN*) genes after the first cloned plant PEBP gene from *Antirrhinum* (Danilevskaya *et al*., 2008a). Out of these 25 genes, *ZCN8* was identified as the most likely homolog to *FT* from Arabidopsis (Danilevskaya *et al*., 2008a; Lazakis *et al*., 2011; Meng *et al*.,

2011). It has also been shown that the expression of *ZCN8* in tropical photoperiod-sensitive maize lines follows a diurnal circadian pattern and its expression is increased under floral inductive short day conditions. Therefore, it was suggested that *ZCN8* acts in the photoperiodic flower inductive pathway (Meng *et al*., 2011). Similar to *FT, ZCN8* is highly expressed in the leaves and its expression is very low in the SAM. The putative mobile ZCN8 protein interacts in the SAM with DELAYED FLOWERING1 (DFL1), the *FD* homolog of maize (Meng *et al*., 2011; Wigge *et al.*, 2005). Overexpression of *ZCN8* leads to an early flowering phenotype, while knockdown of *ZCN8* results in late flowering (Meng *et al*., 2011). The ectopic expression of *ZCN8* can rescue the late flowering phenotype of Arabidopsis *ft* mutants (Lazakis *et al*., 2011). It is thought that *ZCN8* expression is regulated only under long day conditions via *GIGZ1a* and *CONZ1*. It has been shown in *Mutator* transposon insertion lines that a reduced *GIGZ1a* level leads to a comparable increased level of *CONZ1* in SD and LD, but the expression of *ZCN8* is substantially higher in LD than in SD. This comes along with a reduction of leaf number of the transposon insertion lines under LD but not under SD conditions (Bendix *et al*., 2013).

Remarkably, there seems to be a grass-specific flowering time regulation gene. The *indeterminate1* (*id1*) mutant shows the strongest phenotype regarding flowering time in maize so far. This mutant is severely affected in its ability to undergo transition from vegetative to reproductive growth (Singleton, 1946). The mutant shows an increased number of leaves and in some mutants also the flower architecture is abnormal. In these cases vegetative tissues emerge from every spikelet at the tassel and the initiation of female inflorescence fails or the axillary meristems are converted to branch-like vegetative structures. The *ID1* gene is expressed early during development in immature leaf tissue and is a member of a zinc finger gene family (Colasanti *et al.,* 1998). The ID1 protein is also present in developing leaves and is expression level is not altered by light or sink-source transition, so it is most likely that *ID1* acts through the autonomous floral inductive pathway (Wong & Colasanti, 2007). In 2011 it has been shown by Lazakis *et al*. that the activity of ID1 is necessary for expression of *ZCN8*.

In rice, EARLY HEADING DATE2 (EHD2) or OsID1 was identified as a homolog to ZmID1. EHD2 is required to activate the expression of *EHD1* and *FT*-like downstream targets. *Ehd2* mutants show a late flowering phenotype, which is dosage dependent. The expression

behavior of *EHD2* is comparable to the expression of *ZmID1* (Matsubara *et al*., 2008; Park *et al*., 2008). For a more detailed network of the regulation of the 'florigens' in rice see *Figure 4*.

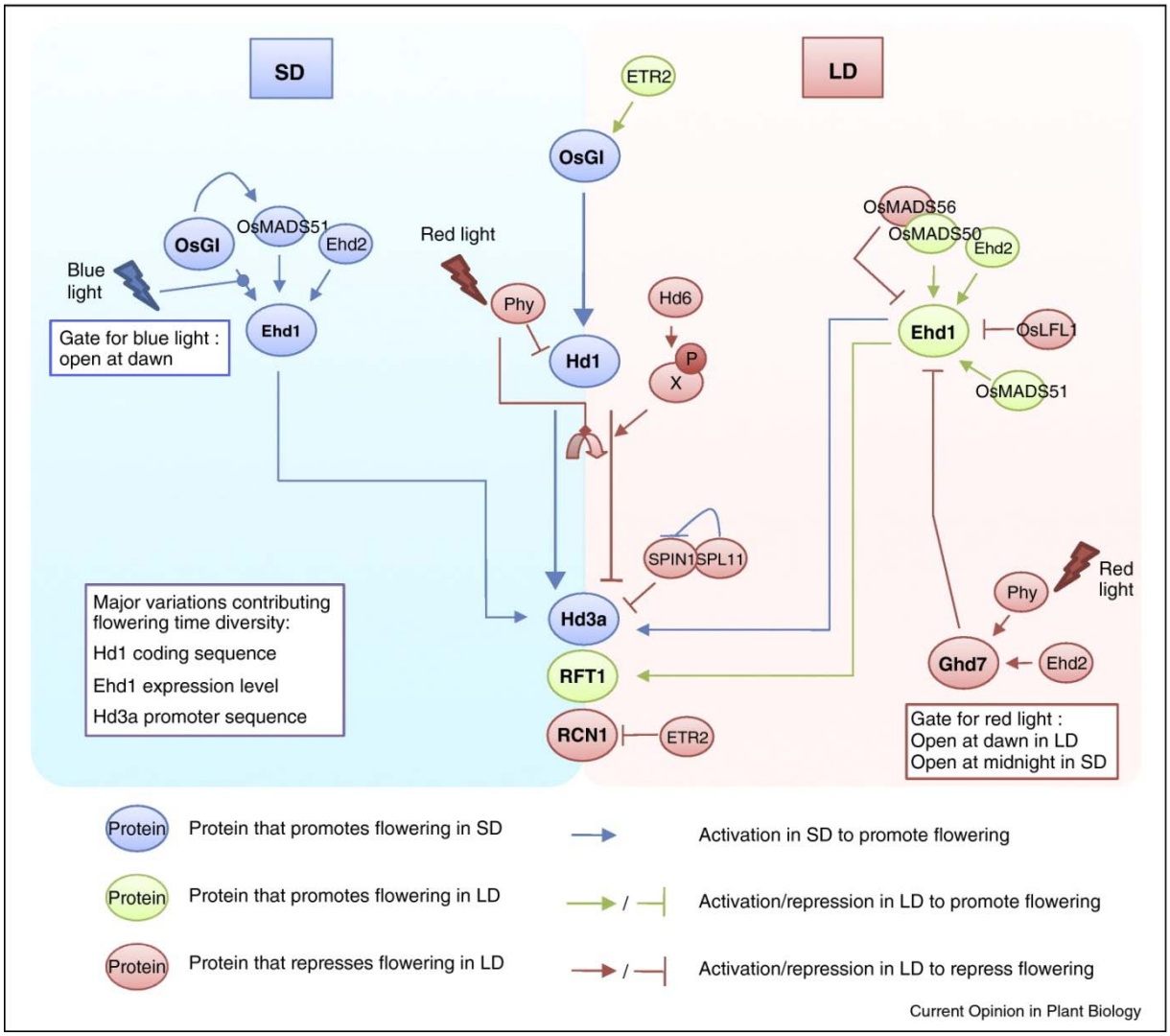

Figure 4. **The molecular network of 'florigen' gene regulation in rice.** The left side shows an overview of the complex network of the regulation of the *FT* homolog *HD3a* under short day (SD) conditions. On the right side the regulation of *HD3a* and its paralog *RFT1* under long day (LD) conditions is depicted. Arrows represent a positive regulation, T-arrows negative regulation. Abbreviations: EHD1/2 (EARLY HEADING DATE1/2), ETR2 (ETHYLENE RECEPTOR2), GHD7 (GRAIN NUMBER, PLANT HEIGHT, AND HEADING DATE7), GI (GIGANTEA), HD1/6 (HEADING DATE1/6), LFL1 (LEC1 AND FUSCA-LIKE1), Phy (Phytochrome), SPL11 (SQUAMOSA PROMOTER-BINDING PROTEIN11), SPIN1 (SPL11 INTERACTING PROTEIN1) (Image taken from Tsuji *et al*., 2011).

3.3. INTEGRATION OF THE FLORAL INDUCTIVE SIGNALS AT THE SHOOT APEX

3.3.1. *FLOWERING LOCUS D*

As previously mentioned, Arabidopsis FT is translocated from the leaf towards the SAM via the phloem (Corbesier *et al.*, 2007; Jaeger & Wigge, 2007). At the SAM it interacts with the basic leucine zipper (bZIP) protein FLOWERING LOCUS D (FD), which is preferentially expressed in the shoot apex. The first indication of FD interacting with FT was demonstrated as an Arabidopsis *fd* mutant was able to suppress the early flowering phenotype caused by *FT* overexpression. The physical interaction of the two proteins was then confirmed using a yeast two-hybrid assay (Abe *et al*., 2005; Wigge *et al.*, 2005). As downstream targets of the FT/FD complex *SUPPRESSOR OF OVEREXPRESSION OF CO1* (*SOC1*) (Michaels *et al*., 2005; Yoo *et al*., 2005) and floral meristem identity genes like *APETALA1* (*AP1*), *FRUITFULL* (*FUL*) and *SEPALLATA3* (*SEP3*) (Abe *et al*., 2005; Corbesier *et al.*, 2007; Wigge *et al.*, 2005) could be identified.

In rice however, the molecular mechanisms of the integration of 'florigens' in the shoot apex seem to be different. The rice FT homolog HD3a does not interact directly with OsFD1, the rice homolog of FD, but requires support by an additional protein. It has been shown that HD3a and OsFD1 are bridged together by the 14-3-3 protein GF14c to form the so-called 'florigen activation complex' (FAC) (Taoka *et al*., 2011). FAC binds to the promoter of *OsMADS15*, which is an ortholog to *AtAP1*, and activates its expression.

Maize *DLF1* is the *FD* homolog and its expression seems to be linked to the floral transition of the SAM. The interaction of ZCN8 and DLF1 has been shown using yeast two-hybrid assays (Danilevskaya *et al*., 2008a; Meng *et al*., 2011). *DLF1* expression increases and peaks at the time point of transition of the SAM, but later during development expression is not detectable anymore (Muszynski *et al*., 2006). Alterations of the expression level of *DLF1* and *ZCN8* both lead to changes in flowering time. Decreased levels of *DLF1* expression lead to an increased leaf number and consequently to a delay in flowering time (Neuffer *et al.*, 1997). This pattern indicates that *DLF1* promotes floral transition (Muszynski *et al*., 2006). A floral meristem identity gene that is activated by the ZCN8/DLF1 complex is the MADS-box transcription factor *Zea mays MADS4* (*ZmM4*). The expression of *ZmM4* is initiated in leaf primordia of the vegetative SAM, increases during the elongation of the SAM and reaches a maximum at the time of spikelet branch meristem initiation. The expression level of *ZmM4*

decreases when the floral development proceeds. Overexpression studies have shown that *ZmM4* promotes floral transition and inflorescence development. Its exact role is not known so far, but it is suggested that it is involved in positive or negative feedback loops similar to LEAFY (LFY), AP1/FUL1 and CAULIFLOWER (CAL) in Arabidopsis (Danilevskaya *et al*., 2008b).

3.3.2. *SUPPRESSOR OF OVEREXPRESSION OF CO1*

The MIKC^{C}-type MADS-box transcription factor *SUPPRESSOR OF OVEREXPRESSION OF CO1* (*SOC1*) or *AGAMOUS LIKE20* (*AGL20*), the target of the FT/FD complex, is one of the major flowering pathway integrators in Arabidopsis. *SOC1* is mainly expressed in developing leaves and meristems. Expression is increasing according to the developmental age (Borner *et al*., 2000; Samach *et al*. 2000). One of the earliest events during floral transition is the up-regulation of *SOC1* expression in the meristem (Lee *et al.*, 2000; Samach *et al*. 2000). The findings that *ft soc1* double null mutants show additive late flowering phenotypes and that *SOC1* expression is not significantly reduced in *ft* mutants compared to autonomous pathway mutants (Lee et al., 2000; Moon *et al*., 2005; Yoo *et al*., 2005), indicate that *SOC1* is not regulated by *FT* alone.

Additionally it has been shown that *SQUAMOSA BINDING FACTOR-LIKE9* (*SPL9*) is positively involved in the age-related regulation of *SOC1* by binding to the first intron of *SOC1*. *SPL9* itself is repressed through *microRNA156* (*miR156*), which is strongly expressed in the juvenile phase of Arabidopsis plants. Its expression decreases while the plant ages and so the expression level of *SPL9* increases during plant growth (Wang *et al.*, 2009). As mentioned earlier also *SOC1* expression increases when the plant ages (Samach *et al*. 2000). The overexpression of *miR156* leads to a late flowering phenotype, similar to *spl9* mutant plants (Schwarz *et al.*, 2008, Wu & Poethig, 2006). The overexpression of other *SPL* genes causes an early transition from vegetative to reproductive growth (Wu & Poethig, 2006).

There are also indications that SOC1 integrates the gibberellic acid (GA) inductive pathway. GA plays an important role in flowering: it had been shown by Wilson and coworkers (1992) that the GA biosynthesis mutant *ga1-3* is not able to flower under short day conditions, whereas under long day conditions the mutation leads to a minor delay of flowering compared to wild type plants. Overexpression of *SOC1* can rescue the late flowering phenotype, while a *soc1* null mutant is less sensitive to GA compared with wild-

type plants (Moon et al., 2003). Moreover, it has been shown by Jung *et al*. (2012) that the integration of the GA pathway into the flowering time regulatory network under short day conditions works via the SOC1-SPL module. However, under inductive long day conditions, GAs are increasing the amount of *FT* in the vasculature, which then activates the floral transition in the shoot apex (Porri *et al*., 2012).

The vernalization pathway and the autonomous pathway are negatively regulating *SOC1* expression in Arabidopsis. One major component in these two pathways is the MADS-box transcription factor *FLOWERING LOCUS C* (*FLC*). To initiate floral transition the regulators of these two pathways are repressing *FLC* expression by changing the epigenetic status of the *FLC* chromatin (Amasino, 2004). FLC itself represses expression of *FT* by binding to the first intron and *FD* and *SOC1* by binding to their promoters. Expression of *FLC* in leaves therefore leads to late flowering due to repression of *FT* and *SOC1* expression. Similarly, expression of *FLC* in the shoot apex leads to late flowering because of repression of *FD* and *SOC1* (Searle *et al.*, 2006). *FLC* forms a floral repressor complex together with another MADS-box transcription factor *SHORT VEGETATIVE PHASE* (*SVP*) (Li *et al.*, 2008). *SVP* is a negative regulator of flowering in Arabidopsis as well (Hartmann *et al*., 2000) and its expression is regulated by the autonomous and the GA pathway. The FLC/SVP complex binds directly to the promoters of *SOC1* and *FT* to repress their expression. Expression of *SOC1* is thus stronger affected by the floral repressor complex than by the activation through FT (Li *et al.*, 2008). Therefore, Arabidopsis *SOC1* is supposed to be an integrator of all five floral inductive pathways, the photoperiodic, the aging, the gibberellin, the autonomous and the vernalization pathway to initiate flower development (*Figure 5*).

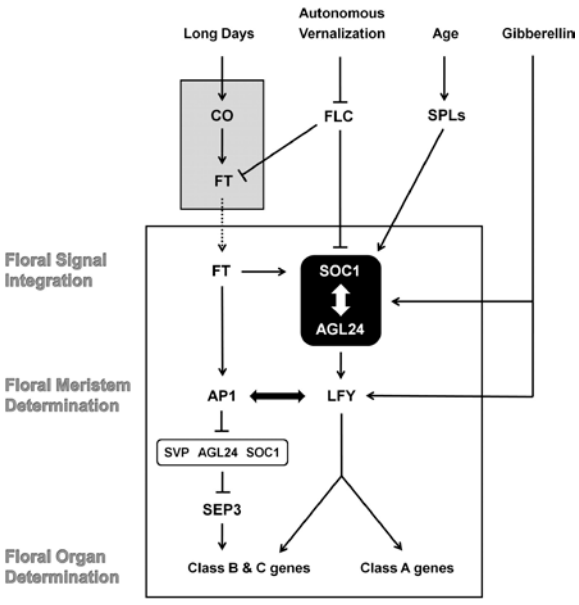

Figure 5. **Integration of the floral inductive pathways by SOC1 at the SAM of *Arabidopsis thaliana*.** SOC1 integrates flowering signals from long day, autonomous, vernalization, plant age and gibberellin pathway. SOC1 and AGL24 interact with each other and regulate each other in a positive feedback loop (black box). SOC1 and AGL24 activate the meristem identity gene *LFY*, which then activates flower meristem identity genes. SOC1 and AGL24 are also involved in the repression of *SEP3*. In this way, SOC1 and AGL24 ensure floral induction and flower development occur in their proper time and space. The grey box indicates the vasculature of the leaf where CO-FT induction occurs, whereas the open rectangle indicates the shoot apical meristem where floral evocation occurs. Arrows indicate activation, T-bars indicate repression (Image taken from Lee & Lee, 2010).

Another MADS-box transcription factor, *AGAMOUS-LIKE24* (*AGL24*), a close homolog of *SVP*, acts as a floral activator like *SOC1* (*Figure 5*) (Michaels *et al*., 2003; Liu *et al*., 2008; Yu *et al*., 2002). Overexpression of *AGL24* causes early flowering, while a loss-of-function mutant exhibits a late flowering phenotype. Expression domains of *SOC1* and *AGL24* are largely overlapping and include leaves, shoot apical meristem, roots, stems and inflorescences (Michaels *et al*., 2003; Yu *et al*., 2002). Expression of *AGL24* is affected by at least three flowering inducing pathways, the photoperiod, the vernalization and the autonomous pathway. AGL24 and SOC1 are thus suggested to integrate flowering signals via a positive feedback loop, because they are able to bind directly to their promoters and thus up-regulate each other (Michaels *et al*., 2003; Liu *et al*., 2008).

In rice two homologous genes to *SOC1*, *OsSOC1* (Tadege *et al*., 2003) or *OsMADS50* (Lee *et al*., 2004) and *OsMADS56* (Ryu *et al*., 2009) were reported. Surprisingly *OsMADS50* and *OsMADS56* have been shown to represent important flowering activators, instead of flowering integrators like *AtSOC1* (Komiya *et al.*, 2009; Lee *et al*., 2004; Ryu *et al*., 2009). Ectopic expression of *OsMADS50*/*OsSOC1* in Arabidopsis leads to early flowering and is able to rescue the *soc1* late flowering phenotype (Tadege *et al*., 2003). *OsMADS50*/*OsSOC1* overexpressing plants flower very early, already at the callus stage, while RNAi plants are late flowering under long day conditions. *OsMADS50*/*OsSOC1* acts upstream of *OsMADS15* and *HD3a*. Both genes are down-regulated if *OsMADS50* is knocked out. *OsGI* and *HD1* are unaffected by down regulation of *OsMADS50*/*OsSOC1*, which indicates that *OsMADS50*/*OsSOC1* works either in parallel with or downstream of *OsGI* and *HD1* (*Figure 4*) (Lee *et al.*, 2004). The situation for the second *SOC1* homolog *OsMADS56* is different. Here, overexpression causes late flowering under long day conditions, but again only transcripts of *HD3a*, *RFT1* and others are reduced, while the mRNA levels of *OsGI*, *HD1* and others appear unaffected. An interaction of OsMADS50/OsSOC1 and OsMADS56 could be shown by yeast two-hybrid and co-immunoprecipitaion analyses. These results indicate, that OsMADS50/OsSOC1 and OsMADS56 are acting antagonistically in long day-specific flowering time regulation likely by forming a complex, which regulates downstream targets (*Figure 4*) (Ryu *et al*., 2009).

ZmMADS1 (also *Zea mays MADS5*, *ZmM5*) is a maize homolog to *SOC1*. *ZmMADS1* was originally isolated from cDNA libraries of maize pollen and egg cells. It was found to be co-

expressed with the *AP1* homolog *ZmMADS3* (or *ZAP1b*) during flower development, in egg cells and early embryogenesis, but its function remained unclear (Heuer *et al.*, 2001).

There are more flowering time regulatory genes known and putative flowering time regulatory genes have been identified in day neutral species maize, but very little is known about their regulatory network. Dong *et al*. (2012) recently published the first gene regulatory network model for floral transition of the shoot apex in maize, in which known information and information based on comparison to flowering time regulatory genes from Arabidopsis and rice are integrated (*Figure 6*). This model gives an overview of the

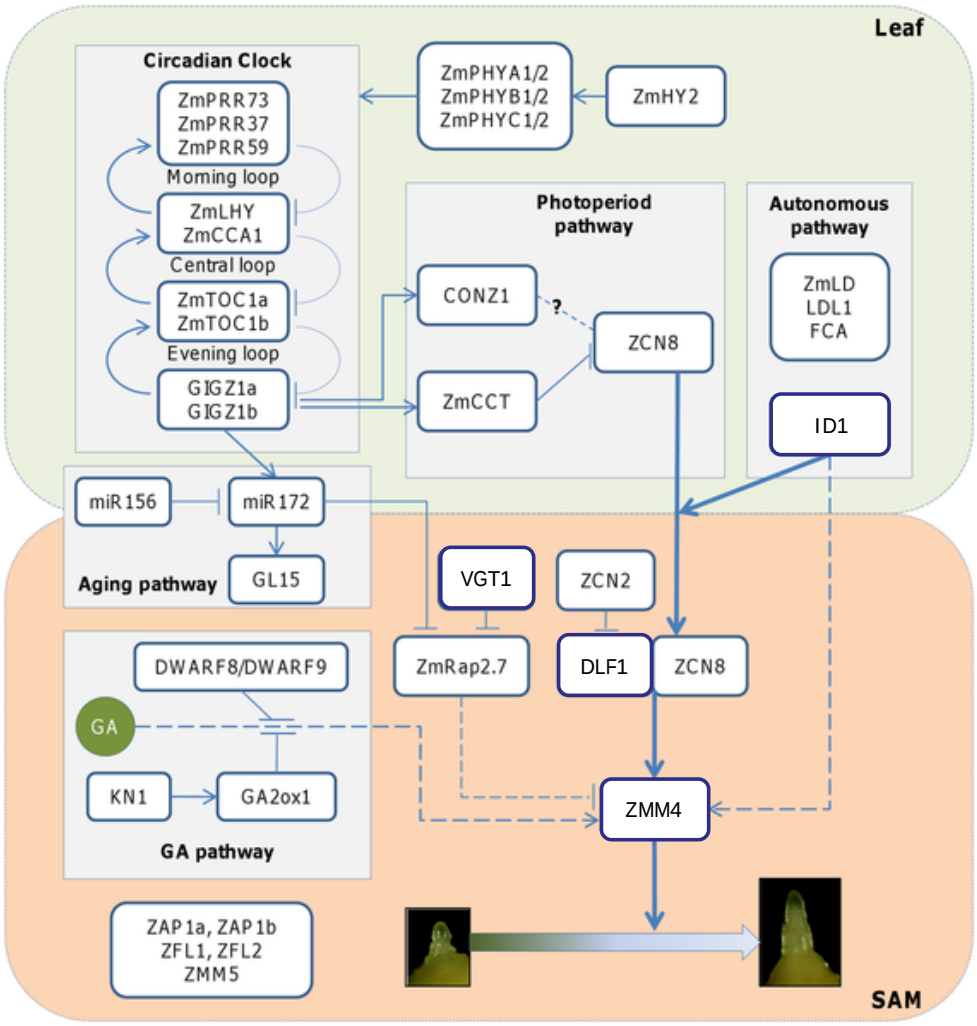

Figure 6. **Gene regulatory network model for floral transition of the shoot apex in maize.** Thick lines are confirmed interaction shown by genetic analysis, thin lines are based on comparative genomics and dashed lines are indicating putative relationship derived from comparative genomics. Arrows represent positive regulation, T-bars represent negative regulation. Genes in boxes without connection to the network could not be allocated. Abbreviations: CCT (CCT domain-containing protein), GL15 (GLOSSY15), HY2 (ELONGATED HYPOCOTYL2), KN1 (KNOTTED1), miR156/172 (microRNA156/172), LD (LUMINIDEPENDENS), LDL1 (LSD1-LIKE1), LHY (LATE ELONGATED HYPOCOTYL), PHYA/B/C (PhytochromeA/B/C), PRR73/37/59 (PSEUDO RESPONSE REGULATOR73/37/59), RAP2.7 (RELATED TO AP2.7), TOC1a/b (TIMING OF CAB EXPRESSION1a/b), VGT1 (VEGETATIVE TO GENERATIVE TRANSITION1), (ZAP1a/b (ZEA APETALA HOMOLOG1a/b), ZFL1/2 (ZEA FLORICAULA/LEAFY1/2) (Image modified from Dong *et al.*, 2012).

complexity of the regulatory network in maize, but additionally points towards numerous unanswered questions.

3.4. OBJECTIVES OF THIS WORK

Maize is the most important crop as it is not only needed for food production, but also as an alternative energy resource for the production of biofuels. Since the area of cultivable land is limited, it is important that the yield of this crop plant is increased, so that farmers can face the demand of food of the increasing world population as well as the increasing demand of biomass for bioenergy production. The limited area of cultivable land is not the only problem by reaching this goal, but also extreme weather situations caused by the climate change constitute big challenges.

The possibility to regulate the time of flowering and with this the time of maturity of a plant represents one part in the puzzle for solving this problem. Maize produces most of its biomass during the corn filling phase, which often falls into the hottest and driest period of the year. Drought, especially during the corn-filling phase, has a huge impact on biomass yield. A change in flowering time and with this a change in time point of the corn-filling phase can help to avoid drought stress and with this may increase yield. Moreover, with shorter growth phases, it would be possible to grow maize in areas, in which summers and the corresponding growth periods are normally too short to grow plants to maturity. By modifying the flowering time of crops, agricultural areas would be available, where cultivation was not promising before. Additionally with a shorter life cycle maize might be sown out more often a year in climate zones with longer summers and thus increase the yield per hectare. Finally, by delaying flowering time maize may produce more vegetative biomass that could be used, for example, for biogas production.

To achieve such effects by genetic modifications of crops, the genetic architecture and network regulating flowering time in maize has to be enlightened. Most of our current knowledge about this regulatory network has been obtained from studies of the LD dicotyledonous model plant *Arabidopsis thaliana*. However, this knowledge is not always easily transferable to the crops, which are often monocotyledonous plants. For example *SOC1* is a flowering time integrator in the shoot apex of Arabidopsis, while its homologs in rice act as flowering time regulatory genes in leaves (Komiya *et al.*, 2009; Lee *et al*., 2004;

Ryu *et al*., 2009). *GIGANTEA* regulates *CONSTANS* in Arabidopsis positively (Suárez-López *et al*., 2001), while *GIGANTEA* influences *CONSTANS* negatively in maize (Bendix et al, 2013). Furthermore, the strongest flowering regulatory effect in maize is attributed to *INDETERMINATE1* (*ID1*) (Colasanti *et al.,* 1998), a gene from which no putative homolog is found in the Arabidopsis genome (Colasanti *et al*., 2006).

To gain more knowledge of the regulatory mechanism controlling flowering time in maize, the major aim of this work was to perform comparative transcriptome analyses of early and late flowering maize genotypes using leaves before and during the floral transition of the shoot apical meristem. The goal of this approach was to identify novel leaf-expressed candidate genes, which play a role in the regulation of floral transition, either by activation or by repression of key flowering time regulators in maize. Activating genes should be up-regulated while repressing genes should be down-regulated after flowering meristem induction. After the identification of candidate genes, functional analyses and complementation assays as well as immunolocalization on maize leaf tissues should be performed. Additionally, the response of the candidates to different day lengths should be analyzed to uncover a potential role in the photoperiodic regulation of flowering.

4. MATERIALS & METHODS

4.1. STANDARD MOLECULAR BIOLOGY WORK

Standard molecular biology methods were performed according to Sambrook *et al.* (1989) using molecular grade reagents.

4.2. BIOINFORMATIC ANALYSES AND STATISTICS

For general information about genes, nucleotides and protein sequences, open resources and software at the National Center for Biotechnology Information (NCBI, http://ncbi.nlm.nih.gov/) was used. Detailed information about genes from maize, Arabidopsis and rice were taken from MaizeSequence (http://www.maizesequence.org/), The Arabidopsis Information Resource (TAIR, http://arabidopsis.org/) and the Rice Genome Annotation Project (http://rice.plantbiology.msu.edu), respectively.

Protein sequences of candidate genes were used as query to identify homologous proteins using the Basic Local Alignment Search Tool (BLASTp) in different genome databases at PlantGDB (http://plantgdb.org) with default settings in *Zea mays*, *Oryza sativa*, and *Arabidopsis thaliana*. For *Hordeum vulgare* and *Triticum aestivum* a BLASTp search was performed at the NCBI homepage with default settings and an E value cut-off of $1e^{-70}$.

Alignments were generated using either the muscle algorithm of the program SeaView Version 4.3.5 (Gouy *et al*. 2010) or using the accurate alignment algorithm using CLC Main Workbench (CLC bio). Alignments generated with SeaView were used for constructing a phylogenetic tree in SeaView using the Neighbor Joining (NJ) method. To test the relationship, the Bootstrap method with 10,000 replicates was applied. SeaView alignments were illustrated using GeneDoc Version 2.7.000.

For *in vitro* cloning procedures Vector NTI® Version 10.3.0 (Invitrogen) software package was used. Data gained from Sanger DNA sequencing, which was performed by the companies GATC Biotech AG (Konstanz, Germany) and LGC Genomics GmbH (Berlin, Germany), were analyzed using the ContigExpress assembly tool of Invitrogen´s Vector NTI® Version 10.3.0.

Tests for significance except for the analysis of the microarray data were calculated in Microsoft Office Excel 2007 with an unpaired *student's t-test* using the TTEST function.

Correlation coefficients were also calculated in Microsoft Office Excel 2007 using the CORREL function.

4.3. PLANT MATERIAL AND GROWING CONDITIONS

Zea mays (L.) lines used during this work are listed in *Table 1*. All lines except A188, Hi II A and Hi II B were selected by the cooperation partner BASF in frame of the OPTIMAS project (http://www.optimas-bioenergy.org/) as genetically closely related pairs for differences in the traits water use efficiency or nitrogen use efficiency. All lines are publicly available and were additionally obtained from the maize stock center at maizecoop.cropsci.uiuc.edu. Maize plants were grown under long day conditions (16 h light, 8 h dark) in greenhouses at 25 °C during the light period and 20 °C in the dark. Temperatures may have been higher when the outside temperature was considerably higher than 25 °C. During the light period the plants were illuminated using Philips MASTER HPI-T Plus 400W/645 E40 1SL and Philips MASTER GreenPower CG T 400W E40 to ensure sufficient light over the 16 h day-period. Experiments under short day conditions (12 h light, 12 h dark) were performed in a climate chamber. The chamber was set to 26 °C during the light period and 18 °C during the dark. Air humidity was kept constant at 60 %. Illumination was provided by above-mentioned illuminants. Seeds were watered overnight and sown in substrate CL TON KOKOS (Einheitserde®) and plants were transferred after 4 weeks to 10 l pots with substrate CL TON KOKOS (Einheitserde®) and fertilized with four pieces Plantosan® Compact (Manna). At the beginning of this work ED73 (Einheitserde®) was used as a substrate.

Arabidopsis thaliana (L.) Heynh. Col-0 accession was used as wild type in this work. The Arabidopsis mutant line *soc1-2* harbors a T-DNA insertion in the gene *SOC1* (*SUPPRESSOR OF OVEREXPRESSION OF CO1*) alias AGL20 (AGAMOUS-LIKE20, AT2G45660) in the first intron at position +710 (Lee *et al*., 2000). Plants were grown in growth chambers under long day conditions (16 h light, 8 h dark) at 20 °C / 70 % air humidity during light and 18 °C / 65 % air humidity during the dark period. Under short day conditions (8 h light, 16 h dark) the chamber was kept constant at 22 °C / 70 % air humidity. Chambers were illuminated by SYLVANIA Luxline Plus F30W/840 cool white deluxe and SYLVANIA Luxline Plus F30W/830

warm white deluxe. Seeds were sown on sieved SPVM (Einheitserde®) substrate mixed with 10 % sand and plants were transferred to SPVM (Einheitserde®) substrate mixed with 10 % sand, 10 % expanded clay (Liapor®) and Osmocote® Start (Scotts) (30 g per 10 l substrate) when they had 4 to 6 leaves.

***Table 1. Zea mays* lines used in this work.** Information of class, pedigree/parents, type and country are taken from the Maize Genetics and Genomics Database (maizegdb.org). For lines marked with * not all informations were available.

Line	Class	Pedigree/Parents	Type	Country
4F-240 BX 16*			unverified	Argentina
4F-350 CN 2*			unverified	Argentina
A6*		Min. #13	Inbred line	USA
A188	White dent	4-29 (Silver King) x 46 (N.W.Dent) 4^4	Inbred line	USA
B73	Yellow dent	Iowa Stiff Stalk Synthetic C5	Inbred line	USA
B77	Yellow dent	BS11 (Pioneer 2-Ear Synthetic)	Inbred line	USA
E2558W	White dent	M162W^3.N6	Inbred line	South Africa
EP1	Yellow flint	Spanish population 'Lizargarate'	Inbred line	Spain
F7	Yellow flint	French population 'Lacaune'	Inbred line	France
Hill A (T940A)*		A188 x B73 F2 selection	Partially inbred line	
Hill B (T940B)*		A188 x B73 F2 selection	Partially inbred line	
IDS69	Popcorn	South American	Inbred line	USA
Ki3	Yellow flint	Suwan 1	Inbred line	Thailand
Ki11*			Inbred line	
Mo1W	White dent	Mo22 x WF9^2	Inbred line	USA
NC304*		Ear-to-row selfing from F2 generation of (Pioneer X105A x H5) x H101	Inbred line	USA
NC320	Yellow dent	SC76^4 x B52	Inbred line	USA
NC332*		Sister line to NC334 and derivative of SC76 x B52	Inbred line	
NC350*		Experimental line sharing the same pedigree of NC296 with an experimental line from the hybrid H101 from El Salvador	Inbred line	
OH43	Yellow dent	Oh40B x W8	Inbred line	USA
PA762	Yellow dent	Oh43 x Pa70L	Inbred line	USA
PA875*		WF9 synthetic (original)	Inbred line	USA
R229	Yellow dent	[479 x B73^2]S6. 479	Inbred line	USA
SA24	Popcorn	South American	Inbred line	USA
Tzi10	White dent	Tlaltizapan 7844 x TZSR	Inbred line	Nigeria
Tzi16*		RppTZSR-Y/N28)	unverified	Nigeria
Tzi25	Yellow dent	B73^3 x RppSR	Inbred line	Nigeria
VA26	Yellow dent	Oh43 x K155	Inbred line	USA
VA102*		Va59 x Va60	Inbred line	USA
Wf9	Yellow dent	Wilson Farm Reid	Inbred line	USA

4.4. DETERMINATION OF FLORAL TRANSITION OF THE SHOOT APICAL MERISTEM (SAM) OF *ZEA MAYS*

Maize plants were cut directly above the substrate. Leaves were removed from the stem one after another using a scalpel. Young and thin leaves were removed under a binocular using a hollow needle. After the shoot apical meristem (SAM) was dissected the developmental stage was determined visually according to Irish and Nelson (1991) under a binocular (ZEISS Discovery.V8 and Nikon SMZ 645). When branch meristems were visible the meristem was designated as 'switched'.

4.5. TOTAL RNA EXTRACTION, DNASE TREATMENT AND REVERSE TRANSCRIPTION

RNA extraction was performed after Logemann *et al.* (1987). 100-200 mg of leaf material was collected in 2.0 ml reaction tubes, frozen in liquid nitrogen, ground using a mixer mill (Retsch® MM200) for 2 min at 30 Hz and homogenized in 400-1000 µl Z6-Buffer (8 M Guanidinium-HCl; 20 mM MES; 20 mM EDTA; pH 7.0; before usage 350 µl 2-mercaptoethanol was added per 50 ml buffer). 500 µl phenol/chloroform/isoamyl alcohol (25:24:1) was added to homogenized leaf material and vortexed for 1 min. Afterwards the mixture was centrifuged for 10 min at 15,000 rpm and 4 °C. RNA was precipitated from the supernatant by mixing with 1/20 vol. 1 N acetic acid and 0.7 vol. 100 % ethanol. Samples were inverted several times and then centrifuged again as described above. Pellets were washed twice in 500 µl 3 M NaOAc pH 5.2 and a third time in 80 % ethanol. Afterwards pellets were dried using a vacuum concentrator (Christ RVC 2-18 or Savant SVC 100H) and resuspended in 50 µl ultra-filtered (Merck Millipore Milli-Q® Biopak®) water for 10 min at 60 °C. RNA concentration was measured with a Peqlab NanoDrop® ND-1000 UV/Vis-spectral photometer. DNase treatment was performed according the manufacturer's protocol of DNase I - RNase-free (Fermentas, now Thermo Scientific). Reverse transcription was performed following the manufacturer's protocol of SuperScript® III Reverse Transcriptase (Invitrogen Life Technologies) using oligo$(dT)_{18}$ primers and RiboLock RNase Inhibitor from Thermo Scientific. For subsequent PCR reactions 1 µl of cDNA was used as a template. For quantitative real-time PCR cDNAs were diluted 1:4 and 1 µl was used each as a template (see also 4.9).

4.6. MICROARRAY ANALYSES

RNA was extracted as described in 4.5. RNA quality was checked using an Agilent 2100 Bioanalyzer and the Agilent RNA 6000 Pico Kit. cDNA and antisense cRNA synthesis was performed at the Friedrich-Alexander-Universität Erlangen-Nürnberg (Division of Biochemistry) by Dr. Urte Schlüter following the one-color microarray-based gene expression analysis protocol (Agilent Technologies). An aliquot of 1.65 mg of the cRNA was each loaded on one-color microarrays. The oligonucleotide probes on the microarrays were custom-designed (Agilent 025271). Microarray data were normalized to the 75th percentile within each array and were analyzed using the Agilent GeneSpring software package according to Pick *et al.* (2011).

4.7. POLYMERASE CHAIN REACTION (PCR)

PCRs for genotyping or primer optimization were performed using recombinant *Taq* DNA polymerase (Thermo Scientific) according to the manufacturer's protocol. dNTPs used for these reactions were also obtained from the same manufacturer. Primers were designed using the primer designing tool/primer-BLAST at NCBI (http://www.ncbi.nlm.nih.gov/tools/primer-blast/) (see also 4.8).

For amplification of nucleic acid fragments for DNA cloning (4.10) and sequencing the Peqlab KAPAHiFi™ PCR Kit was used following the manufacturer's manual. Annealing was performed at 60 °C.

4.8. PRIMER DESIGN

Primers were designed using the primer designing tool/primer-BLAST at NCBI (http://www.ncbi.nlm.nih.gov/tools/primer-blast/). Parameters for product length for qRT-PCR were set from 100 bp to 400 bp and melting temperatures between 55 °C and 65 °C with a maximum difference of 1 °C. Furthermore primers should have a GC content of 40 - 60 % and a length of 18 – 22 bp. The specificity check of the tool was set to the refseq mRNA database of *Zea mays*. Primer sequences were chosen that are predicted to be specific for

the desired product according to the database. If specificity was not possible, primer sequences were chosen to avoid side products by using a stringent elongation time according to the properties of the used DNA polymerase. All primer sequences can be found in the appendix (8.3 and 8.4).

Primers for the amplification the complete coding sequences of *ZmMADS1* (GRMZM2G171365) and *Zmm26* (GRMZM2G046885) comprised the first and the last 20 nucleotides of the respective coding sequence including start and stop codon referring to the maizesequence.org database. The primers designed for the 5' end of the genes contained additionally the nucleotides CACC at the very 5'- end for pENTR/D-TOPO cloning.

A 1951 bp fragment of the Arabidopsis *SOC1* (AT2G45660) promoter from -1951 bp to -1 bp was amplified using as forward primers the nucleotide sequences from -1951 to -1931 bp upstream of the start codon/translational start and as reverse primer the nucleotide sequence -1 to -21 bp. A *Sac*I restriction side was added to the 5'- end of the forward primer and a *Spe*I restriction side was added to the reverse primer at its 5'- end to allow cloning into the vector pB7FWG2 (Karimi *et al*., 2007) after removing the *35S* promoter (see section 4.10.2).

4.9. QUANTITATIVE REAL TIME PCR (QRT-PCR)

Quantitative real time PCR was performed using an Eppendorf Mastercycler realplex^2 and the Peqlab KAPA™ SYBR® Fast QPCR MasterMix Universal Kit. cDNA templates were synthesized as described in 4.5. Primers were designed using the primer designing tool/primer-BLAST at NCBI (4.8). Primer sequences are given in the appendix. The optimal annealing temperature of each primer pair was first determined by performing an annealing temperature gradient PCR. For amplificates smaller than 200 bp a two-step cycle program was used, for larger products a three-step cycle program was chosen. In both cases 40 cycles were performed followed by a melting curve to assess product purity and to analyze the specificity of the reaction. The detection of the SYBR green fluorescence was set to the annealing step in case of a two-step cycle and to the elongation step in case of a three-step cycle. qRT-PCR data were analyzed using the $\Delta\Delta C_T$ method described by Livak & Schmittgen (2001). *Glyceraldehyde-3-phosphatase dehydrogenase* (*GAP-DH*; GRMZM2G046804) was used as a reference gene for normalization.

4.10. CLONING STRATEGIES

For cloning purposes nucleic acids were generally amplified using the Peqlab KAPAHiFi™ PCR Kit with the exception of the *MADS1*-RNAi construct to generate p*UBI*:*MADS1*-RNAi where the Platinum® *Taq* DNA polymerase (Invitrogen Life Technologies) was used. The amplified nucleic acids were checked on an agarose gel and purified from the gel using the QIAquick® Gel Extraction Kit (QIAGEN). DNA concentration was determined using a Peqlab NanoDrop® ND-1000 UV/Vis-spectral photometer. Sequence accuracies of all finished constructs were verified by Sanger DNA sequencing. All primers and vector maps can be found in the appendix (8.4 and 8.5).

4.10.1. CONSTRUCTS FOR MAIZE TRANSFORMATION

Four constructs were generated for Agrobacterium-mediated transformation of maize. DNA fragments were all cloned into the binary vector pTF101. (Paz *et al.*, 2004): p*UBI*:MADS1 (pTF101.1), p*UBI*:*ZmM26* (pTF101.1), p*UBI*:amiR-*ZmM26* (pTF101.1) and p*UBI*:*MADS1*-RNAi (pTF101.1). The RNAi construct is a modified version of the *ZmEAL1*-RNAi construct described by Krohn *et al*., 2012. As sequence of the stem loop a 163 bp sequence (5'-AAGCAGAAGGAGATGAGTCTGCGCAAGAGCAACGAAGATTTGCGTGAAAAGTGCAAGAAGCAG CCGCCTGTGCCGATGGCTTCGGCGCCGCCTCGTGCGCCGGCAGTCGACAACGTGGAGGACGGTCAC CGGGAGCCGAAGGACGACGGGATGGACGTGGAGA-3') from the 3'-end of the coding sequence of *ZmMADS1* was chosen. The stem loop was amplified from cDNA and introduced into the *ZmEAL1*-RNAi construct replacing the *ZmEAL1* specific stem loop using the restriction enzymes *Bsr*GI and *Mlu*I for the sense strand and *Bam*HI and *Eco*RI for the antisense strand, resulting in p*UBI*:*MADS1*-RNAi. The artificial microRNA construct was designed based on the microRNA396 (McGonigle, 2012; Zhang *et al.*, 2009) and the stem loop region (amiR-ZmM26 5'-GGGACGTATCTCTAAAGTT-3', amiR-ZmM26* 5'-ATAACTTAAGAGATACGTTCC-3') was calculated using the WMD3 (Web MicroRNA Designer, http://weigelworld.org). The amiRNA construct was cloned based on the amiR396-IVR2 construct (M. Gahrtz, unpublished) as described at WMD3 resulting in amiR-ZmM26. The amiR-ZmM26 construct was cloned into the pCR-Blunt II-TOPO vector using the Zero Blunt® TOPO® PCR Cloning Kit (Invitrogen Life Technologies), transformed and propagated in *E. coli* (4.11), cut out and introduced into the

amiR396-IVR2 (M. Gahrtz, unpublished) vector using the restriction enzymes *Sac*I and *BspE*I. The resulting vector (amiR396-ZmM26) is an entry vector. The entry vector was transformed and propagated in *E. coli* cells (4.11). Afterwards the coding sequences of *ZmMADS1* (GRMZM2G171365) and *ZmM26* (GRMZM2G046885) and the construct *MADS1*-RNAi were amplified with primers adding a CACC motif to the 5'-end of the amplicon. The PCR products were cloned into an entry vector using the pENTR™ Directional TOPO® Cloning Kits (Invitrogen Life Technologies). These entry vectors were transformed and propagated in *E. coli* cells (4.11). Afterwards all four entry vectors were recombined with the destination vectors p*UBI*:Gate (M. Gahrtz, unpublished) using the Gateway® LR Clonase® II enzyme mix (Invitrogen Life Technologies), resulting in the intermediate vectors p*UBI*:*MADS1*, p*UBI*:*ZmM26*, p*UBI*:amiR-*ZmM26* and p*UBI*:*MADS1*-RNAi. The p*UBI*:Gate vector is based on the p*NOS*-AB-M vector (DNA Cloning Service, Hamburg). A 2 kb fragment of the *POLYUBIQUITIN* promoter (GRMZM2G409726; Christensen *et al*., 1992), including the sequence from -2000 bp to -1 bp upstream of the start codon followed by the Gateway cassette was introduced in front of the *NOS* terminator. The *UBI* promoter was amplified from pBract303 (www.bract.org). Complete constructs, composed of promoter, coding sequence or knock-down construct and terminator, were amplified with primers containing a for the nascent amplicon unique restriction site (see appendix 8.4) at the very 5'-end and introduced using these restriction enzymes into the plant expression vector pTF101.1 (Paz *et al.*, 2004). The amplicons p*UBI*:*MADS1*-RNAi and p*Ubi*:amiR-*ZmM26* were cloned in an intermediate step into the pCR-Blunt II-TOPO vector using the Zero Blunt® TOPO® PCR Cloning Kit (Invitrogen Life Technologies) to increase the yield by propagation in *E. coli*. After multiplication, the constructs and the vector pTF101.1 (Paz *et al.*, 2004) were digested by corresponding restriction enzymes (Thermo Scientific or New England Biolabs) following the respective manufacturer's protocol. T4 DNA Ligase (Thermo Scientific) was used to ligate constructs into the vector pTF101.1 (Paz *et al.*, 2004) resulting in p*UBI*:*MADS1* (pTF101.1), p*UBI*:*ZmM26* (pTF101.1), p*UBI*:amiR-*ZmM26* (pTF101.1) and p*UBI*:*MADS1*-RNAi (pTF101.1). Cloned vectors were transformed into *E. coli* cells (4.11).

4.10.2. CONSTRUCTS FOR ARABIDOPSIS TRANSFORMATION

Three constructs were made for Arabidopsis transformation: p*35S*:*MADS1*, p*35S*:*MADS1-GFP* and p*SOC1*:*MADS1-GFP*. First, the coding sequence of *ZmMADS1* (GRMZM2G171365) was amplified using a forward primer (CDS MADS1 5' pENTR) introducing a CACC motif to the very 5'-end of the amplicon and a reverse primer containing a degenerated *Bam*HI restriction site (GGATCM), which introduces either a stop codon or a functional restriction site at the end of the coding sequnce. The PCR products were cloned into an entry vector using the pENTR™ Directional TOPO® Cloning Kits (Invitrogen Life Technologies). These entry vectors were transformed into *E. coli* cells (4.11), propagated and extracted (4.13). Afterwards, the constructs were recombined either with the destination vector pB7FWG2 (Karimi et al., 2007) or a modified version of pB7FWG2, in which the *CaMV 35S* promoter was replaced with a *SOC1*-promoter fragment from position -1951 bp to -1 bp upstream of the start codon of the *SOC1* gene (AT2G45660) using *Sac*I and *Spe*I restriction enzymes. Recombination was done using the Gateway® LR Clonase® II enzyme mixture (Invitrogen Life Technologies) resulting in p*35S*:*MADS1*, p*35S*:*MADS1-GFP* and p*SOC1*:*MADS1-GFP*. Recombined expression vectors were transformed into *E. coli* cells (4.11).

4.11. HEAT SHOCK TRANSFORMATION OF *ESCHERICHIA COLI*

Transformation of *E. coli* was performed according to Inoue *et al.* (1990). *E. coli* (DH5α or DB3.1) cells were grown in 250 ml LB medium (10 g/l tryptone, 5 g/l yeast extract, 10 g/l NaCl, pH 7.0) at 18 °C to an OD_{600} of 0.6, put on ice for 10 minutes and centrifuged for 10 min at 2,500 rpm at 4 °C. The pellet was suspended in 80 ml ice cold TB buffer (10 mM Pipes, 15 mM $CaCl_2$, 250 mM KCl, adjusted to pH 6.7 before addition of $MnCl_2$ to a final concentration of 55 mM) and incubated 10 min on ice. Suspensions were centrifuged for 10 min at 2,500 rpm at 4 °C, the pellets were resuspended in 20 ml ice cold TB buffer, DMSO was added to a final concentration of 7 % and incubated 10 min on ice. Cells that were not used immediately were stored at -80 °C.

50 ng of plasmid DNA was added to 100 µl of chemically competent *E. coli* cells and incubated for 30 min on ice. After a heat shock for 1.5 min at 42 °C cells were immediately

placed on ice before addition of 0.8 ml of LB medium. After 1 h incubation at 37 °C with shaking cells were centrifuged for 1 min, supernatants discarded and cells suspended in 100 µl of LB medium. Cells were plated on solid LB medium containing the appropriate antibiotic(s) for selection of transformed cells and incubated at 37 °C overnight.

4.12. DIRECT DNA TRANSFER INTO *AGROBACTERIUM TUMEFACIENS*

A single colony of *A. tumefaciens* cells (LB4404 or C58C1) was each grown in 2 ml YEP medium (10 g/l yeast extract, 10 g/l peptone, 5 g/l NaCl, pH 7.0) at 28 °C overnight. 50 ml of YEP medium were inoculated with the 2 ml-culture and cultivated at 28 °C to an OD_{600} of 0.5. This culture was centrifuged for 5 min at 5,000 rpm and the pellet resuspended in 10 ml 0.15 M NaCl. Suspension were centrifuged for 5 min at 5,000 rpm and pellets resuspended in 1 ml of 20 mM ice cold $CaCl_2$. Glycerol was added to a final concentration of 15 % to cells that were not used immediately and they were stored at -80 °C.

1 µg of plasmid DNA was added to 200 µl of competent *A. tumefaciens* cells and incubated for 30 min on ice. Cells were frozen for 1 min in liquid nitrogen and incubated at 37 °C until they were thawed. 1 ml of YEP medium was added and cells were incubated at 28 °C for 2 to 4 h with gentle shaking. Cells were centrifuged for 1 min, supernatants discarded and cells resuspended in 100 µl YEP-medium. Cells were plated on solid YEP medium containing the appropriate antibiotic(s) for selection of transformed cells and incubated at 28 °C. Transformed colonies appeared after 2 to 3 days (Höfgen & Willmitzer, 1988).

4.13. PLASMID DNA EXTRACTION FROM *E. COLI* OR *A. TUMEFACIENS*

A single colony of bacteria was each picked and grown in 5 ml cultivation medium (*A. tumefaciens* in YEP, *E. coli* in LB) containing the appropriate antibiotic(s) for selection. 3 ml of the culture were each harvested by centrifugation for 1 min at 14,000 rpm and plasmids extracted using the High-Speed Plasmid Mini Kit following the manufacturer's guidelines (Avegene, now Geneaid). The concentration of the extracted plasmid DNA was determined using a Peqlab NanoDrop® ND-1000 UV/Vis-spectral photometer.

The plasmid DNA of the constructs p*UBI*:*MADS1* (pTF101.1), p*UBI*:*ZmM26* (pTF101.1) and p*UBI*:miRNA396-*ZmM26* (pTF101.1) used for Agrobacterium mediated transformation of maize (conducted by Iowa State University Plant Transformation Facility) was extracted from 50 ml cultures using the NucleoBond® PC100 kit (Macherey-Nagel).

4.14. AGROBACTERIUM MEDIATED TRANSFORMATION OF *ARABIDOPSIS THALIANA*

A. thaliana was transformed using the floral dip method according to Clough & Bent (1998). A single colony of *A. tumefaciens* was each grown in 5 ml YEP medium at 28 °C overnight with shaking. The next day, these cultures were used for inoculation of 500 ml YEP medium containing the appropriate antibiotics and grown overnight at 28 °C with shaking. Cultures were centrifuged at 9,000 rpm for 5 minutes and the pellets resuspended in 250 ml 3 % sucrose solution containing 100 µl Silwet® L-77. *A. thaliana* plants with mature flower buds, still closed or slightly open, were dipped into bacteria suspensions for 1 min. Afterwards plants were covered with a plastic bag to keep the humidity high for 1 to 2 days. Plastic bags were removed and plants grown for 2 weeks before they were put aside for ripening. After additional 2 weeks seeds were collected. Transformed plants were selected according to their glufosinate resistance. Plantlets at the four leaf state were sprayed 3 times with a solution containing 1 % Basta® (Bayer CropScience) and 1 % Tween 20.

4.15. AGROBACTERIUM MEDIATED TRANSFORMATION OF *ZEA MAYS*

Transformation of maize was performed with Agrobacteria according to Frame *et al.* (2002). For the generation of Agrobacterium transformation cultures a freshly grown *A. tumefaciens* LB4404 30 ml overnight culture, containing the binary plasmid for maize transformation, was each centrifuged 5 min at 5,000 rpm, pellets were washed with 15 ml 10 mM $MgSO_4$, centrifuged 5 min at 5,000 rpm and resuspended in 1x infection medium (20 ml: 10 ml 2x infection medium, 10 ml H_2O, 2 µl 1 M acetosyringone; 2x infection medium contained the following: 200 ml 10x N6 macro salts (1 l: 4.63 g $(NH_4)_2SO_4$, 28.3 g KNO_3, 4 g KH_2PO_4, 1.85 g $MgSO_4$ * 7 H_2O, $CaCl_2$ * 2 H_2O), 2 ml 1,000x N6 micro salts (100 ml: 387 mg $MnSO_4$ * 1 H_2O, 150 mg $ZnSO_4$ * 7 H_2O, 160 mg H_3BO_3, 80 mg KI), 2 ml 1,000x N6 vitamins

(100 ml: 200 mg glycine, 100 mg thiamine-HCl, 50 mg pyridoxine-HCl, 50 mg niacin), 4 ml 50 mM NaFe-EDTA, 1.4 g L-proline, 136.8 g sucrose, 72 g glucose, filled up to 1 l with H_20, pH 5.2) and adjusted to an OD_{600} of 0.5. Immature zygotic maize embryos (1.5 – 2 mm) were isolated from Hi II A ears 10 to 13 days post pollination, previously pollinated with Hi II B pollen (or *vice versa*), of greenhouse-grown plants and transferred to a 2 ml reaction tube containing 1x infection medium. Embryos were washed twice with 1x infection medium, medium was removed and 2 ml Agrobacterium suspension containing 30 µl Silwet® L-77 was added. After 5 min Agrobacterium suspension culture containing the embryos was poured out to CoCu plates (80 ml: 40 ml 2x co-cultivation medium, 30 µl $AgNO_3$ (3.4 mg/ml), 8 µl 1 M acetosyringone, 480 µl L-cysteine (50 mg/ml), 180 µl 2,4-D (1 mg/ml) 40 ml 0,6 % Gelrite®; 2x co-cultivation medium contained the following: 200 ml 10x N6 macro salts, 2 ml 1,000x N6 micro salts, 2 ml 1,000x N6 vitamins, 4 ml 50 mM NaFe-EDTA, 1.4 g L-proline, 60 g sucrose, filled up to 1 l with H_2O, pH 5.8). Liquid medium was removed using a pipette and the plates were incubated overnight at 21 °C in the dark. Afterwards, embryos were turned upside down and transferred to new CoCu plates and incubated overnight at 21 °C in the dark. Thereafter embryos were transferred to REME plates (200 ml: 100 ml 2x resting medium, 50 µl $AgNO_3$ (3.4 mg/ml), 201 µl cefotaxime (100 mg/ml), 400 µl vancomycin (50 mg/ml) 300 µl 2,4-D (1 mg/ml), 100 ml 0.6 % Gelrite®; 2x resting medium was composed as follows: like co-cultivation medium, but additionally including 1 g MES ($C_6H_{12}NO_4S$)) with the embryo-axis side facing the medium (scutellum side up) and incubated for 7 days at 28 °C in the dark. Embryos were transferred to SEME I plates (200 ml: 100 ml 2x resting medium, 50 µl $AgNO_3$ (3.4 mg/ml), 201 µl cefotaxime (100 mg/ml), 400 µl vancomycin (50 mg/ml) 15 µl glufosinate (20 mg/ml) 100 ml 0.6 % Gelrite®) and incubated for 2 weeks at 28 °C in the dark followed by 2 times 2 weeks on SEME II plates (like SEME I, but with double concentration of glufosinate) at 28 °C in the dark. Occasionally, emerging coleoptiles were dissected from embryos. Thereafter, embryos that had initiated embryogenic type II callus were transferred to Reg I plates (200 ml: 100 ml 2x regeneration medium I, 201 µl cefotaxime (100 mg/ml), 30 µl glufosinate (20 mg/ml), 100 ml 0.6 % Gelrite®; 2x regeneration medium I contained the following: 200 ml 10x MS macro salts (1 l: 16.5 g NH_4NO_3, 19 g KNO_3, 1.7 g KH_2PO_4, 3.7 g $MgSO_4$ * 7 H_2O, 4.4 g $CaCl_2$ * 2 H_2O), 2 ml 1,000x MS micro salts (100 ml: 1690 mg $MnSO_4$ * H_2O, 860 mg $ZnSO_4$ * 7 H_2O, 620 mg H_3BO_3, 83 mg KI, 25 mg Na_2MoO_4 * 2 H_2O, 2.5 mg $CoCl_2$ * 6 H_2O, 2.5 mg $CuSO_4$ *5 H_2O), 2 ml 1,000x MS

vitamins (100 ml: 200 mg glycine, 10 mg thiamine-HCl, 50 mg pyridoxine-HCl, 50 mg niacin), 4 ml 50 mM NaFe-EDTA, 4 ml myo-inositol (50 mg/ml), 120 g sucrose, filled up to 1 l H_2O, pH 5.8) and incubated for 3 weeks at 28 °C in the dark. Afterwards calli were transferred to Reg II plates (200 ml: 100 ml 2x regeneration medium II, 30 µl glufosinate (20 mg/ml), 100 ml 0.6 % Gelrite®; 2x regeneration medium II was composed as follows: like 2x regeneration medium I, but with half the sucrose concentration) and placed in light until plantlets had been regenerated.

4.16. AGROBACTERIUM INFILTRATION INTO *NICOTIANA BENTHAMIANA* LEAVES

Infiltration of *Agrobacterium tumefaciens* was performed according to Bartetzko *et al.* (2009). 5 ml freshly grown overnight culture of *A. tumefaciens* containing the binary plasmid of interest was centrifuged at 5,000 rpm for 15 minutes to harvest cells and resuspended afterwards in infiltration buffer (10 mM $MgCl_2$, 10 mM MES-KOH pH 5.7, 100 µM acetosyringone) to an OD_{600} of 1. The mixture was pressed carefully into the abaxial side of tobacco leaves using a syringe. After an incubation time of 2 days infiltrated leaves were analyzed by microscopy. *N. benthamiana* leaf epidermis cells were examined with the HC PL APO CS2 20x/0.75 Leica glycerol-immersion objective using a Leica SP8 confocal microscopy system. GFP was excited by a 488-nm argon laser and emission was detect by a hybrid detector at 500 to 550 nm. At the same time a bright field image was measured.

4.17. GENOMIC DNA EXTRACTION FROM PLANT MATERIAL

50-200 mg leaf material, from maize or Arabidopsis, was each collected in a 2 ml reaction tube, frozen in liquid nitrogen and ground using a mixer mill (Retsch® MM200) for 2 min at 30 Hz. 400 µl extraction buffer (200 mM Tris-HCl pH7.5, 250 mM NaCl, 25 mM EDTA, 0,5 % SDS) was added and mixed by vortexing for 5 sec. After centrifugation for 1 min at 14,000 rpm supernatants were transferred to a fresh reaction tube. Afterwards 300 µl of 2-propanol was added and incubated for 2 min at room temperature. The mixture was each centrifuged for 5 min at 14,000 rpm and supernatants discarded. Pellets were washed using 70 % ethanol, dried using a vacuum concentrator (Christ RVC 2-18 or Savant SVC 100H) and

resuspended in 100 µl water. 1 µl was each was used for following PCR analysis (Edwards *et al*., 1991).

4.18. ANTIBODY DESIGN AND PRODUCTION

Amino acid sequences of MADS1 and ZmM26 and their close homologs MADS56 and ZmM19 were sent to the company Pineda Antibody-Service where an epitope analysis based on Parker *et al*. (1986) was performed to detect specific peptide sequences for MADS1 and ZmM26 with a predicted strong immunogenicity. The peptide sequence NH_2-CASAPPRAPAVDNVEDGHRE-$CONH_2$ was chosen for MADS1 and NH_2-CIDKYNTHSKNLGKTEQPSL-$CONH_2$ for ZmM26 antibody production. The company Biotem synthesized these peptides, conjugated keyhole limpet hemocyanin (KLH) to the N-terminus and injected the conjugates each into three 'New Zealand' white rabbits for immunization. 63 days after initial immunization antibody production was tested via western blots (4.22) with total protein extracts from maize leaves (4.21). Immunization of two rabbits injected with the MADS1 peptide was prolonged to 105 days. Immunization of rabbits injected with ZmM26 peptide was stopped after 65 days.

4.19. EMBEDDING OF PLANT MATERIAL IN METHACRYLATE

Leaf material was cut into pieces of about 1 x 5 mm in size, transferred into 2 ml reaction tubes, filled with 2 ml fixing solution (ethanol p.a.: acetic acid = 3 : 1) and exposed to vacuum 3 to 5 times until air bubbles were forming in the solution and tissue pieces sunk to the bottom of the tubes. Fixing solution was removed carefully and 2 ml of fresh fixing solution was added to samples and incubated for 1 to 2 h at 4 °C. Samples were washed 3 times with 70 % EtOH and incubated with 70 % EtOH + 1 mM DTT at 4 °C overnight. After sample dehydration in an ethanol series of increasing ethanol concentration (20 min 85 % EtOH + 1 mM DTT, 20 min 90 % EtOH + 1 mM DTT, 20 min 95 % EtOH + 1 mM DTT, 2 x 30 min 100 % EtOH p.a. + 10 mM DTT) they were infiltrated using a methacrylate mix (75 % v/v butylmethacrylate, 25 % v/v methylmethacrylate, 10 mM DTT, 0.5 % benzoinethylether). The methacrylate mix was aerated with nitrogen before each usage to remove oxygen, which

disturbs final polymerization. Samples were incubated first for 6 h in EtOH p.a. + 10 mM DTT: methacrylat mix 2:1, then 6 h in EtOH p.a. + 10 mM DTT: methacrylat mix 1:1 and then 6 h in EtOH p.a. + 10 mM DTT: methacrylate mix 1:2 always at 4 °C. Afterwards samples were incubated 2 times for 6 h in methacrylate mixture at 4 °C and then for 24 h. Finally, samples were transferred into 200 µl reaction tubes, correctly adjusted and irradiated with UV light (310 – 360 nm) from 15 cm distance for 15 h to polymerize methacrylate.

4.20. SECTIONING OF EMBEDDED TISSUES AND IMMUNOLOCALIZATION OF MADS1 AND ZMM26

Embedded tissues (4.19) were released from surrounding PCR tubes and cut into sections of 2 to 4 µm thickness using an ultramicrotome (Reichert Om U2, Reichert Austria, now Leica) with glass knives. Sections were collected in a water filled collecting tray glued to the knife with dental wax and transferred to a drop of water on adhesive polysine® microscope slides (Thermo Scientific) which were placed on a heatable stretching table (TFP 40, Medite), set to 56 °C, until water had evaporated. Methacrylate surrounding the sections attached to the microscope slides was removed by treating the slides for 2 min with 100 vol % acetone p.a.. Then, sections were rehydrated in an ethanol series of decreasing ethanol concentration (100 %, 85 %, 70 %, 50 % and 30 % for 2 min each) followed by 3 washing steps in TBS (50 mM Tris-HCl pH 7.5, 150 mM NaCl) for 1 min each. Sections were blocked for 30 minutes in blocking solution (TBS, 1 % w/v milk powder, 0.1 % v/v Triton X-100). During blocking solutions were changed twice. Slides were briefly dried and covered with cover slips prepared with small plasticine feet at each corner as a spacer. Crude immune serum was diluted 1:20 in blocking solution, purified antibody was used undiluted, and 200 µl were pipetted carefully between sections and cover slip, which was then carefully pressed down to equally distribute the antibody solution. Sections were incubated overnight at 4 °C in a wet chamber. Cover slips were removed and sections washed 30 min in blocking solution, which was again changed twice during washing. The secondary antibody (Cy2-conjugated AffiniPure goat anti rabbit IgG, Dianova) was used in a 1:40 dilution in the same way as the primary antibody and samples were incubated in a wet chamber for 90 min at room temperature in the dark. The secondary antibody was washed off using blocking solution as described above, however, washing was performed in the dark. Finally, slides were washed 3 times for 1 min with TBS in the dark. Briefly dried samples were mounted in

water. Microscopy analyses were performed using an Axioskop FL epifluorescence microscope (Zeiss) with the Zeiss filter set no. 46 (Cy2, excitation: BP 500/20, beam splitter: FT 515, emission: BP 535/30).

4.21. PROTEIN EXTRACTION FROM MAIZE LEAVES

100-200 mg of leaf material was each collected in 2.0 ml reaction tubes, frozen in liquid nitrogen and ground using a mixer mill (Retsch® MM200) for 2 min at 30 Hz. 600 µl of extraction buffer (50 mM K_3PO_4 pH 7.2, 2 mM 2-mercaptoethanol, 1 mM EDTA, 1% v/v Protease Inhibitor Cocktail for plant cell and tissue extracts, Sigma-Aldrich) was each added to samples, vortexed and centrifuged at 9,000 rpm for 20 min at 4 °C. Supernatants containing proteins were transferred to a fresh reaction tube. Protein concentration was determined using the Bradford assay (Bradford, 1976). Samples were stored at -20 °C until they were used for SDS-PAGE and western blot (4.22).

4.22. SDS-PAGE, DOT AND WESTERN BLOT

Protein solutions (4.21) containing 20 ng proteins were supplied with 6x sample buffer (375 mM Tris-HCl pH 6.8, 12 % w/v SDS, 30 % v/v glycerol, 30 % v/v 2-mercaptoethanol, 0.6 % w/v bromophenol blue), boiled and loaded on a polyacrylamide gel (12 % separation gel: 1.6 ml H_2O, 2 ml 3x separation gel buffer (1,126 M Tris-HCl pH 8.8, 0.3 % w/v SDS), 2.4 ml 30 % acrylamide/0.8 % bisacrylamide mix, 3 µl TEMED, 60 µl 10 % ammonium persulfate; stacking gel: 2.25 ml stacking gel buffer (0.139 M Tris-HCl pH 6.8, 0.11 % w/v SDS), 0.4 ml 30 % acrylamide/ 0.8 % bisacrylamide mix, 2 µl TEMED, 16 µl 10 % APS) in running buffer (25 mM Tris, 0.1 % w/v SDS, 192 mM glycine). SDS-PAGE was performed at 200 V until the dye bromophenol blue reached the lower edge of the gel. Proteins were transferred to nitrocellulose membranes (Amersham™ Hybond ECL, GE Healthcare Life Science) along an electrical field (150 mA, 30 min) using the western blot technique (Towbin *et al.* 1979). The western blot was performed as a tank blot in blotting buffer (2 l 5x western transfer buffer: 24.2 g Tris, 112.7 g glycine, 20 ml 10 % SDS, fill up to 2 l with H_2O; 1 l 1x western transfer buffer: 200 ml 5x western transfer buffer, 200 ml

methanol, 600 ml H_2O). After blotting membranes were stained with Ponceau S solution (Sigma Life Science) to check for successful protein transfer. After destaining with water, membranes were blocked in blocking solution (50 mM Tris-HCl pH 7.5, 150 mM NaCl, 5 % w/v milk powder, 0.1 % v/v Tween 20) for 1 h at room temperature. Membranes were incubated with the antiserum against MADS1 or ZmM26 (1:200 diluted in blocking solution) overnight at 4 °C. Afterwards membranes were washed 3 times in blocking solution for 15 min at room temperature. The secondary antibody (goat anti-Rabbit IgG (whole molecule)-peroxidase, Sigma Aldrich®) was diluted 1:5,000 in blocking solution, incubated with membranes for 1 h at room temperature and afterwards washed off as described above. Membranes were shortly washed in TBS, then a luminal-based solution was applied to detect horseradish peroxidase (HRP-Juice, P.J.K.) and chemiluminescence was detected by exposing a medical x-ray film (Super RX, Fujifilm Corporation). Western blots were scanned and quantified using the software ImageJ Version 1.47 (http://imagej.nih.gov/ij/). Intensities were normalized to the intensity of the RuBisCO band.

4.23. PURIFICATION OF IMMUNE SERA ("POOR MAN'S MONOCLONALS")

About 1 µg of ZmMADS1 and ZmM26 peptide conjugated to KLH were solubilized in 1 ml H_2O each. In a first test these solutions were used to perform dot blots with decreasing concentration of the peptide to determine the peptide concentration, which gives the optimal signal. Crude immune sera against peptides were diluted 1:200. In a second test, dot blots, with the optimal peptide concentration according to the first test, were performed against decreasing immune serum concentration, to determine the immune serum concentration, which is still good enough to give a strong detection signal. For the ZmMADS1 immune serum this was a dilution of 1:600 and for the ZmM26 immune serum it was 1:200. Afterwards peptide amount was calculated from the result of the first test, which is needed to scale the blot up from a dot (0.2 cm^2) towards a membrane area of 54 cm^2 and spotted directly onto a nitrocellulose membrane (Amersham™ Hybond ECL, GE Healthcare Life Science) of that size. After this membrane was dried, it was blocked in 5 % milk powder in TBS for 30 min. Immune sera were diluted as determined in the second test in TBS and incubated with plain rotary motions overnight. The membrane was washed twice shortly with TBS-T (TBS containing 0.5 % Tween 20) and 5 min again with TBS-T followed by 5 min

with TBS. Antibodies were relieved from the membrane by incubation with 5 ml 100 mM glycine pH 2.8 and 1 mM NaN_3 for 1 min and immediately neutralized by adding 200 µl 1 M NaOH and stabilized by adding BSA to a final concentration of 1 %.

5. RESULTS

5.1. IDENTIFICATION OF THE DATE OF FLORAL TRANSITION AND GROWTH BEHAVIOR OF SELECTED MAIZE INBRED LINES

To gain universal knowledge of the regulatory mechanism controlling flowering time in maize, the aim of this work was to perform comparative transcriptome analyses of maize leaves before and during the floral transition of the shoot apical meristem (SAM). The goal of this approach was to identify leaf-derived genes, which play a role in the regulation of floral transition, either by activation or by repression. To achieve this it was important at the beginning of this work to identify closely related maize inbred lines, which differ in the time point of transition of the SAM from vegetative to reproductive growth. These lines were considered to be the ideal material for transcriptome analysis. In total, 30 maize lines in 15 pairs were analyzed using stereomicroscopy regarding the developmental stage in which the floral transition of the SAM occurred. Differences of 0 to 11 days within genetically related pairs were observed (*Table 2*). The largest differences were identified for the pair 4F-240 BX 16 / 4F-350 CN 2 and the pair B77 / E2558W (*Table 2*). 4F-240 BX16 undergoes the transition of the SAM 24 days after sowing (DAS) at the developmental stage V5 according to the "leaf collar method" recapped by Abendroth *et al*. (2011), whereas in 4F-350 CN 2 this transition occurs 35 DAS at developmental stage V8. In the second pair the difference of the transition was 2 days shorter with

Table 2. **Identification of the point of transition of the SAM from vegetative to reproductive growth.** Time points in days after sowing (DAS) of the transition of the SAM from vegetative to reproductive growth in all maize lines analyzed for this trait and the developmental stage of the plants (according to Abendroth *et al*., 2011) at that time are shown. Inbred lines are ordered as genetically closely related pairs except for the pair A188 and B73 (Rgbg). Lines in grey boxes were selected for transcriptome analysis.

Maize genotype	Develop-mental stage	Transition of the SAM (DAS)
B73	V5/V6	26
R229	V5/V6	25
IDS69	V6	28
SA24	V7	29
PA762	V4/V5	20
OH43	V4/V5	20
Mo1W	V5/V6	26
Wf9	V5/V6	23
VA102	V5	26
VA26	V4	20
A6	V10	40
Tzi10	V11	40
4F-240 BX 16	V5	24
4F-350 CN 2	V8	35
A188	V5	19
B73 (Rgbg)	V6	26
NC304	V9	35
NC350	V7	31
Tzi16	V10	36
Tzi25	V8	33
Ki11	V7	33
Ki3	V10	36
NC320	V7	29
NC332	V5/V6	29
PA875	V8	29
Mo1W	V5/V6	26
EP1	V3/V4	18
F7	V3/V4	18
B77	V6	24
E2558W	V8	33

B77 'switching' at 24 DAS at stage V6 and E2558W 'switching' at 33 DAS at stage V8.

These results were produced under long day conditions (LD) in the greenhouse. Later short day (SD) experiments were additionally performed in a growth chamber. To test whether the growth behavior of plants of the four above selected maize lines was comparable under LD conditions in both greenhouse and growth chamber, respectively, all four lines were grown in the greenhouse under LD conditions and in the growth chamber under LD and SD conditions. Total leaf number and total plant size were analyzed (*Figure 7*). Line 4F-240 BX 16 produced on average 18.7 (± 1.1) leaves in the greenhouse and

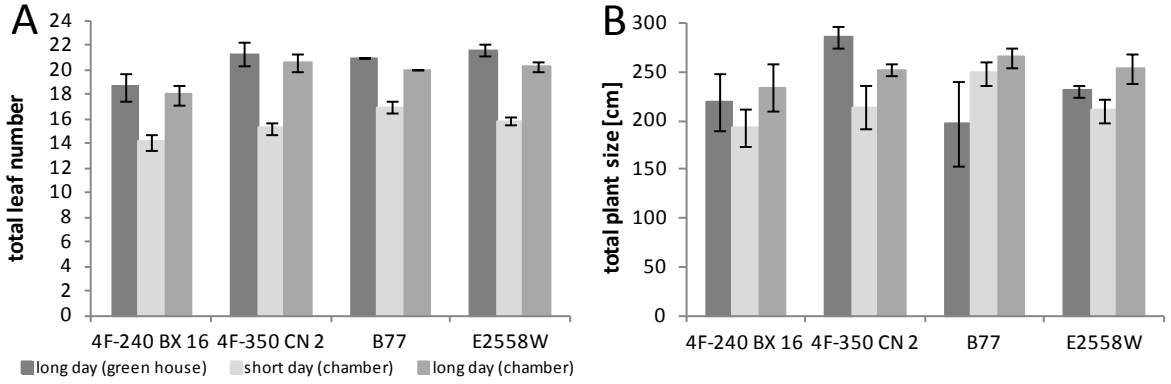

Figure 7. **Growth behavior of four selected maize inbred lines in the greenhouse and in the growth chamber.** (A) Total leaf number and (B) plant size in cm of plants of the genotypes 4F-240 BX 16, 4F-350 CN 2, B77 and E2558W grown in the greenhouse under LD conditions (dark grey) and grown in the growth camber both under SD (light grey) and LD conditions (medium grey) are shown. Mean values ± standard deviation of n=7 (growth chamber) or n=6 (greenhouse; except B77 n=2 and E2558W n=3) individual plants per genotype are shown.

18.0 (± 0.8) leaves in the growth chamber. Total leaf number of 4F-350 CN 2 was 21.3 (± 0.9) in the greenhouse and 20.6 (± 0.7) in the growth chamber (*Figure 7 A*). For the other two lines total leaf number was also nearly the same both in the greenhouse and growth chamber. B77 generated on average 21.0 (± 0.0) and E2558W 21.7 (± 0.5) leaves in the greenhouse and 20.0 (± 0.0) and 20.3 (± 0.5) leaves in the growth chamber, respectively (*Figure 7 A*). Leaf number of SD grown plants differed significantly ($p \leq 0.02$, student's t-test) from in chamber grown LD plants. 4F-240 BX 16 plants contained on average 14.1 (± 0.6) leaves, 4F-350 CN 2 plants 15.3 (± 0.5) leaves, B77 plants 17.0 (± 0.5) leaves and E2558W plants 15.9 (± 0.3) leaves (*Figure 7 A*).

To compare size plants were measured from the soil towards the tip of the tassel. In three out of four cases plant height was comparable between the greenhouse and growth chamber. 4F-240 BX 16 plants were 219.0 (± 28.9) cm high in the greenhouse and 234.1 (± 24.0) cm in the chamber, 4F-350 CN 2 plants measured 285.8 (± 10.6) cm and

252.4 (± 5.6) cm and plants of the line E2558W 230.7 (± 6.1) cm and 253.4 (± 15.4) cm, respectively (*Figure 7 B*). Only plants of line B77 showed a difference of more than half a meter, 197.0 ± 44.0 cm and 265.1 ± 10.3 cm (*Figure 7 B*), but in this case only two plants survived the growth phase in the greenhouse. SD grown plants differed significantly in plant size from chamber grown LD plants ($p \leq 0.02$, student's t-test). 4F-240 BX 16 plants were 193.4 (± 18.4) cm high, 4F-350 CN 2 plants were 214.1 (± 22.9) cm high, B77 plants were 248.9 (± 11.5) cm high and E2558W plants were 210.4 (± 12.5) cm high (*Figure 7 B*).

To analyze the time point of floral transition in SD and LD condition, plants were grown in the greenhouse in three (B77, E2558W) or four (4F-240 BX16, 4F-350 CN2) successive independent experiments and in the growth chamber once in LD and once in SD. Floral transition of the SAM was overall comparable in the greenhouse and growth camber under LD conditions calculated as time point in days after sowing or at time point during development of the plant (*Table 3*). However, transition of the SAM took place in

Table 3. **Comparison of the time point of transition of the SAM in SD and LD condition.** The time of floral transition and the developmental stage of 4F-240 BX 16, 4F-350 CN 2, B77 and E2558W grown in the greenhouse under LD conditions and in the growth chamber in SD and LD are shown. The greenhouse data are mean values ± standard deviation of 4 (4F-240 BX 16, 4F-350 CN 2) and 3 (B77, E2558W) independently grown populations, grown over a period of two years. Time is given in days after sowing (DAS), developmental stage (dev. stage) is indicated according to Abendroth *et al*., 2011.

	long day (greenhouse)		short day (chamber)		long day (chamber)	
	time (DAS)	dev. stage	time (DAS)	dev. stage	time (DAS)	dev. stage
4F-240 BX 16	24.5 (± 1.29)	V5	24	V4	28	V4/V5
4F-350 CN 2	34.5 (± 1.29)	V7/V8	31	V5	35	V8
B77	24.7 (± 0.58)	V5	26	V4	26	V5
E2558W	35.0 (± 1.73)	V8	31	V5	33	V6

4F-240 BX 16 plants about 4 days later in the growth chamber than in the greenhouse, but the developmental stage of the plants was nearly the same with transition from V4 to V5 compared to V5 in the greenhouse. Plants were grown in the growth chamber only once (*Table 3*). In plants of the line E2558W the developmental stage was differing between greenhouse (V8) and growth chamber (V6) but the time period until transition was nearly identical with 35.0 (± 1.73) DAS in the greenhouse and 33 DAS in the growth chamber (*Table 3*). Interestingly, the time period between sowing and transition of the SAM was the same for lines with early transition (4F-240 BX 16 and B77) in LD and SD condition, but for the lines with late transition (4F-350 CN 2 and E2558W) the period was slightly shorter in SD

compared with LD. The developmental stage at which the plants reached transition of the SAM was for all lines earlier in SD than in LD condition, except for the line 4F-240 BX 16, where this was less pronounced with V4 in SD and transition from V4 to V5 in LD in the chamber, but with V5 in LD in the greenhouse (*Table 3*). These results of the earlier developmental stage at the transition of the SAM in SD compared with LD are in agreement with the findings that plants grown in SD contain fewer leaves compared to plants grown in LD (*Figure 7*). Again, it has to be mentioned that plants were grown in the growth chamber only once in LD and SD during this work. To obtain a clearer result this has to be repeated more often.

Taken together, the pairs 4F-240 BX 16 / 4F-350 CN2 and B77 / E2558W were selected for transcriptome analyses. The growth conditions in the greenhouse and the growth chamber were comparable and all four lines showed a day length sensitive growth behavior.

5.2. TRANSCRIPTOME ANALYSIS OF LEAVES DURING TRANSITION OF THE SAM FROM VEGETATIVE TO REPRODUCTIVE GROWTH

After maize lines 4F-240 BX 16 / 4F-350 CN 2 and B77 / E2558W had been identified as suitable pairs for transcriptome analysis, all four lines were grown in the greenhouse under LD conditions to take leaf samples for RNA extraction. To identify putative flowering time regulatory genes in leaves, samples from the uppermost fully expanded leaf were taken at three different developmental stages. These time points were (i) when plants of both lines per pair had reached V3 and before any line had 'switched' its SAM, (ii) one day before the transition of the 'early switching' line (4F-240 BX 16 or B77) and (iii) one day before the transition of the 'late switching' line (4F-350 CN 2 or E2558W). The developmental stages of the SAMs during the sampling is shown exemplarily for the pair 4F-240 BX 16 / 4F-350 CN 2 in *Figure 8 A*. Sampling was performed in the same way for the maize pair B77 / E2558W.

Putative flowering time regulatory genes with activating functions were expected to display an expression profile that was low in both lines before the switch and increased to a maximum in the early switching line at the 'early switch' time point, while it would further increase for the late switching line, and be still at the maximum or decreased at the 'late switch' time point (*Figure 8 B*). *Vice versa*, a repressor of floral transition was expected to

show a high transcript level at the beginning and a lower expression after the transition of the SAM (*Figure 8 C*). These profiles were expected, because the putative candidate(s) would need to reach a certain level to induce or to stop repressing the development of floral organs.

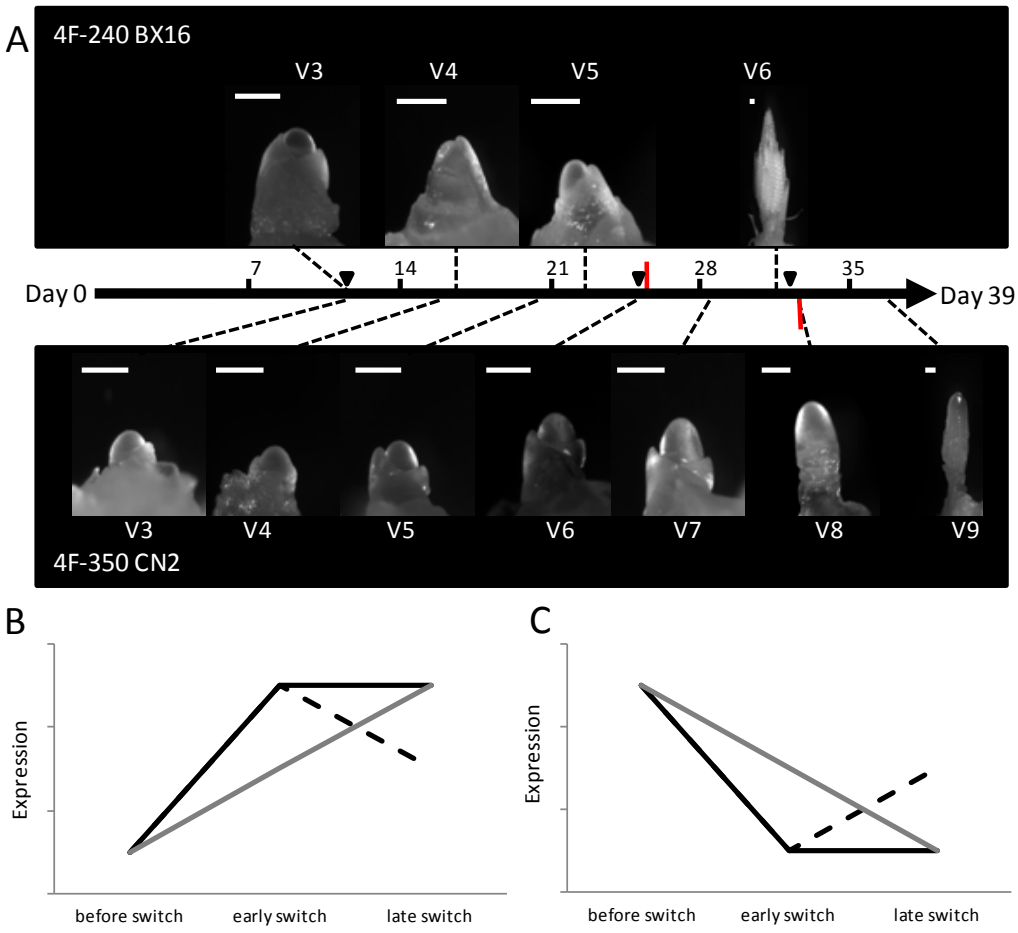

Figure 8. **Developmental stage of the SAM and expected transcript profiles of putative flowering time regulatory genes at sampling time points for transcriptome analysis.** (A) Microscopy images of the SAM of the genotypes 4F-240 BX 16 (upper lane) and 4F-350 CN 2 (lower lane) at indicated developmental stages over a time period of 39 days (black horizontal arrow) after sowing. The transition of the SAM is marked by a vertical red bar and the time points of leaf material sampling each of the upper most fully expanded leaf are indicated by black arrowheads. Scale bars = 200 µm. (B) Expression profiles for a putative flowering time activator and (C) a putative flowering time repressor. The black line represents the expected expression in genotypes with an early transition of the SAM, and the grey line for genotypes with a late transition. Dashed lines indicate the possibility that expression of a putative activator/repressor returns to its initial level after the switch in lines of showing early transition.

It was further expected that the transcriptome of the lines of each pair would be very similar. The working hypothesis was that putative flowering time regulatory genes could be identified by subtracting the transcriptome of the 'late switcher' from the transcriptome of the 'early switcher' at the 'early switch' time point. By focusing on these differentially

expressed genes it was intended to identify exclusively putative flowering time regulatory genes and to mask all other genes that are not related to the floral transition. In this assumption the transcriptome data would be nearly identical at the time points 'before switch' and 'late switch'.

As quality control of the transcriptome data a principle component analysis (PCA) was made first. The PCA showed that the transcriptome data of the three time points of each genotype are grouping together and that the genotypes are clearly separated (*Figure 9*).

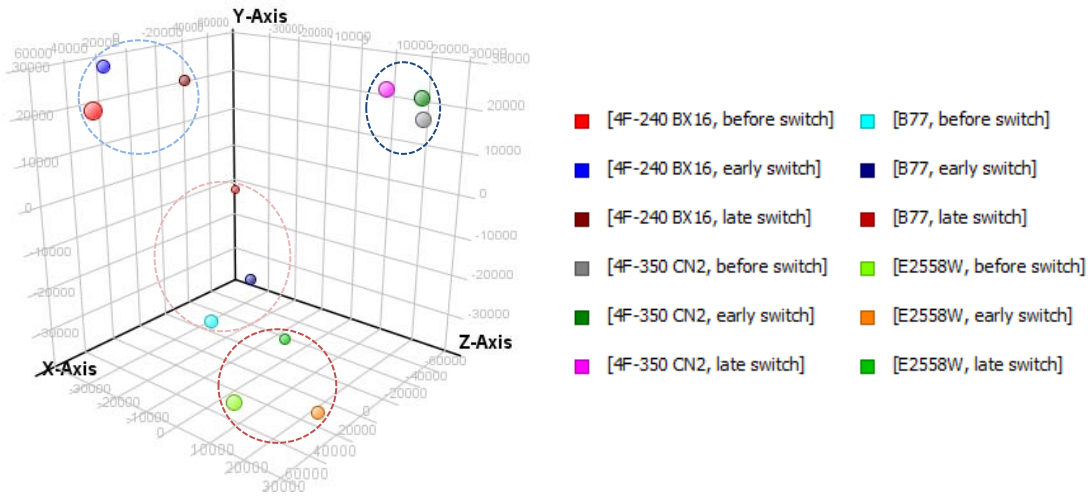

Figure 9. **Principal component analysis (PCA) of the transcriptome samples analyzed to identify flowering time regulatory genes.** PCA depicting the mean of transcriptome triplicates per time point and line. X-axis shows component 1 (27.72 %), Y-axis component 2 (18.85 %) and Z-axis component 3 (17.2 %). Data sets of 4F-350 CN 2 are encircled in dark blue, 4F-240 BX 16 in light blue, E2558W in dark red and B77 in light red.

Moreover, it turned out that it was not possible to analyze the transcriptome data like described above as the genotype-dependent effects were more significant compared with the developmental stage. The lines 4F- 240 BX16 and 4F-350 CN 2 showed 11,535 genes differentially expressed (Fold change (FC) ≥ 2, p-value ≤ 0.05) between both lines at the time point 'before switch'. At the early switch there were 9,911 genes differentially expressed and at the late switching state there were only 1,641 differentially expressed genes. For the other pair B77 / E2558W however, it was the other way around. These lines showed 4,216 differentially expressed genes 'before switch' time point and the transcriptome was more distinguished between the lines later during development. At the early switch 5,090 genes were differentially expressed and finally 8,311 genes at the 'late switch' point.

Since the analysis was not accomplishable as initially planned, the transcriptome data of each line was screened for genes that changed their expression level between the time point 'before switch' and the time point of the transition of the SAM of the line ('early switch' for 4F-240 BX 16 and B77, 'late switch' for 4F-350 CN 2 and E2558W). This resulted in four data sets with 4,417 differentially expressed genes (FC ≥ 2, p-value ≤ 0.05) in total (*Figure 10*).

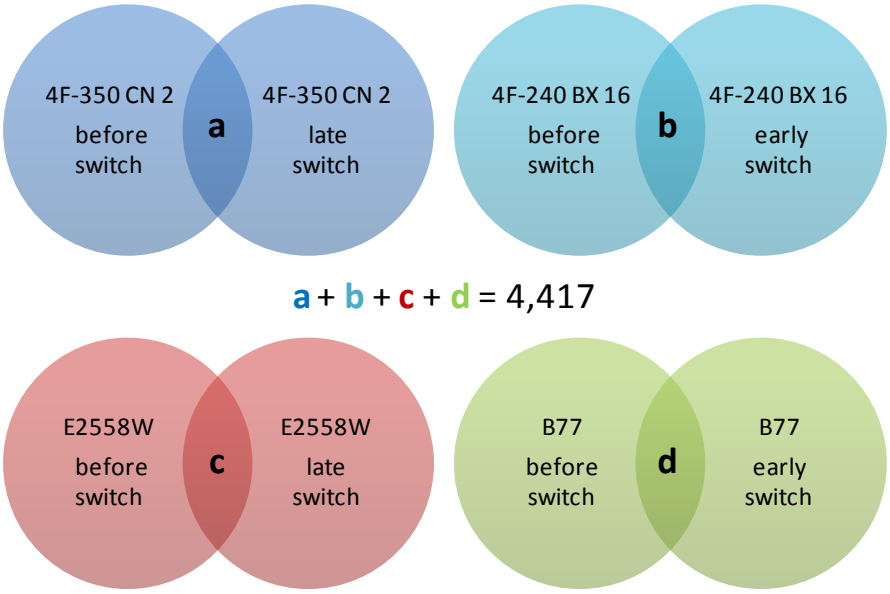

Figure 10. **Total number of putative flowering time regulatory genes in four maize lines.** Schematic depiction of the transcriptome data sets is indicated 'before switch' and the respective switching time point of the lines 4F-350 CN 2 (dark blue), 4F-240 BX 16 (light blue), E2558W (red) and B77 (green). The overlap (a – d) and the total number of putative flowering time regulatory genes (sum of a, b, c, d) is also shown.

Because the number of 4,417 genes was too high to characterize all genes during this work, it was necessary to use a more stringent filter method. Therefore, I made use of the closely related pairs and the data sets were therefore compared between the lines in these pairs. This reduced the number of putative flowering time regulatory genes to 29 (overlap of a and b in *Figure 10*) in the pair 4F-240 BX 16 / 4F-350 CN 2 (*Table 4 A*) and 25 (overlap of c and d in *Figure 10*) in the pair B77 / E2558W (*Table 4 B*). To identify genes that are differentially expressed over time in both pairs these two data sets were compared. Finally, two genes were identified with a putative function in flowering time regulation in all lines (*Figure 11 A, Table 5*).

Table 4. **Candidate flowering time regulatory genes in leaves (A) of the maize lines 4F-240 BX 16 and 4F-350 CN 2 and (B) of the lines B77 and E2558W, respectively.** The table shows the OPTIMAS-ID, the identifier of the oligo on the microarray chip, transcript ID (MaizeSequence Version 4a.53) of the coding sequence from which the oligo was derived, and for both lines fold change (FC), p-value, whether expression was up or down regulated, and the annotation. Values are calculated between transcriptome data obtained from leaf samples at V3 and one day before transition of the SAM from vegetative to flowering meristem. Oligo sequences can be found in the appendix (8.1).

A

OPTIMAS-ID	4a.53 Coding Sequence	4F 240 BX 16			4F-350 CN 2			Annotation
		FC	p-value	Regulation	FC	p-value	Regulation	
OptiV1N35942	GRMZM2G125853_T06	45,72	0,02	down	72,40	0,04	down	POUF
OptiV1C09461	GRMZM2G053977_T01	40,18	0,02	up	13,11	0,05	up	short-chain dehydrogenase/reductase (SDR) family protein
OptiV1C01178	GRMZM2G152801_T02	26,68	0,02	down	11,75	0,04	down	FLS (FLAVONOL SYNTHASE)
OptiV1S17892	GRMZM2G060866_T01	24,65	0,02	down	30,02	0,04	down	Anther-specific proline-rich protein
OptiV1S18863	GRMZM2G700665_T02	19,07	0,02	down	4,16	0,03	down	RAP2.7
OptiV1S26761	GRMZM2G152801_T01	16,36	0,03	down	17,64	0,04	down	FLS (FLAVONOL SYNTHASE)
OptiV1C11740	GRMZM2G036203_T01	13,25	0,05	up	4,29	0,04	up	cysteine proteinase, putative
OptiV1C06259	GRMZM2G113480_T01	10,27	0,03	down	6,50	0,04	down	POUF
OptiV1S29412	GRMZM2G088964_T01	9,02	0,04	up	4,05	0,05	up	ATKT1 (POTASSIUM TRANSPORTER 1)
OptiV1C17237	GRMZM2G171365_T01	8,73	0,02	up	5,78	0,02	up	MADS1
OptiV1S20394	GRMZM2G363229_T01	7,87	0,02	down	3,07	0,04	down	MATE efflux family protein
OptiV1C05995	GRMZM2G070034_T01	7,77	0,02	up	43,86	0,01	up	AtAGL20 (AGAMOUS-LIKE 20)
OptiV1S21916	GRMZM2G046885_T02	7,59	0,02	up	3,24	0,04	up	M26
OptiV1C10423	GRMZM2G029912_T02	6,81	0,03	up	11,23	0,04	up	CER3 (ECERIFERUM 3)
OptiV1S18200	GRMZM2G055446_T01	5,99	0,02	up	12,07	0,01	up	UDP-glycosyltransferase/ sinapate 1-glucosyltransferase/ transferase
OptiV1S30318	GRMZM2G131266_T01	5,93	0,02	up	86,15	0,02	up	ovule development protein, putative
OptiV1C13062	GRMZM2G322047_T01	5,92	0,03	down	11,01	0,02	down	exostosin family protein
OptiV1S28227	AC197143.3_FGT007	4,53	0,02	down	4,68	0,05	down	ATPRB1
OptiV1S24670	GRMZM2G073969_T01	3,93	0,02	up	15,62	0,03	up	POUF
OptiV1C01853	GRMZM2G055178_T01	3,66	0,02	down	265,51	0,02	up	PTAC5 (PLASTID TRANSCRIPTIONALLY ACTIVE5)
OptiV1C08761	GRMZM2G004748_T01	3,44	0,02	up	5,72	0,00	up	PGP2 (P-GLYCOPROTEIN 2)
OptiV1N40004	AC213612.3_FGT001	3,20	0,02	up	17,85	0,05	up	Glycine-rich cell wall structural protein
OptiV1S24539	GRMZM2G034471_T01	3,19	0,03	up	4,28	0,03	up	Cytochrome P450 CYP2 subfamily protein
OptiV1N37090		2,58	0,02	up	27,57	0,02	up	
OptiV1S21266	GRMZM2G006806_T01	2,56	0,02	down	2,35	0,04	down	Ssu72-like family protein
OptiV1S18426	GRMZM2G108153_T01	2,55	0,03	down	74,54	0,04	up	peroxidase 12 (PER12) (P12) (PRXR6)
OptiV1C01437	GRMZM2G459841_T01	2,48	0,02	up	2,38	0,05	down	POUF
OptiV1C03164	GRMZM2G127581_T01	2,41	0,03	up	2,48	0,04	up	Tubulin-specific chaperone B
OptiV1S26447	GRMZM2G019993_T01	2,03	0,02	up	6,94	0,03	up	ZCN21

B

OPTIMAS-ID	4a.53 Coding Sequence	B77			E2558W			Annotation
		FC	p-value	Regulation	FC	p-value	Regulation	
OptiV1S24287	GRMZM2G159105_T01	222,58	0,03	down	56,78	0,02	down	protein kinase family protein
OptiV1C11764	GRMZM2G109627_T01	87,32	0,04	up	6,34	0,02	up	PPR repeat containing protein
OptiV1C02818	GRMZM2G168898_T01	35,29	0,03	down	8,82	0,04	down	HB2 (Hemoglobin 2)
OptiV1N40037	GRMZM2G006210_T01	11,87	0,04	down	32,18	0,02	down	
OptiV1S32916	GRMZM2G061751_T01	10,30	0,05	down	16,07	0,04	down	UNE1 (Unfertilized Embryo Sac 1)
OptiV1S26715	GRMZM2G052461_T01	8,95	0,03	up	3,14	0,02	up	LHT2 (LYSINE HISTIDINE TRANSPORTER 2)
OptiV1C17237	GRMZM2G171365_T01	7,07	0,05	up	6,63	0,04	up	MADS1
OptiV1S31605	GRMZM2G052034_T02	6,85	0,05	down	8,50	0,04	down	zinc finger (C3HC4-type RING finger) family protein
OptiV1S21916	GRMZM2G046885_T02	6,29	0,03	up	7,01	0,03	up	M26
OptiV1S19217	GRMZM2G009475_T01	6,20	0,04	down	4,71	0,02	down	POUF
OptiV1N35188	AC233893.1_FGT001	5,66	0,05	down	4,82	0,03	down	Homocysteine S-methyltransferase
OptiV1C06771	GRMZM2G179264_T01	5,60	0,03	up	43,90	0,04	up	ZCN8
OptiV1S20894	GRMZM2G134502_T01	5,22	0,03	down	5,02	0,03	down	Fiber annexin
OptiV1S29802	GRMZM2G066291_T01	4,97	0,04	up	3,84	0,02	up	POUF
OptiV1S33653	GRMZM2G370777_T04	4,02	0,03	up	3,72	0,04	up	M19
OptiV1C05996	GRMZM2G370777_T05	3,87	0,04	up	4,24	0,04	up	M19
OptiV1C09078	GRMZM2G046885_T01	3,68	0,03	up	3,59	0,05	up	M26
OptiV1C04175	GRMZM2G128466_T02	3,30	0,05	up	3,85	0,03	up	NQR (NADPH:QUINONE OXIDOREDUCTASE)
OptiV1S18918	GRMZM2G107839_T01	2,72	0,04	down	6,54	0,04	down	putative LTP
OptiV1C03183	GRMZM2G469898_T01	2,59	0,04	down	4,99	0,03	down	GDSL-motif lipase/hydrolase family protein
OptiV1S29722	GRMZM2G101634_T01	2,39	0,03	down	5,30	0,02	down	Serine/threonine protein phosphatase 2A, regulatory subunit
OptiV1C10635	AC233935.1_FGT005	2,37	0,04	down	5,41	0,04	down	OBP3 (OBF-BINDING PROTEIN 3)
OptiV1S19635	GRMZM2G055447_T01	2,32	0,03	up	3,47	0,04	up	POUF
OptiV1C00462	GRMZM2G174942_T02	2,21	0,03	up	2,70	0,04	up	eukaryotic translation initiation factor SUI1, putative
OptiV1C01938	GRMZM2G443715_T01	2,06	0,04	up	3,00	0,04	down	mannan synthase

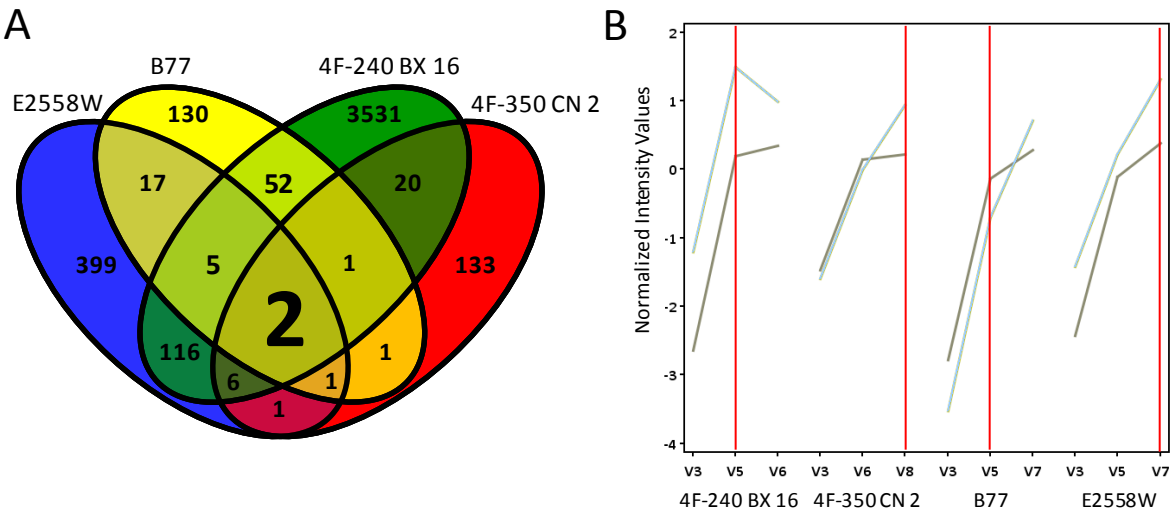

Figure 11. **Putative flowering time regulatory genes.** (A) Venn-Diagram showing the number of genes differentially expressed shortly before transition of the SAM at developmental stage V3 in the upper most fully expanded leaf in the lines 4F-240 BX 16 (green), 4F-350 CN 2 (red), B77 (yellow) and E2558W (blue). Two genes are differentially expressed in all four lines. (B) Expression profiles of the two candidate genes *ZmMADS1* (light blue) and *ZmM26* (grey). Red lines are indicating the time of the SAM transition.

Both candidates were identified as MADS-box transcription factors. The first candidate is *ZmMADS1* also known as *ZmM5*. Fold changes of *ZmMADS1* from 'before switch' to the time point of the actual switch ranged from 5.8-fold up-regulation in 4F-350 CN 2 to 8.7 fold up-regulation in 4F-240 BX 16 (*Figure 11 B, Table 5*). Therefore this gene is a candidate flowering inductive gene. The second putative flowering time regulatory gene is *ZmM26* or *ZmMADS22*. *ZmM26* is also up regulated from 3.2 fold in 4F-350 CN 2 to 7.6 fold in 4F-240 BX 16 (*Figure 11 B, Table 5*) and represents therefore also a putative flowering inductive gene. Taking the transcriptome data of the third, so far not included time point, for 4F-240 BX 16 and B77 'late switch' and for 4F-350 CN 2 and E2558W 'early switch', into account, the expression profiles of these two candidates resemble the expected expression profile (*Figure 8 B, Figure 11 B*).

Table 5. **Expression of candidate flowering time regulatory genes.** The fold changes (FC), p-values and the regulation of *ZmMADS1* and *ZmM26* expression in leaves of the maize lines 4F-240 BX 16, 4F-350 CN 2, B77 and E2558W between V3 and one day before switching of the SAM.

	ZmMADS1			***ZmM26***		
	FC	p-value	Regulation	FC	p-value	Regulation
4F-240 BX 16	8.7	0.019	up	7.6	0.023	up
4F-350 CN 2	5.8	0.016	up	3.2	0.045	up
B77	7.1	0.049	up	6.3	0.029	up
E2558W	6.6	0.040	up	7.0	0.026	up

5.3. *ZmMADS1* AND *ZmM26* HOMOLOGOUS GENES

To gain first ideas, which roles the candidate genes *ZmMADS1* and *ZmM26* could play, homology analyses were performed. For this purpose, BLASTp analyses were performed using protein sequence data bases of the crop plants rice, barley and wheat as well as of the dicotyledonous model plant *Arabidopsis thaliana*, the best studied species in terms of flowering regulation. Additionally, the genome of maize was screened for homologous genes. The identifier of the proteins can be found in the appendix (8.2).

Homology analyses for *ZmMADS1* resulted in the identification of two homologs in maize itself; *ZmMADS56* and a putative uncharacterized gene with the identifier *GRMZM2G070034* at MaizeSequence (http://www.maizesequence.org/) (*Figure 12*). Two

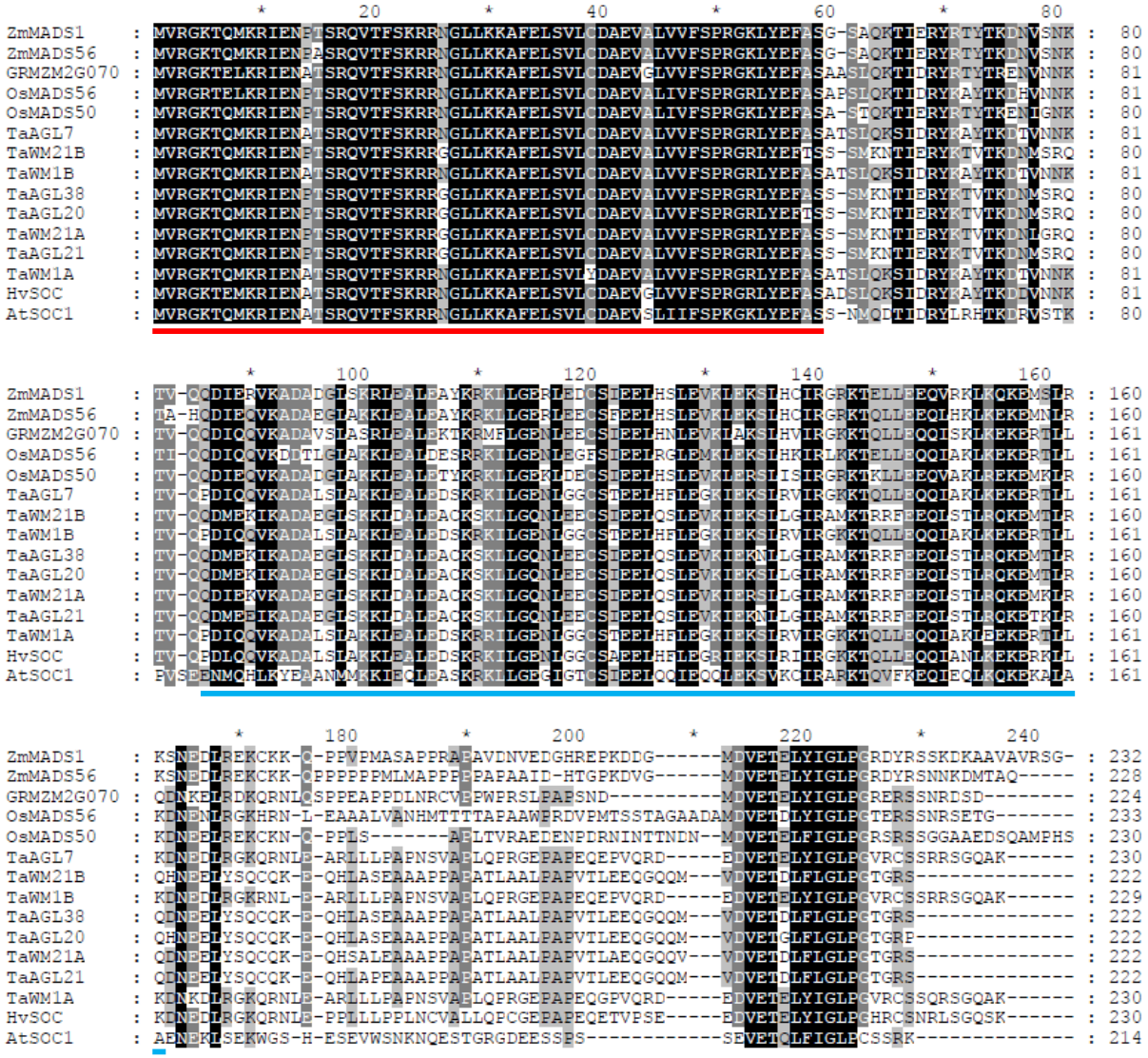

Figure 12. **Multiple protein sequence alignment of ZmMADS1 and homologous proteins from maize, rice, wheat, barley and Arabidopsis**. Conserved regions between the sequences are shown with a black background. The red bar below the sequences marks the region of the MADS-domain of ZmMADS1 and the blue bar indicates the K-domain.

genes from rice, *OsMADS50* and *OsMADS56*, eight genes from wheat including *TaAGL21 (TaAGAMOUS-like 21),* and *AtSOC1* (*AtSUPPRESSOR OF OVEREXPRESSION OF CO1*) from *Arabidopsis thaliana* were identified as homologous genes to *ZmMADS1* in other species (*Figure 12*). In barley, only one predicted gene was identified. The MADS-domain (*Figure 12*, red bar), which is usually N-terminally located and consists of 58 amino acids necessary for DNA binding of the MADS-box proteins (reviewed by Gramzow & Theissen, 2010), is highly conserved with a sequence identity of 78 % between all proteins. The K-domain (*Figure 12*, blue bar), which is usually 70 amino acids long and located in the middle of the protein between the I-domain and the C-terminal domain and which is needed for protein-protein interactions (reviewed by Gramzow & Theissen, 2010), is also conserved with a sequence identity of 23 %.

There are three homologous genes to *ZmM26* in maize, *ZmM19*, *ZmM21* and *ZmMADS47* (*Figure 13*). In rice there are also three putative homologs, *OsMADS22*, *OsMADS47* and *OsMADS55* (*Figure 13*). The barley genome encodes three *ZmM26* homologs, *HvBM1* (*HvBarley MADS1*) with two splice variants, *HvBM10* (*HvBarley MADS10*) and *HvVRT-2* (*HvVegetative to Reproductive Transition-2*). Eleven genes were identified in wheat, amongst them *TaVRT-2* and one gene in *Arabidopsis thaliana, AtSVP (AtShort Vegetative Phase)* (*Figure 13*). Additionally, *AtAGL24* was included to this analysis due to its close homology to *AtSVP* and its function in flowering time regulation (*Figure 13*). The MADS domain (*Figure 13*, red bar) of all genes showed sequence identity of 59 %. Remarkably, OsMADS47 seems to have an extended N-terminus. The K-domain (*Figure 13*, blue bar) shows a similarity of 31%.

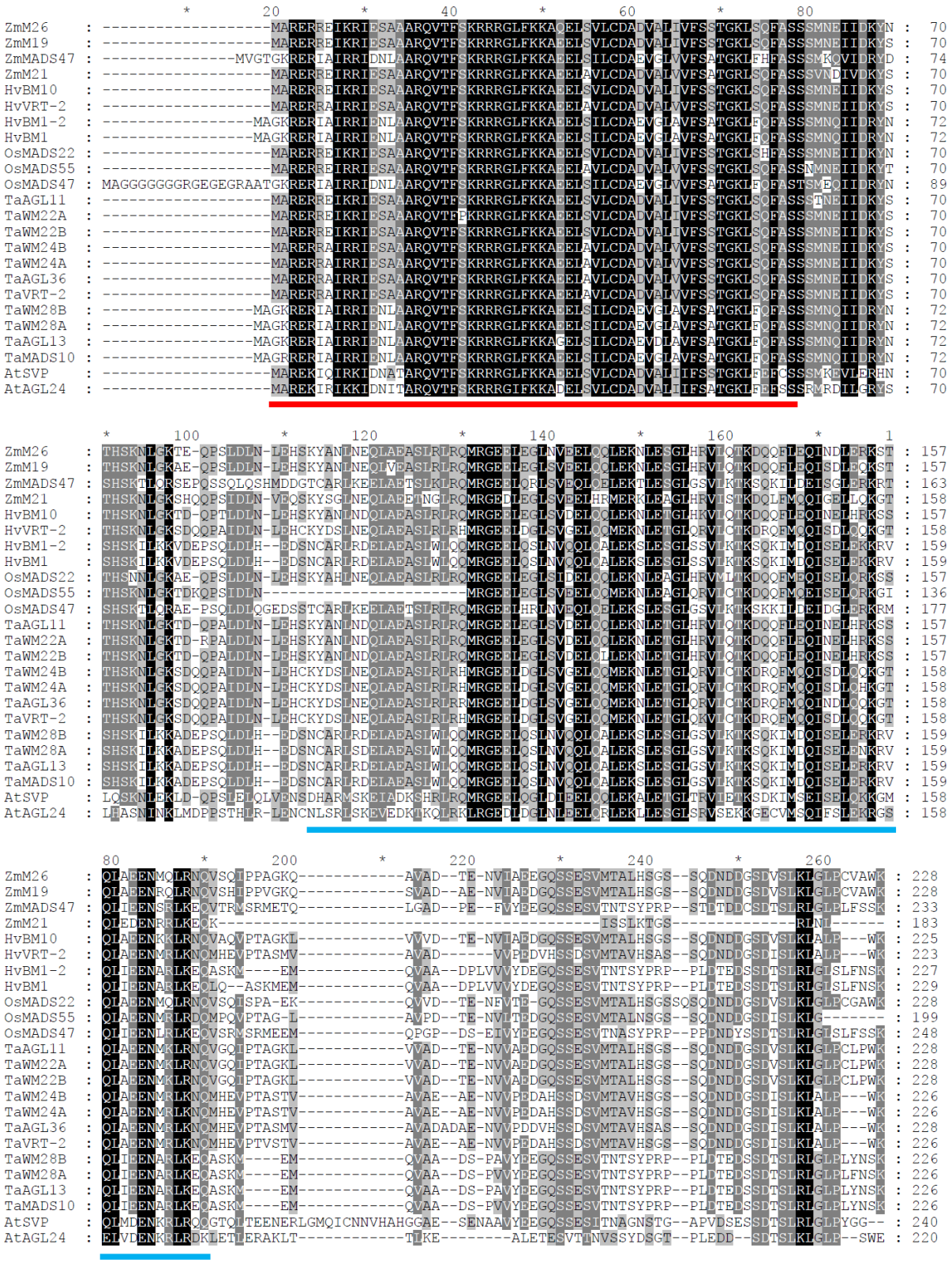

Figure 13. **Multiple protein sequence alignment of ZmM26 and its putative homologs from maize, barley, rice, wheat and Arabidopsis.** Conserved amino acids between the sequences are shown with a black background. The red bar under the sequences marks the region of the MADS-domain of ZmM26 and the blue bar indicates the K-domain.

All mentioned homologs of ZmMADS1 and ZmM26 were used to construct a phylogenetic tree (*Figure 14*). The outcome was a two-armed tree with all the *ZmMADS1* homologs on one branch and all the *ZmM26* homologs on the other branch. Within these branches *ZmMADS1* clusters together with the two other genes *ZmMADS56* and *OsMADS50* (*Figure 14*, blue bar). The subgroup to which *ZmM26* clusters is slightly larger and contains six additional genes, namely *ZmM19*, *OsMADS22*, *HvBM10*, *TaWM22A*, *TaWM22B* and *TaAGL11* (*Figure 14*, red bar).

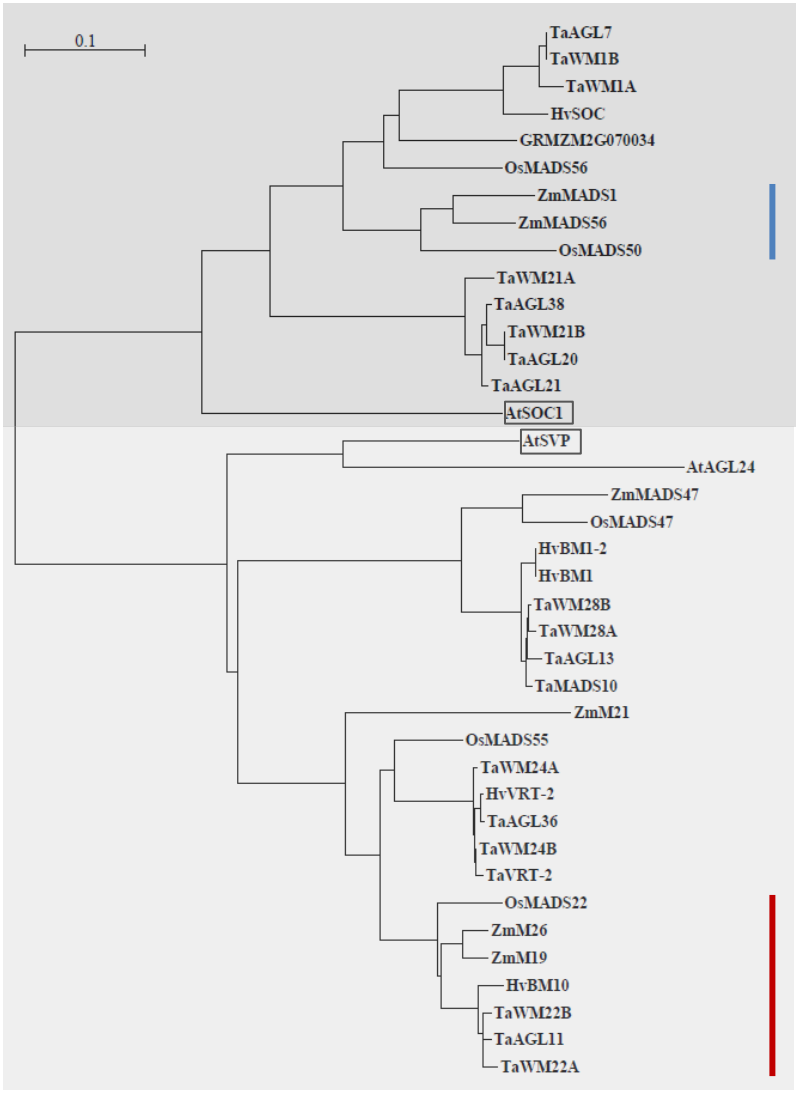

Figure 14. **Phylogenetic tree of ZmMADS1, ZmM26 and homologous proteins**. ZmMADS1 and homologs are shaded in dark gray. The subgroup containing ZmMADS1 is marked by a blue bar. The subgroup containing ZmM26 is marked by a red bar. ZmM26 and homologs are shaded in light grey. AtSOC1 and AtSVP are framed in black. Bar = number of substitutions per site.

5.4. CONSERVATION OF *ZMMADS1* AND *ZMM26* IN DIFFERENT MAIZE GENOTYPES

After screening for homologous genes in different plant species, the coding sequence and the deduced amino acid sequence of *ZmMADS1* and *ZmM26* were analyzed in the maize lines, in which these genes were identified as putative flowering time regulators. This was done to study whether the genes were identical in all lines or if the difference observed in the transition of the SAM (*Table 2 & Table 3*) could be addressed to natural variations in one of these genes.

The protein coding sequences of *ZmMADS1* and *ZmM26* reported on MaizeSequence (http://www.maizesequence.org/) were amplified from cDNA derived from the maize lines 4F-240 BX 16, 4F-350 CN 2, B77 and E2558W. Additionally, B73 was included as a control. The amplicons were sequenced and the gained nucleotide sequences were translated to amino acid sequences to analyze changes in the primary protein structure in the four maize lines used in this study.

The amino acid sequences for both ZmMADS1 and ZmM26 derived from B73 were identical to the annotated sequences at MaizeSequence data base. The protein sequence for ZmMADS1 from 4F-240 BX 16, 4F-350 CN 2 and B77 was identical to the sequence of B73. The sequence of E2558W was slightly different, because several nucleotide exchanges led to an exchange of six amino acids. At position 143 glutamic acid was replaced by glutamine, at position 176 valine by methionine, at position 177 proline by threonine, at position 180 serine by proline, at position 190 asparagine by threonine and at position 194 glycine by aspartic acid (*Figure 15 A*, red asterisks). Only one of these six substitutions, namely E143Q is located within the conserved K-domain (*Figure 15 A* blue bar). All other substitutions are in the less conserved C-terminal domain, suggesting that protein function is likely not affected. The deduced amino acid sequence of ZmM26 is identical to the published B73 sequence in the genotypes 4F 350 CN 2, E2558W and B77. In line 4F-240 BX 16 one amino acid exchange from glutamic acid to aspartic acid took place at position 121 (*Figure 15 B*, red asterisks). This is a conservative exchange located within the K-domain (*Figure 15 B* blue bar), thus a functional change is unlikely.

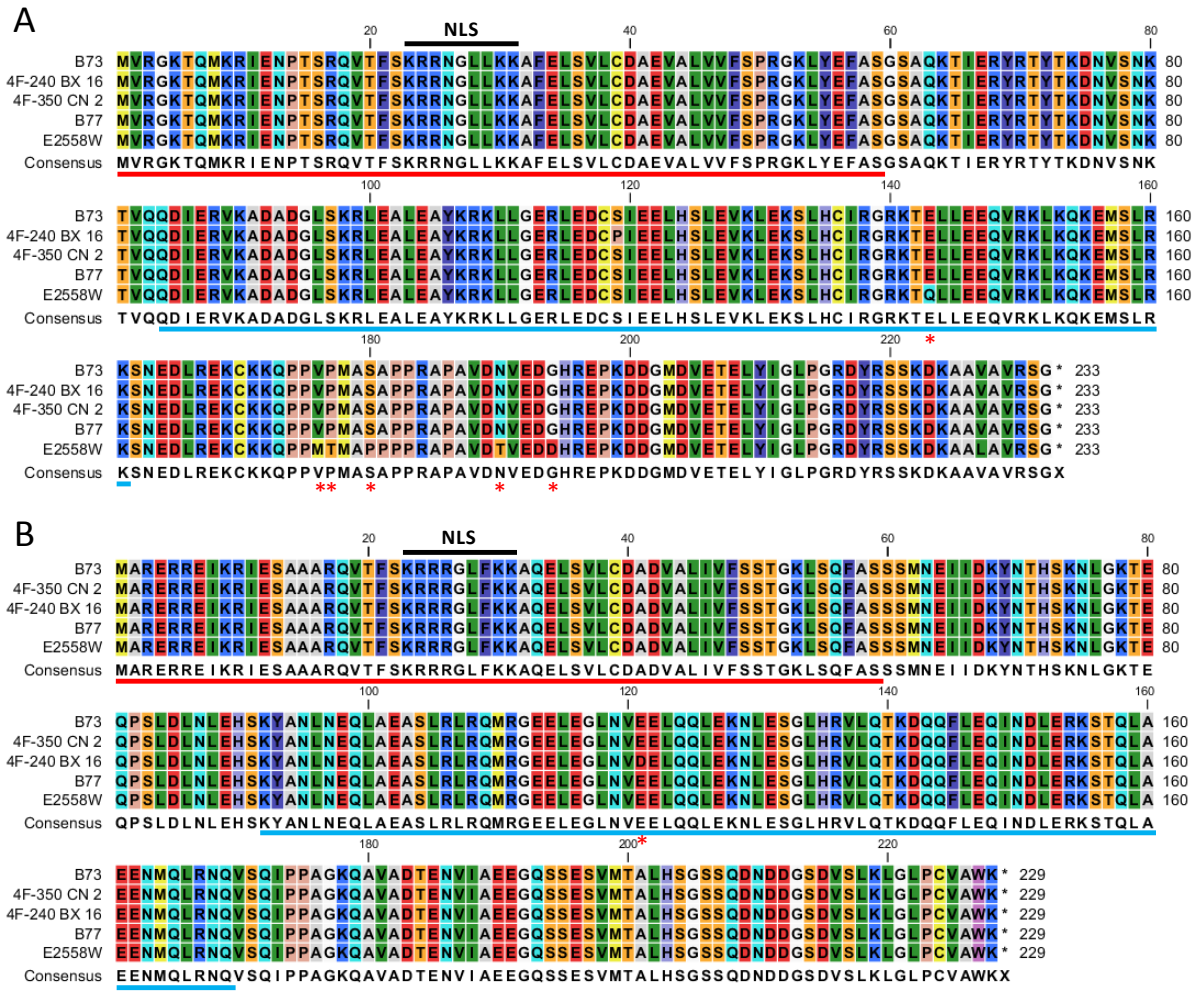

Figure 15. **Alignment of deduced amino acid sequences of (A) ZmMADS1 and (B) ZmM26 in the maize lines 4F-240 BX 16, 4F-350 CN2, B77 and E2558W.** Protein sequences are derived from nucleotide sequences generated by Sanger sequencing. The MADS domain is underlined in red, the K-domain in blue. Nuclear localization signal (NLS) is indicated with a black bar. Amino acid exchanges are indicated by red asterisk under the consensus sequnece.

5.5. COMPLEMENTATION OF ARABIDOPSIS *SOC1-2* MUTANT WITH *ZMMADS1*

Homology studies of *ZmMADS1* indicated that the important flowering time regulator *SOC1* from Arabidopsis might represent a homologous protein. When *AtSOC1* is mutated flowering is delayed (Borner *et al*., 2000; Lee *et al.,* 2000). To assess whether ZmMADS1 has a similar function in flowering time and is able to rescue the late flowering phenotype of the Arabidopsis *soc1-2* mutant (Lee *et al.,* 2000) a complementation assay was set up. The coding sequence of *ZmMADS1* was cloned behind a 1951 bp fragment of the *AtSOC1* promoter (p*SOC1*:*MADS1*) for complementation and behind the *CaMV 35S* promoter (p*35S*:*MADS1*) for overexpression studies. Both constructs were used for transformation of Arabidopsis *soc1-2* mutant plants. Additionally, a C-terminal translational fusion of

ZmMADS1 and the green fluorescent protein (GFP) was cloned behind the *AtSOC1* promoter fragment (p*SOC1*:*MADS1-GFP*) and transformed into Arabidopsis wild-type (Col 0) and *soc1-2* mutant plants. Transgenic plants of the first generation were analyzed regarding *ZmMADS1* expression (data not shown). Afterwards, offspring of plants expressing *MADS1* without the translational fusion were grown in SD and plants containing the fusion protein were grown in LD conditions. Plants were genotyped for bearing ZmMADS1 (data not shown). In both cases wild-type and mutant plants were grown side by side with transformed plants as controls.

In SD conditions, wild-type plants were bolting on average after 140.2 (±2.99) days after sowing and *soc1-2* mutants after 181.0 (±10.0) days (*Figure 16 A & C*). Three lines containing the construct p*35S*:*MADS1* in a *soc1-2* background were analyzed. Line 7 bolted after 140.0 (±2.0), line 12 after 119.3 (±7.6 days) and line 14 after 135.4 (±22.6) days (*Figure 16 A & C*), respectively. Mutant line and overexpressing line 12 differed significantly ($p \leq 0.05$). Two lines bearing the p*SOC1*:*MADS1* construct in the mutant background were analyzed. Line 6 was bolting after 122.2 (±6.41) days and line 18 after 126.3 (±5.0) days (*Figure 16 A & C*), respectively. Here lines 6 and 18 differed significantly from the mutant ($p \leq 0.05$).

Under LD conditions wild type plants bolted on average 44.8 (±4.2) days after sowing and *soc1-2* plants after 73.7 (±7.7) days (*Figure 16 B*). Two lines were analyzed with p*SOC1*:*MADS1-GFP* in a wild type background (p*SOC1*:*MADS1-GFP*). Line 6 bolted after 40.5 (±0.9) days and line 9 after 32.6 (±1.0) (*Figure 16 B*). The difference between WT plants and plants of the line p*SOC1*:*MADS1-GFP* 9 were significant ($p \leq 0.05$). Three lines were analyzed with this construct in the mutant background (*soc1-2*/p*SOC1*:*MADS1-GFP*). Line 2 bolted after 64.8 (±1.6) days, line 4 after 66.2 (±4.0) and line 8 bolted after 40.3 (±3.9) days (*Figure 16 B*), respectively. The differences between *soc1-2* mutants and plants of the lines *soc1-2*/p*SOC1*:*MADS1-GFP* 2 and 8 were significant ($p \leq 0.05$). Originally, *soc1-2* plants were transformed additionally with the p*35S*:*MADS1-GFP* construct, but unfortunately the offspring of these plants did not produce any seeds. Therefore, it was not possible to use the second generation for complementation analyses.

Taken together, *ZmMADS1* is able to rescue the late flowering phenotype of the Arabidopsis *soc1-2* mutant. In addition, it was possible to show that the translational fusion of ZmMADS1 and GFP is functional, since the late flowering phenotype can be rescued.

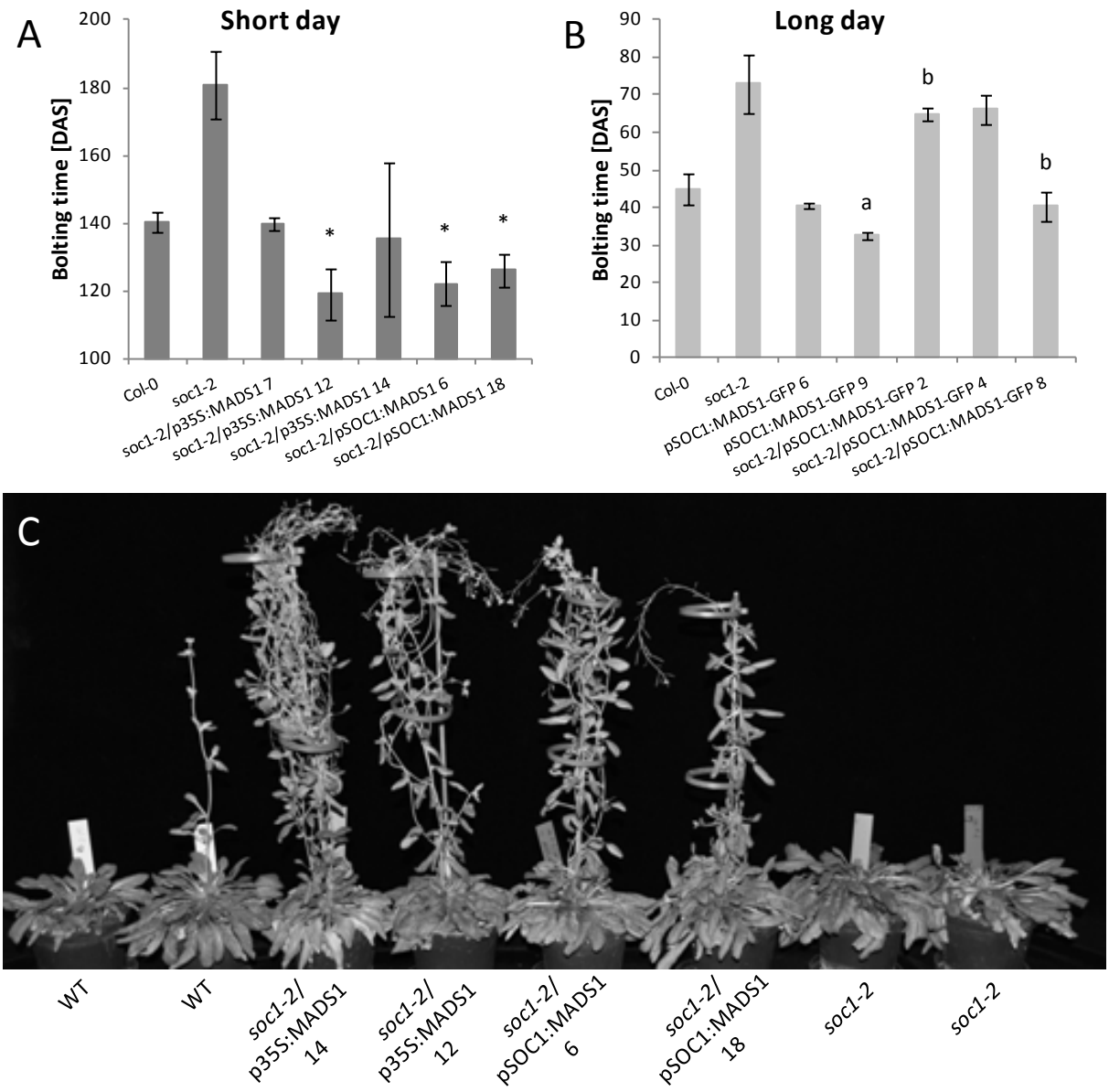

Figure 16. **Complementation of the *Arabidopsis thaliana soc1-2* mutant by expressing *ZmMADS1*.** Plants were grown in (A) LD and (B) SD conditions, respectively. The expression of *ZmMADS1* was driven either by the *AtSOC1* or the *CaMV 35S* promoter in the *soc1-2* mutant background. In SD *ZmMADS1* was expressed in wild type plants as well (n = 2-7, mean values are shown, error bars = standard deviation). (A) * = significantly different to *soc1-2* ($p \leq 0.05$), (B) a = significantly different to Col-0 ($p \leq 0.05$), b = significantly different to *soc1-2* ($p \leq 0.05$)). (C) Comparison of growth behavior/plant architecture of Col-0 (wild type, WT), *soc1-2*, *soc1-2*/p*35S*:*MADS1*_14 and _12, *soc1-2*/p*SOC1*:*MADS1*_6 and _18 grown in SD. All plants grew for a period of 148 days under short day conditions.

5.6. SUBCELLULAR LOCALIZATION OF *ZMMADS1*

As shown in the previous chapter the MADS1-GFP fusion protein was functional, since the *soc1-2* flowering phenotype was rescued by its overexpression. To analyze the subcellular localization of the MADS1 protein, these plants were also used for confocal laser scanning microscopy.

Fluorescence signals were detectable at various places in the cells in different strength (*Figure 17 A*). In the merge of bright field and fluorescence channel it became obvious that the weaker signals localize to chloroplasts (*Figure 17 A & B*, blue arrow heads). It is thus likely that these signals were autofluorescence signals. The stronger signals were only present once per cell and over a larger area in a dotted way. The size, shape and number are indicating that this signal corresponds to the nucleus of the cells (*Figure 17* A & B, red arrow heads).

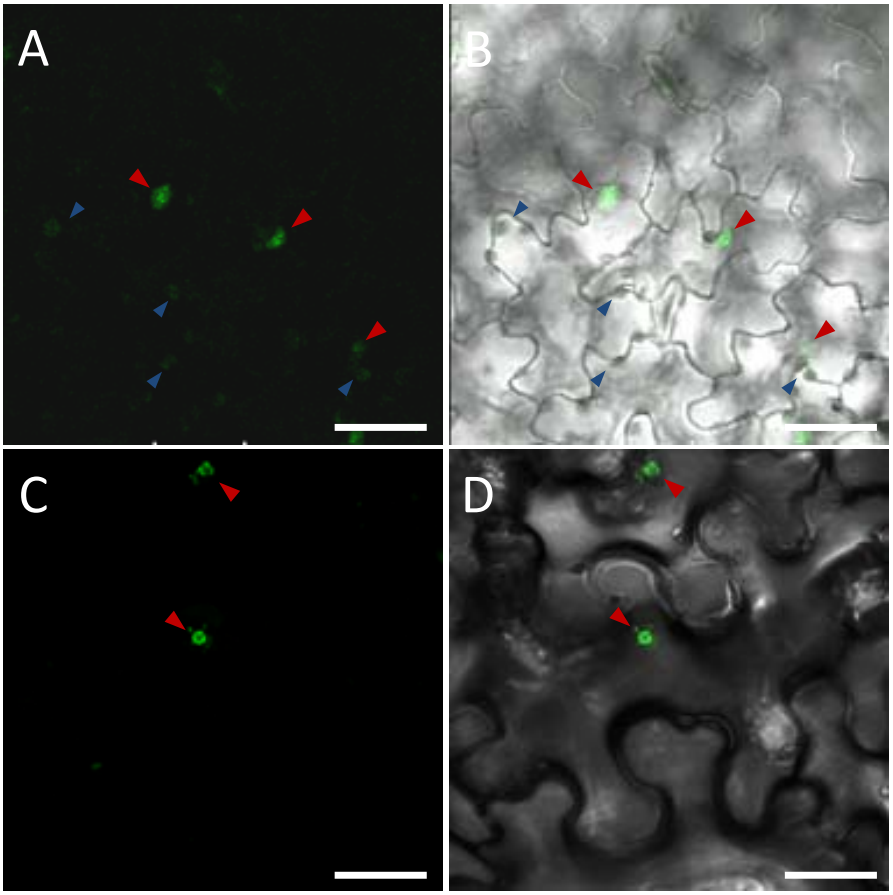

***Figure 17.* Subcellular localization of ZmMADS1**. (A) Confocal laser scanning microscopy (CLSM) image of the fluorescence signal emitted by p*35S:MADS1-GFP* in leaf epidermis cells of *A. thaliana soc1-2* mutant. Fluorescence signals were detected in the nucleus (red arrow heads) and the chloroplasts (blue arrow heads). (B) Merge of image A and corresponding bright field image. (C) CLSM image of the fluorescence signal emitted by p*35S:MADS1-GFP* infiltrated into *N. benthamiana* leaves. Fluorescence signals were detected in the nucleus of epidermal cells (red arrow heads). (D) Merge of image C and the corresponding bright field image. Scale bars = 25 µm.

To confirm this result, the p*35S*:*MADS1-GFP* construct was used for infiltration of leaf epidermal cells of *Nicotiana benthamiana*. This time, autofluorescence of the chloroplasts was filtered out, so it was possible to clearly identify the GFP fluorescence. Again, the signal was detected in a dotted manner in the nucleus (*Figure 17 C & D,* red arrow heads) confirming the previously identified subcellular localization of the MADS1-GFP fusion protein in transgenic Arabidopsis plants.

5.7. CELLULAR LOCALIZATION OF ZMMADS1 AND ZMM26

Peptide antibodies were produced against ZmMADS1 and ZmM26 to analyze the distribution of the proteins in maize leaves using immunolocalization. Immune sera were first tested against their corresponding peptides and purified using the synthesized peptide (*Figure 18*).

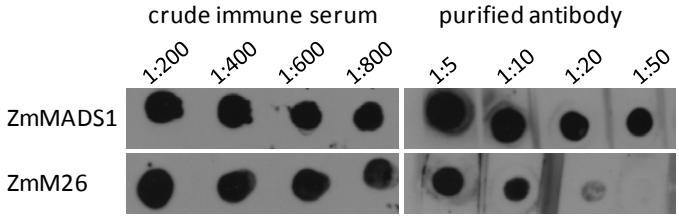

Figure 18. **Result of the purification of antibodies against peptides of ZmMADS1 and ZmM26.** Dot blots of the peptides ZmMADS1 (upper row) and ZmM26 (lower row) treated with the crude immune sera in different dilutions, from 1:200 to 1:800 (left) and the purified antibody in dilutions from 1:5 to 1:50 (right). Films for detecting chemiluminescence of crude immune sera were exposed 10 sec and for the purified antibodies were exposed for 1 min.

Since purified antibodies were able to recognize their corresponding peptides (*Figure 18*), they were used for immunolocalization of cross sections of maize leaves, collected at the time period around the transition of the SAM from vegetative to flowering. Unfortunately, with both purified antibodies it was not possible to detect any signal on cross sections besides weak autofluorescence signals derived from chloroplasts (data not shown), even when antibodies were used undilutedly. Therefore, crude immune sera were used to analyze cellular localization of ZmMADS1 and ZmM26 (*Figure 19*).

In cross sections of maize B73 leaves treated with the immune serum against the ZmMADS1 peptide a fluorescence signal of the Cy2-coupled secondary antibody was detected strongly in bundle sheath cells of young vascular bundles (*Figure 19 A – C*). Additionally, there might also be a weak signal inside the vascular bundle and in the mesophyll cells and some dot-like structures were visible at cell walls epidermis cells (*Figure 19 A – C*). In leaves

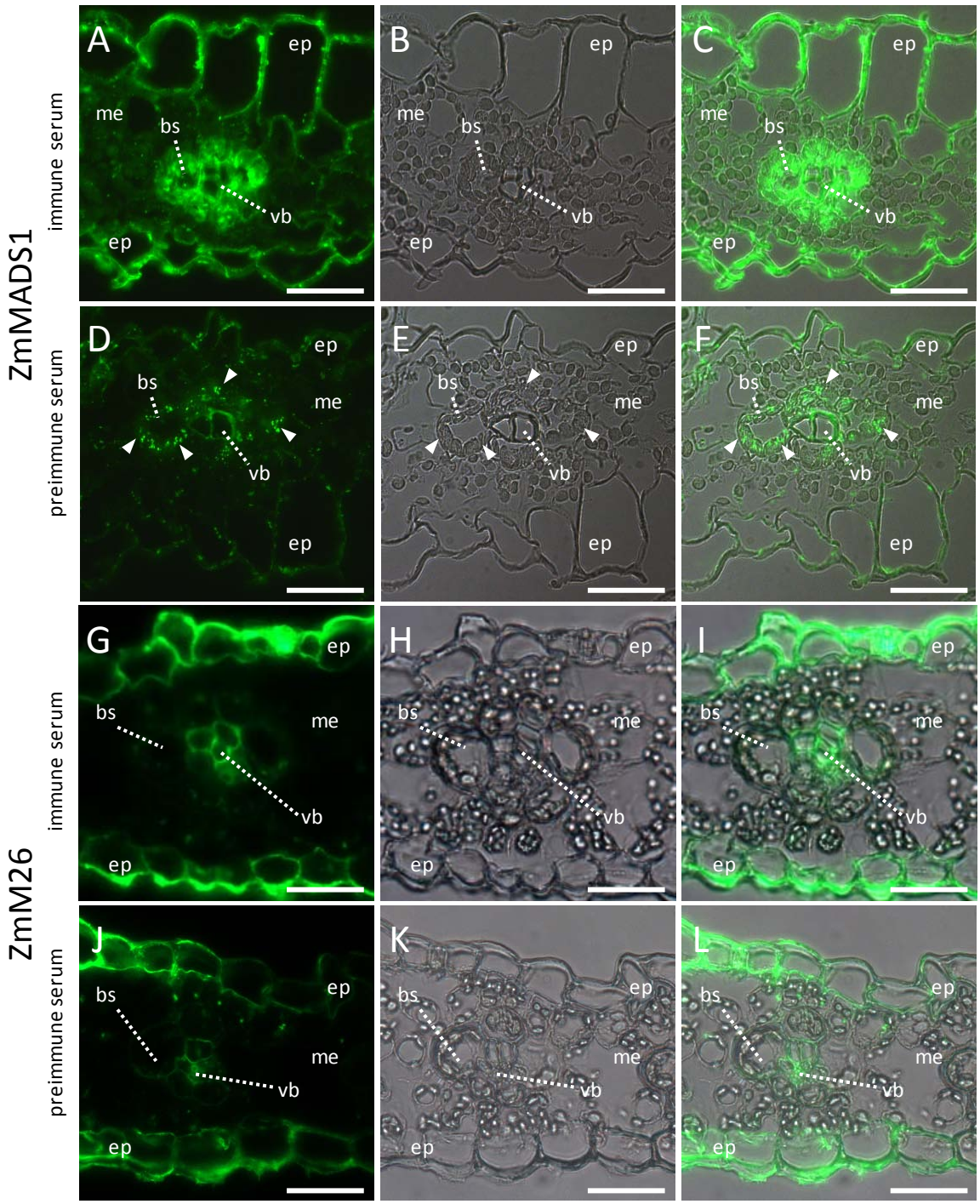

Figure 19. **Immunolocalization of ZmMADS1 and ZmM26 on cross sections of maize leaves.** Microscopy images of fluorescence signals emitted by a Cy2-coupled secondary antibody (A, D, G, J), corresponding bright field image (B, E, H, K) and the merge of both channels (C, F, I, L). (A-C) Leaf sections were treated with immune serum against the ZmMADS1 peptide. Cy2 signals are detectable strongly in the bundle sheath cells (bs) and weaker in the epidermal cell layer (ep) and the mesophyll (me). Signals in the vascular bundle (vb) cannot be distinguished from signals in bs. (D-F) Leaf sections were treated with corresponding preimmune serum. Cy2 signals can be detected weakly in bs, ep and me. Stronger signals in vb and in chloroplasts (arrow heads) in bs. (G-I) Leaf sections were treated with immune serum against the ZmM26 peptide. Cy2 signals are detectable in ep and vb. (J-L) Leaf sections were treated with corresponding preimmune serum. Cy2 signals are detectable in ep and vb. Scale bars = 50 µm.

treated with preimmune serum, dotted signals were detectable, co-localizing with chloroplasts in bundle sheath cells (*Figure 19 D – F*, arrow heads). Since these dots are only visible in chloroplasts of bundle sheath cells and not in the mesophyll chloroplasts, it is most likely that these are signals derived from Ribulose-1,5-bisphosphate carboxylase (RuBisCo). Additionally, there is a signal localized to the vascular bundles and weak signals in mesophyll and epidermis cells (*Figure 19 D – F*). The dot-like structures at the cell walls of the epidermis cells were also detected (*Figure 19 D - F*).

In case of the immunolocalization of ZmM26 in maize B73 leaves, it was not possible to detect differences in cross sections treated with the immune serum (*Figure 19 G – I*) compared to cross sections treated with preimmune serum (*Figure 19 J – L*).

5.8. CIRCADIAN ACCUMULATION OF ZMMADS1 AND ZMM26

To analyze accumulation of ZmMADS1 and ZmM26 during the day or photoperiod and to analyze possible genotypic differences, leaf samples were taken from the four maize lines 4F-240 BX 16, 4F-350 CN 2, B77 and E2558W in 4 hour intervals over a period of 2 days starting at dawn in SD and LD conditions, respectively. Samples were taken from the uppermost fully expanded leaf, when plants were shortly before or at the time of transition of the SAM. Proteins were extracted and samples analyzed using a western blot. First, purified antibodies against ZmMADS1 and ZmM26 were used, but signals were not detected on blots in both cases. Again, crude immune sera were used for protein detection. However, also with these immune sera it was not possible to detect any signal at the expected sizes of 26.4 kDa in the case of ZmMADS1 and of 25.5 kDa for ZmM26. Solely in the case of the SD samples of B77 it was possible to detect a signal corresponding to a molecular weight of approximately 90 kDa with the immune serum against of ZmMADS1, which was fluctuating over the day (*Figure 20*, red arrow head). The band was strongest at time points 4 h, 8 h, 28 h and 32 h. These time points correspond to 4 and 8 hours after beginning of the light period, respectively (*Figure 20*). In the dark periods, 16 – 24 h and 40 – 48 h, two bands are visible at this molecular weight (*Figure 20*). A signal of this size was not detectable when preimmune serum was used (data not shown). Additionally, a second signal at the size of about 50 to 55 kDa (*Figure 20*, asterisk) was detected in any of the samples at a similar intensity. This signal might be caused by a putative cross-reaction with the large subunit of

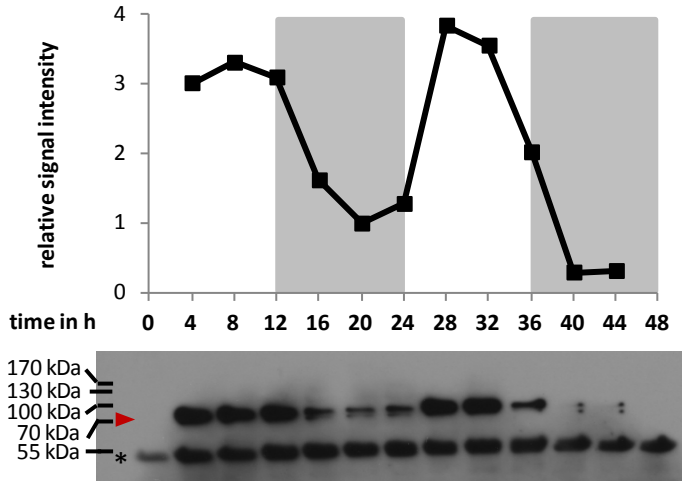

Figure 20. **ZmMADS1 accumulation in B77 leaves during the course of two days.** Proteins were detected using immune serum against a ZmMADS1 peptide. Samples were taken in 4 h intervals over 2 d in protein extracts of B77 leaves grown in SD condition. Grey areas indicate dark period. Red arrowhead marks a putative ZmMADS1 higher order complex, asterisk marks a putative crossreaction with the large subunit of RuBisCO. For quantification putative MADS1 containing bands were normalized to the RuBisCo band.

the RuBisCo enzyme (*Figure 20*). Since it was not possible to clarify if ZmMADS1 was part of this putative protein complex showing a fluctuating intensity, it was decided to analyze the dependency of photoperiod and day length on transcript level using quantitative real-time PCR.

5.9. TRANSCRIPT ACCUMULATION OF *ZMMADS1, ZMM26* AND HOMOLOGOUS GENES DURING THE COURSE OF TWO DAYS

Many photoperiodic flowering time regulatory genes are expressed in a circadian manner. Therefore candidate genes were investigated regarding this possibility. To analyze the transcript level of *ZmMADS1* and *ZmM26* during the course of a day, sister samples were used, which were collected from leaves in parallel to samples taken for the analyses of protein accumulation during the course of a day (5.8). Total RNA was extracted from three biological replicates. All quantitative real-time PCR (qRT-PCR) results were normalized to the expression of *glyceraldehyde-3-phosphatase dehydrogenase* (*GAP-DH*; GRMZM2G046804) and given relatively to the time point with the lowest expression value of each gene and maize line.

The transcript of *ZmGIGZ1a* (*Gigantea 1a,* GRMZM2G107101) shows a day time specific expression pattern (Miller *et al.*, 2008) and was therefore used as control to check if the sampling was performed correctly and if day time specific analyses were possible. Indeed, the expression pattern of *ZmGIGZ1a* agreed with published data in all four analyzed maize lines. (*Figure 21, Table 6*). In SD condition, transcript reached its highest level after 12 h and

36 h (at the beginning of the dark period), respectively, while the lowest expression was observed at the end of the dark period at time points 0 h, 24 h and 48 h (*Figure 21, Table 6*). At LD condition transcript maximum was 4 h to 8 h before the dark period and lowest expression was at the end of the dark period (*Figure 21, Table 6*), like at SD condition.

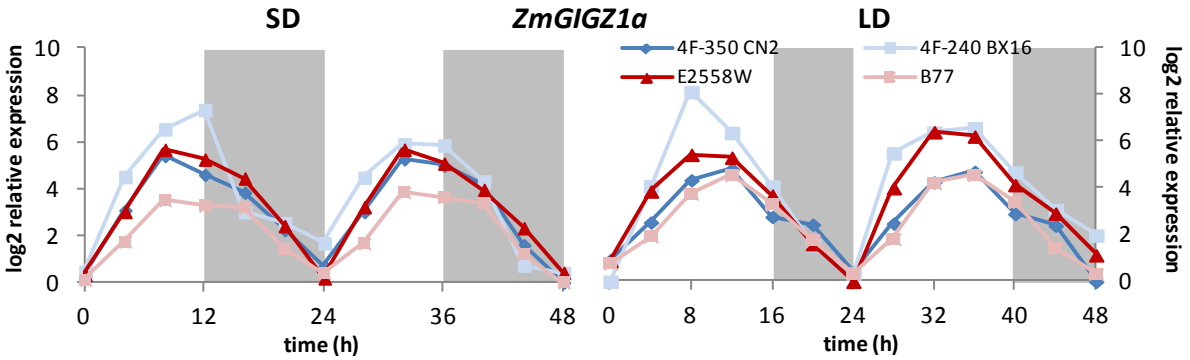

***Figure 21.* Graphical representation of *ZmGIGZ1a* expression.** Relative expression level of *ZmGIGZ1A* in the genotypes 4F-350 CN 2 (dark blue), 4F-240 BX 16 (light blue), E2558W (dark red) and B77 (light red) over a period of 2 days in 4 h intervals under SD (left) and LD (right) conditions is shown as mean of three biological replicates. The relative expression values are log2 transformed. Standard deviations are not depicted (*Table 6*). Grey areas indicate dark periods.

***Table 6.* Expression values of *ZmGIGZ1a*.** Log2 transformed relative expression values of *ZmGIGZ1A* in the genotypes 4F-350 CN 2, 4F-240 BX 16, E2558W and B77 over a period of 2 days in 4 h intervals under SD (left) and LD (right) conditions. Mean values of biological triplicates and the standard deviations (st dev) are indicated.

SD *GIGZ1a*	4F-350 CN2		4F-240 BX16		E2558W		B77	
time (h)	mean	st dev	mean	st dev	mean	st dev	mean	st dev
0	0,30	0,46	0,49	0,60	0,36	0,13	0,13	0,18
4	3,11	0,56	4,53	1,05	3,04	0,58	1,76	0,90
8	5,42	0,07	6,56	1,33	5,69	0,88	3,53	0,84
12	4,62	0,67	7,38	0,20	5,27	0,76	3,30	0,40
16	3,86	0,07	3,03	0,73	4,47	0,39	3,22	0,61
20	2,27	0,67	2,56	1,72	2,44	0,63	1,46	0,61
24	0,73	0,32	1,70	1,33	0,21	0,30	0,43	0,24
28	3,03	0,34	4,50	1,11	3,25	0,62	1,68	0,73
32	5,28	0,14	5,92	0,93	5,69	0,63	3,87	0,70
36	5,01	0,30	5,87	1,02	5,10	0,47	3,66	0,49
40	4,20	0,23	4,34	1,49	3,98	0,98	3,40	0,85
44	1,62	0,35	0,76	0,81	2,35	0,40	1,25	0,60
48	0,03	0,04	0,43	0,55	0,45	0,42	0,02	0,03

LD *GIGZ1a*	4F-350 CN2		4F-240 BX16		E2558W		B77	
time (h)	mean	st dev	mean	st dev	mean	st dev	mean	st dev
0	0,93	0,31	0,00	0,00	0,88	0,35	0,77	0,55
4	2,54	0,11	4,10	0,59	3,87	0,34	1,93	0,63
8	4,35	0,40	8,14	0,79	5,45	0,64	3,76	0,24
12	4,83	0,28	6,38	0,45	5,32	0,29	4,56	0,66
16	2,78	0,15	4,08	0,76	3,70	0,21	3,30	0,58
20	2,45	0,06	1,57	0,67	1,61	0,47	1,76	0,57
24	0,42	0,23	0,35	0,26	0,00	0,00	0,31	0,27
28	2,49	0,34	5,51	1,03	4,01	0,42	1,82	0,68
32	4,26	0,18	6,40	0,28	6,42	0,29	4,22	0,62
36	4,72	0,51	6,59	0,88	6,23	0,27	4,56	0,27
40	2,90	0,28	4,68	0,57	4,15	0,46	3,41	0,47
44	2,40	0,47	3,08	1,92	2,92	0,69	1,43	0,33
48	0,00	0,00	1,98	2,17	1,13	0,12	0,33	0,33

Expression of *ZmMADS1* was strongest at the end of the dark period in all four maize lines (*Figure 22, Table 7*). The expression maxima were higher in lines 4F-350 CN 2 and B77 compared with 4F-240 BX 16 and E2558W. Expression minimum was 4 to 8 h before the beginning of the dark period (*Figure 22, Table 7*). Similar in SD condition, expression maxima of *ZmMADS1* in all lines were visible at dawn, but were increased compared to LD condition (*Figure 22, Table 7*). Expression minima were detected 4 h before the dark period. These data indicate that in all four analyzed maize lines *ZmMADS1* is regulated by the photoperiod and that this regulation is even more pronounced in SD compared with LD conditions.

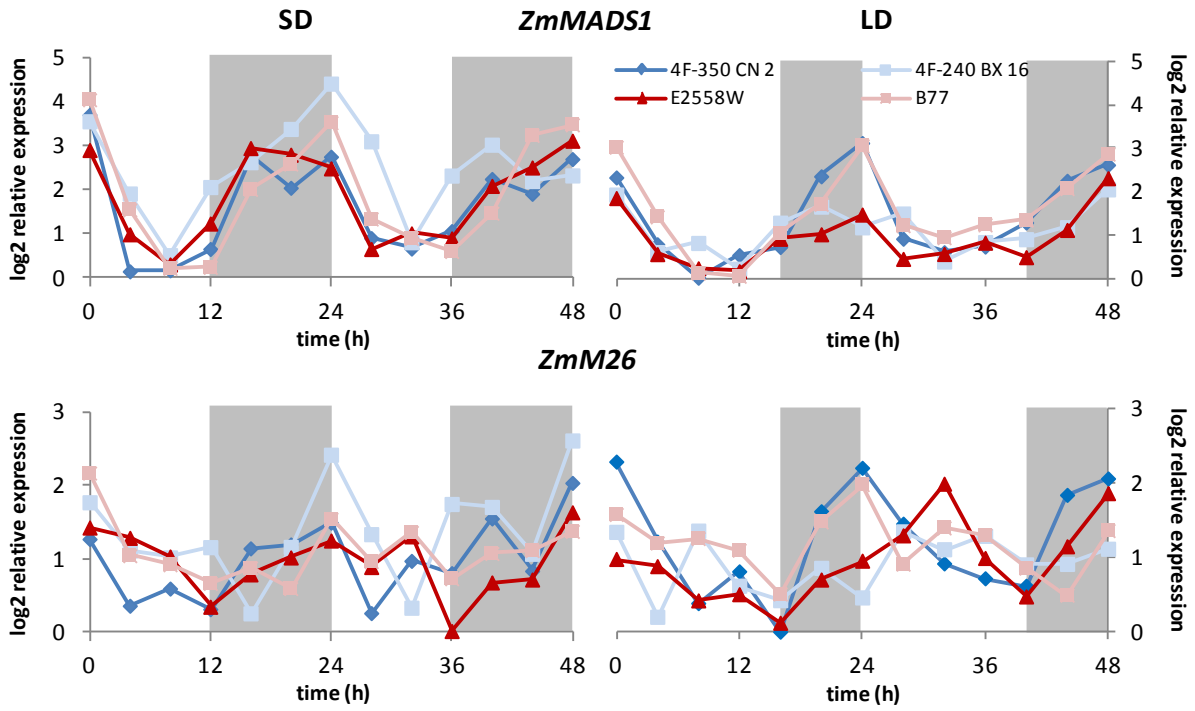

Figure 22. **Graphical representation of *ZmMADS1* and *ZmM26* expression levels over a period of 2 days in 4 h intervals under SD (left) and LD (right) conditions, respectively.** Log2 transformed relative expression values are shown for the genotypes 4F-350 CN 2 (dark blue), 4F-240 BX 16 (light blue), E2558W (dark red) and B77 (light red). Mean values of three biological replicates are shown. Standard deviations are not depicted (*Table 7*). Grey areas indicate dark periods.

Table 7. **Expression values of *ZmMADS1* and *ZmM26***. Log2 transformed relative expression values of *ZmMADS1* and *ZmM26* in the genotypes 4F-350 CN 2, 4F-240 BX 16, E2558W and B77 over a period of 2 days in 4 h intervals under SD (left) and LD (right) conditions. Mean values of biological triplicates and standard deviations (st dev) are indicated.

SD MADS1	4F-350 CN2		4F-240 BX16		E2558W		B77	
time (h)	mean	st dev	mean	st dev	mean	st dev	mean	st dev
0	3,70	0,03	3,55	0,66	2,90	0,30	4,04	0,35
4	0,15	0,14	1,92	2,43	0,99	0,32	1,55	0,63
8	0,18	0,13	0,52	0,69	0,31	0,44	0,22	0,31
12	0,66	0,47	2,06	1,46	1,24	0,23	0,24	0,30
16	2,77	0,21	2,63	1,92	2,95	0,58	2,01	0,52
20	2,05	0,48	3,38	1,59	2,80	0,17	2,58	0,68
24	2,75	0,15	4,41	0,30	2,49	0,32	3,52	0,55
28	0,91	0,70	3,10	1,05	0,66	0,33	1,34	0,33
32	0,67	0,31	0,81	0,42	1,01	0,72	0,90	0,39
36	1,07	0,31	2,32	0,67	0,90	0,29	0,60	0,31
40	2,25	0,57	3,02	1,40	2,09	0,57	1,47	0,98
44	1,91	0,43	2,20	0,48	2,51	0,17	3,23	0,53
48	2,70	0,44	2,33	0,60	3,11	0,82	3,47	0,89

LD MADS1	4F-350 CN2		4F-240 BX16		E2558W		B77	
time (h)	mean	st dev	mean	st dev	mean	st dev	mean	st dev
0	2,33	0,29	1,94	1,06	1,86	0,23	3,03	0,35
4	0,80	0,12	0,62	0,25	0,57	0,42	1,43	0,43
8	0,03	0,04	0,83	0,58	0,24	0,34	0,13	0,16
12	0,55	0,09	0,23	0,17	0,18	0,06	0,06	0,08
16	0,73	0,16	1,29	0,91	0,92	0,40	1,06	0,34
20	2,36	0,16	1,66	0,67	1,03	0,19	1,72	0,48
24	3,13	0,54	1,19	0,34	1,48	0,32	3,06	0,20
28	0,92	0,05	1,50	0,19	0,46	0,07	1,22	0,44
32	0,61	0,16	0,40	0,32	0,57	0,48	0,95	0,31
36	0,74	0,63	0,85	0,61	0,83	0,28	1,24	0,11
40	1,30	0,40	0,91	0,64	0,50	0,17	1,35	0,38
44	2,26	0,36	1,19	0,64	1,13	0,70	2,08	0,50
48	2,62	0,22	2,06	0,27	2,32	0,14	2,87	0,56

SD ZmM26	4F-350 CN2		4F-240 BX16		E2558W		B77	
time (h)	mean	st dev	mean	st dev	mean	st dev	mean	st dev
0	1,27	0,23	1,77	0,66	1,43	0,39	2,17	0,60
4	0,37	0,47	1,12	0,73	1,29	0,67	1,05	0,83
8	0,60	0,14	1,02	0,51	1,04	0,51	0,92	0,40
12	0,32	0,42	1,16	0,07	0,35	0,27	0,67	0,50
16	1,15	0,48	0,26	0,37	0,79	0,20	0,88	0,63
20	1,20	0,55	1,17	0,54	1,02	0,31	0,60	0,85
24	1,50	0,25	2,42	0,83	1,25	0,37	1,54	0,35
28	0,27	0,19	1,34	0,34	0,89	0,29	0,97	0,32
32	0,98	0,33	0,34	0,27	1,31	0,49	1,36	0,55
36	0,81	0,31	1,75	0,50	0,02	0,03	0,73	0,33
40	1,55	0,68	1,71	0,46	0,68	0,61	1,08	0,68
44	0,84	0,43	1,07	0,50	0,72	0,29	1,12	0,43
48	2,04	0,41	2,61	1,42	1,64	0,57	1,38	0,87

LD ZmM26	4F-350 CN2		4F-240 BX16		E2558W		B77	
time (h)	mean	st dev	mean	st dev	mean	st dev	mean	st dev
0	2,28	0,15	1,34	0,13	0,98	0,24	1,57	0,19
4	1,21	0,26	0,20	0,22	0,88	0,74	1,19	0,44
8	0,38	0,10	1,36	0,35	0,42	0,28	1,25	0,18
12	0,81	0,24	0,62	0,47	0,50	0,09	1,09	0,23
16	0,00	0,00	0,42	0,23	0,12	0,17	0,51	0,47
20	1,62	0,17	0,86	0,15	0,70	0,44	1,47	0,28
24	2,20	0,00	0,46	0,60	0,95	0,15	1,97	0,61
28	1,45	0,35	1,35	0,56	1,29	0,55	0,91	0,18
32	0,92	0,24	1,11	0,52	1,99	0,22	1,39	0,68
36	0,72	0,31	1,29	0,52	0,99	0,27	1,29	0,41
40	0,62	0,11	0,90	0,41	0,47	0,29	0,85	0,20
44	1,84	0,25	0,91	0,23	1,15	0,56	0,49	0,69
48	2,06	0,13	1,11	0,53	1,86	0,01	1,36	0,64

The expression of *ZmM26* was day time specifically regulated in a circadian manner in 4F-350 CN 2 and B77 lines in LD condition (*Figure 22, Table 7*), but the standard deviations in B77 were relatively high compared to the relative expression values, so that these data have to be handled with care (*Table 7*). At SD condition *ZmM26* transcript was slightly regulated in all lines, but the standard deviations were again relatively high in all lines compared to relative expression values (*Figure 22, Table 7*). Most likely, *ZmM26* is not regulated significantly by the photoperiod.

Expression of *ZmMADS56* and the gene *GRMZM2G070034* were also investigated (*Figure 23, Table 8*) because *ZmMADS56* is the closest homolog to *ZmMADS1* in maize (*Figure 14*). *GRMZM2G070034* was included in the analysis, because it represents a homolog of *ZmMADS1* and additionally appeared in the list for putative flowering time regulatory genes of the pair 4F-240 BX 16 and 4F-350 CN2 (*Table 4 A*). *ZmMADS56* is slightly regulated by day time in the lines 4F-350 CN 2 and B77 in LD, with expression maxima at the end of the dark period. However, standard deviation was relatively high in both cases compared to the relative expression values (*Figure 23, Table 8*). In SD condition day time dependent

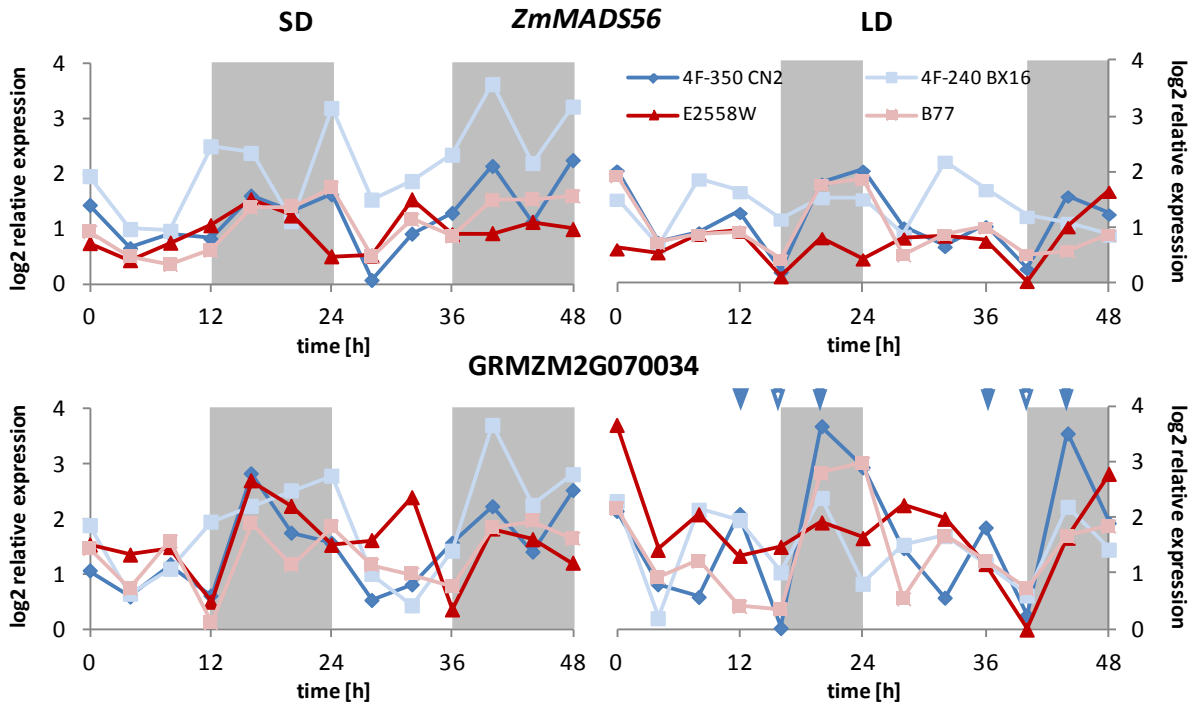

***Figure 23.* Graphical representation of *ZmMADS56 and GRMZM2G070034* expression levels over a period of 2 days in 4 h intervals under SD (left) and LD (right) conditions, respectively.** Log2 transformed relative expression values are shown for the genotypes 4F-350 CN 2 (dark blue), 4F-240 BX 16 (light blue), E2558W (dark red) and B77 (light red). Mean values of three biological replicates are shown. Standard deviations are not depicted (*Table 8*). Grey areas indicate dark periods. Open arrow heads indicate expression minimum of *GRMZM2G07003* in 4F-350 CN 2 in LD condition, closed arrow heads indicate expression maxima of *GRMZM2G07003* in 4F-350 CN 2 in LD condition.

Table 8. **Expression values of *ZmMADS56* and *GRMZM2G070034.*** Log2 transformed relative expression values of *ZmMADS56* and *GRMZM2G070034* in the genotypes 4F-350 CN 2, 4F-240 BX 16, E2558W and B77 over a period of 2 days in 4 h intervals under SD (left) and LD (right) conditions. Mean values of biological triplicates and the standard deviations (st dev) are indicated.

SD MADS56	4F-350 CN2		4F-240 BX16		E2558W		B77	
time (h)	mean	st dev	mean	st dev	mean	st dev	mean	st dev
0	1,43	0,34	1,95	1,53	0,74	0,54	0,94	0,74
4	0,64	0,69	0,99	0,79	0,43	0,37	0,50	0,23
8	0,90	0,26	0,96	0,73	0,74	0,45	0,35	0,49
12	0,82	0,71	2,49	1,23	1,06	0,76	0,61	0,49
16	1,60	0,24	2,37	1,26	1,53	0,43	1,39	0,11
20	1,30	0,53	1,13	1,17	1,24	0,10	1,39	0,55
24	1,62	0,25	3,18	1,21	0,50	0,45	1,74	0,22
28	0,07	0,09	1,52	0,67	0,51	0,16	0,49	0,44
32	0,91	0,05	1,86	0,86	1,53	0,65	1,16	0,27
36	1,28	0,12	2,34	0,88	0,89	0,27	0,86	0,51
40	2,13	0,12	3,62	0,37	0,92	0,65	1,52	0,45
44	1,12	0,24	2,19	1,40	1,12	0,09	1,52	0,12
48	2,24	0,55	3,21	1,65	0,99	0,67	1,59	0,14

LD MADS56	4F-350 CN2		4F-240 BX16		E2558W		B77	
time (h)	mean	st dev	mean	st dev	mean	st dev	mean	st dev
0	2,04	0,26	1,52	0,52	0,63	0,28	1,93	0,46
4	0,76	0,54	0,68	0,79	0,56	0,44	0,73	0,47
8	0,93	0,28	1,88	0,33	0,89	0,67	0,87	0,45
12	1,28	0,29	1,65	1,39	0,95	0,35	0,93	0,68
16	0,22	0,19	1,16	1,06	0,13	0,18	0,43	0,20
20	1,80	0,18	1,55	1,03	0,83	0,49	1,78	0,31
24	2,04	0,19	1,52	1,38	0,45	0,21	1,86	0,67
28	1,02	0,45	0,87	0,66	0,82	0,63	0,51	0,41
32	0,67	0,15	2,20	0,38	0,86	0,37	0,89	0,77
36	1,04	0,47	1,69	0,25	0,77	0,23	1,01	0,29
40	0,28	0,29	1,21	1,03	0,05	0,02	0,52	0,37
44	1,58	0,01	1,10	0,22	1,03	0,70	0,59	0,58
48	1,25	0,15	0,88	0,62	1,66	0,22	0,87	0,38

SD GRMZM2G 070034	4F-350 CN2		4F-240 BX16		E2558W		B77	
time (h)	mean	st dev	mean	st dev	mean	st dev	mean	st dev
0	1,06	0,73	1,88	1,05	1,52	0,54	1,45	0,29
4	0,58	0,11	0,63	0,46	1,34	0,54	0,73	0,53
8	1,17	0,23	1,09	0,57	1,48	0,39	1,59	0,93
12	0,60	0,85	1,94	1,00	0,49	0,41	0,11	0,08
16	2,82	0,52	2,23	0,85	2,69	0,38	1,91	0,61
20	1,74	1,12	2,51	1,37	2,23	0,70	1,16	0,83
24	1,56	0,29	2,77	0,93	1,52	0,11	1,85	0,68
28	0,52	0,49	0,99	0,40	1,61	0,84	1,16	0,62
32	0,80	0,49	0,42	0,60	2,38	0,81	1,00	0,30
36	1,56	0,15	1,41	0,16	0,35	0,25	0,77	0,71
40	2,22	0,85	3,69	0,92	1,82	0,51	1,83	0,92
44	1,40	0,45	2,24	0,82	1,62	0,38	1,96	0,52
48	2,51	0,08	2,80	0,66	1,20	0,87	1,64	0,44

LD GRMZM2G 070034	4F-350 CN2		4F-240 BX16		E2558W		B77	
time (h)	mean	st dev	mean	st dev	mean	st dev	mean	st dev
0	2,12	0,21	2,30	0,36	3,66	0,55	2,17	0,41
4	0,81	0,35	0,20	0,29	1,43	0,22	0,94	0,68
8	0,58	0,32	2,14	0,24	2,06	0,45	1,22	0,64
12	2,07	0,32	1,96	1,22	1,32	0,64	0,41	0,13
16	0,03	0,04	1,02	0,56	1,48	1,18	0,36	0,46
20	3,64	0,31	2,36	0,29	1,92	0,45	2,79	0,69
24	2,90	0,06	0,82	0,87	1,64	0,74	2,98	1,05
28	1,46	0,52	1,52	1,07	2,23	0,57	0,55	0,41
32	0,57	0,37	1,67	0,45	1,98	0,46	1,67	0,56
36	1,83	0,70	1,17	0,67	1,17	0,47	1,23	0,42
40	0,25	0,32	0,61	0,25	0,00	0,00	0,73	0,81
44	3,51	0,93	2,20	0,43	1,64	0,42	1,67	0,58
48	1,91	0,48	1,43	0,55	2,79	1,02	1,85	0,10

regulation could not be detected, which is higher than the significance cut-off of a twofold difference (*Figure 23, Table 8*). In LD condition expression of *GRMZM2G070034* was day time specific in the line 4F-350 CN 2. Expression showed two maxima per day. The first maximum was 4 h before the beginning of the dark period, while the second one appeared just 4 h after the beginning of the dark period (*Figure 23*, closed arrow heads). The expression minimum was directly in between both expression maxima (*Figure 23*, open arrow heads). This pattern was not detectable in SD condition, but still a day time specific expression was visible, indicating that *GRMZM2G070034* expression is influenced by LD condition (*Figure 23, Table 8*). In case of the line 4F-240 BX 16 it was the other way around. Here, a regulation was detectable in SD, with the maxima at the end of the dark period, while it is seemed not to be regulated in LD condition (*Figure 23, Table 8*). In the other two lines there was neither a regulation in SD nor in LD conditions. Taken together, a clear statement about the influence of day time and day length on the expression of *GRMZM2G070034* cannot be made.

The *ZmM26* homolog *ZmM19* was also included in the expression analysis, because it appeared in the list for flowering time regulatory genes of the pair B77 and E2558W (*Table 4 B*) and is the closest homolog for *ZmM26* (*Figure 14*). The expression level started to

increase at the beginning of the day and reached its maximum 4 h prior to the end of the light period and then it decreased to the starting level during the dark period. This pattern was observed in all lines in LD as well as in SD (*Figure 24, Table 9*). The day length did not have any significant influence on the relative expression level of *ZmM19*.

Taken together, the expression profile of *GIGZ1a* showed that a day time specific regulation of gene expression could be detected in all four maize lines. *ZmMADS1* was also day time specifically regulated in LD and SD conditions, but the effect was stronger in SD. Besides *ZmMADS1*, it was only possible to detect a diurnal expression profile for *ZmM19* in all four lines in SD and LD. For the other genes investigated no significant conclusion could be made about a circadian regulation of their expression in levels.

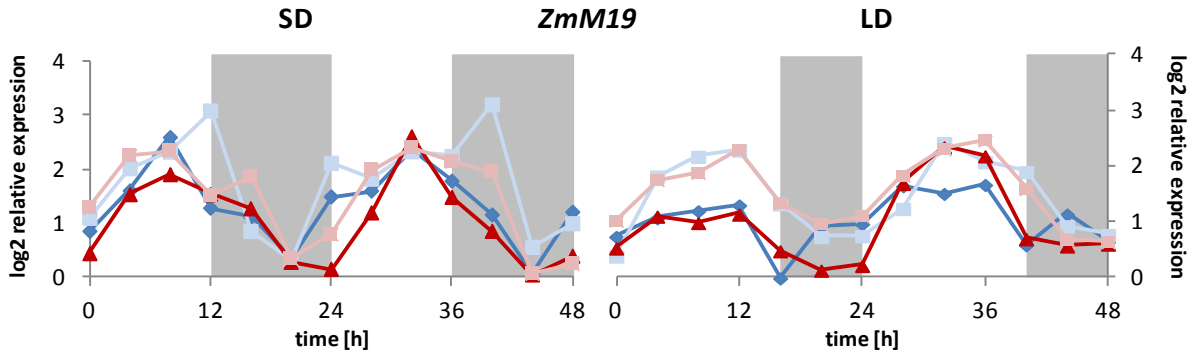

***Figure 24.* Graphical representation of *ZmM19* expression level over a period of 2 days in 4 h intervals under SD (left) and LD (right) conditions.** Log2 transformed relative expression values are shown for the genotypes 4F-350 CN 2 (dark blue), 4F-240 BX 16 (light blue), E2558W (dark red) and B77 (light red) Mean values of three biological replicates are shown. The standard deviations are not depicted (*Table 9*). Grey areas indicate dark periods.

***Table 9.* Expression values of *ZmM19*.** Log2 transformed relative expression values of *ZmM19* in the genotypes 4F-350 CN 2, 4F-240 BX 16, E2558W and B77 over a period of 2 days in 4 h intervals under SD (left) and LD (right) conditions. Mean values of biological triplicates and the standard deviations (st dev) are indicated.

SD ZmM19	4F-350 CN2		4F-240 BX16		E2558W		B77	
time (h)	mean	st dev	mean	st dev	mean	st dev	mean	st dev
0	0,86	0,16	1,10	1,01	0,44	0,16	1,29	0,31
4	1,60	0,53	2,01	1,35	1,53	0,36	2,25	0,63
8	2,59	0,12	2,32	0,83	1,90	0,35	2,34	0,19
12	1,28	0,55	3,08	0,62	1,53	0,65	1,51	0,06
16	1,11	0,23	0,85	0,63	1,27	0,44	1,86	0,34
20	0,34	0,48	0,31	0,44	0,28	0,22	0,35	0,25
24	1,49	0,46	2,11	1,18	0,15	0,19	0,80	0,38
28	1,60	0,24	1,82	1,05	1,20	0,31	1,98	0,34
32	2,37	0,25	2,33	1,22	2,60	0,37	2,39	0,35
36	1,78	0,30	2,24	0,77	1,48	0,29	2,14	0,08
40	1,16	0,19	3,19	1,06	0,86	0,53	1,95	0,51
44	0,07	0,09	0,56	0,64	0,05	0,05	0,07	0,10
48	1,21	0,04	1,00	0,51	0,40	0,66	0,25	0,22

LD ZmM19	4F-350 CN2		4F-240 BX16		E2558W		B77	
time (h)	mean	st dev	mean	st dev	mean	st dev	mean	st dev
0	0,74	0,51	0,39	0,38	0,54	0,27	1,03	0,37
4	1,08	0,36	1,82	0,34	1,11	0,33	1,75	0,19
8	1,20	0,71	2,18	0,58	0,99	0,32	1,88	0,11
12	1,31	0,48	2,29	0,50	1,14	0,30	2,29	0,60
16	0,00	0,00	1,33	0,32	0,49	0,39	1,34	0,41
20	0,93	0,52	0,74	0,82	0,14	0,10	0,96	0,78
24	0,97	0,14	0,76	0,67	0,22	0,18	1,11	0,79
28	1,65	0,61	1,24	0,23	1,69	0,38	1,83	0,33
32	1,51	0,37	2,42	0,25	2,35	0,42	2,30	0,57
36	1,67	0,90	2,08	0,48	2,19	0,06	2,46	0,25
40	0,59	0,34	1,90	0,83	0,70	0,22	1,59	0,19
44	1,14	0,68	0,93	0,81	0,57	0,42	0,68	0,59
48	0,65	0,35	0,78	0,66	0,61	0,30	0,64	0,46

5.10. FUNCTIONAL ANALYSES OF *ZMMADS1* AND *ZMM26* IN MAIZE

To study the role of *ZmMADS1* and *ZmM26* for flowering time, overexpression constructs of both genes were generated under control of the ubiquitin promoter of maize (Christensen *et al*., 1992). Additionally an artificial microRNA construct was made against *ZmM26.* The three constructs, p*UBI*:*MADS1*, p*UBI*:*ZmM26* and p*UBI*:amiR-*ZmM26*, were sent to the Plant Transformation Facility at Iowa State University, where they were used for transformation of HiII A x HiII B F2 hybrid maize according to Frame *et al*. (2002). A fourth construct was planned to be transformed in Regensburg. An RNAi construct against the *ZmMADS1* coding region was generated using also the ubiquitin promoter as it was not possible to design a specific amiRNA against *ZmMADS1*. Unfortunately, the transformation was not successful as plants could not be generated. The Plant Transformation Facility delivered 35 plantlets bearing the p*UBI*:*MADS1* construct, 39 for p*UBI*:*ZmM26* and 51 for p*UBI*:amiR-*ZmM26*. Plantlets of the p*UBI*:*MADS1*, p*UBI*:*ZmM26* and p*UBI*:amiR-*ZmM26* transformations were derived from 6, 7 and 8 independent transformation events, respectively. Plantlets were genotyped and grown to maturity in the greenhouse and self-crossed if possible. If a self-cross was not possible, plants were crossed either with HiII A or HiII B. Because of space limitation in the greenhouse only a limited number of offspring could be grown in the next generation. To study the overexpression of *ZmMADS1* and down-regulation of *ZmM26*, offspring of 3 plants from 2 independent transformation events were each selected. In the case of overexpression studies of *ZmM26* offspring of 8 plants of in total 4 independent transformation events were selected. From these plants always 5 seeds were sown out in the greenhouse to analyze the next generation. These were 29 out of 30 seed germinated in case of p*UBI*:*MADS1* and 30 out of 40 in case of p*UBI*:*ZmM26*. All 30 *pUBI*:amiR-*ZmM26* seeds germinated. To make sure, that observed phenotypes were correlated with the transgene, RNA levels of *ZmMADS1* or *ZmM26* were determined in RNA extracts derived from the uppermost leaf 3 weeks after sowing (*Figure 25 A*, *C*, *E*). The expression levels were set into relation of the average expression level of 3 plants of HiII A and HiII B each, respectively. In the 29 p*Ubi*:*MADS1* plants *ZmMADS1* expression levels appeared 1.8 to 1,355.9 fold higher compared to the HiII control (*Figure 25 A*). Compared with the HiII control expression of *ZmM26* varied from 51.2 fold down-regulation to 2.85 fold higher expression in plants carrying the overexpression construct for *ZmM26* (*Figure 25 C*).

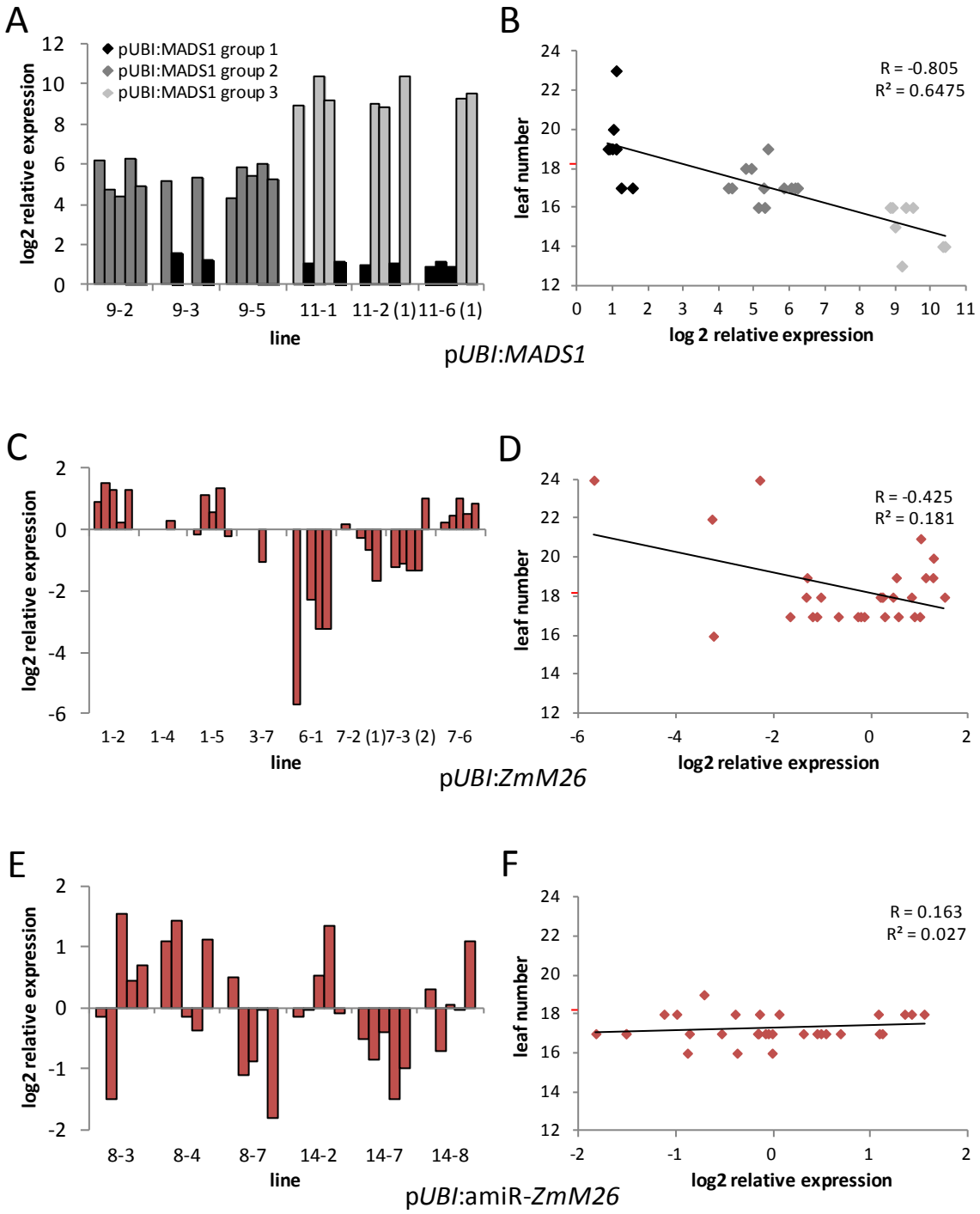

Figure 25. **Characterization of the transgenic maize plants bearing p*Ubi*:*MADS1* (A & B), p*Ubi*:*ZmM26* (C & D) and p*Ubi*:amiR-*ZmM26* (E & F).** (A, C, E) Log2 transformed expression values relative to the average expression of 3 HiII A and 3 HiII B plants of either *ZmMADS1* in transgenic maize plants carrying the p*Ubi*:*MADS1* construct (A), *ZmM26* in transgenic maize plants carrying the construct p*Ubi*:*ZmM26* (C) and p*Ubi*:amiR-*ZmM26* (E). 5 plants per line were sown out and every germinated plant was analyzed individually, shown in (A) black bars for p*UBI*:*MADS1* group 1, dark grey for group 2 and light green for group 3, in (C, E) red bars for *ZmM26*. (B, D, F) Correlation of leaf number and the log2 transformed relative expression values of the corresponding gene of plants carrying p*Ubi*:*MADS1* (B), p*Ubi*:*ZmM26* (D) and p*Ubi*:amiR-*ZmM26* (F) are shown. The regression line, the correlation coefficients (R) and the coefficients of determination (R^2) are indicated. Red mark at the y-axis indicates the mean value of 8 HiII F1 hybrid plants. Colors are as described for (A, C, E).

Expression of *ZmM26* in p*UBI*:amiR-*ZmM26* plants varied from 2.8 fold lower to 2.9 fold higher expression compared to the HiII control (*Figure 25 E*).

The total leaf number was observed as a characteristic trait for flowering time (*Figure 25 B*, *D*, *F*). Total leaf number for plants carrying the p*UBI*:*MADS1* construct was between 13 and 23 leaves per plant, for plants bearing the p*UBI*:*ZmM26* construct the number of leaves was between 16 and 24 and plants containing the p*UBI*:amiR-*ZmM26* construct had between 16 and 19 leaves. The leaf number correlates with the overexpression level of *ZmMADS1* with a correlation coefficient (R) of -0.805 in *ZmMADS1* overexpressing plants (*Figure 25 B*). Three groups of *ZmMADS1* overexpressing plants can be recognized in *Figure 25 B*. Firstly, a group with plants that are slightly overexpressing *ZmMADS1* (group 1: log2 relative expression < 3.3, black color code), secondly, a medium overexpressing group (group 2: 3.3 < log2 relative expression < 6.6, dark grey color code), and thirdly, a highly overexpressing group (group 3: 6.6 < log 2 relative expression, light grey color code). These three groups differ significantly from each other in the average leaf number ($p \leq 0.01$), having 19.1 (± 1.66); 17.2 (± 0.8) and 15.0 (± 1.12) leaves, respectively. This classification was kept for the rest of the analyses.

Leaf number correlates with the expression of *ZmM26* in p*UBI*:*ZmM26* plants with a correlation coefficient of -0.425, but this correlation is forced by only 3 plants, in which *ZmM26* is down-regulated by 4 to 50 times (log2 transformed -2 to -6) (*Figure 25 D*). The increased number of leaves in these three plants cannot be attributed to the action of the transgene, because increased leaf numbers appeared also in slightly overexpressing plants (*Figure 25 D*). The average leaf number in p*UBI*:*ZmM26* plants was 18.4 (± 1.99). F1 HiII hybrids showed an average leaf number of 18.1 (± 0.33) (n=8) in previous experiments in the greenhouse (data not shown). This difference is not significant.

In p*UBI*:amiR-*ZmM26* plants a significant trend was not visible regarding leaf number and expression level of *ZmM26*. These plants had 17.3 (± 0.68) leaves (*Figure 25 F*). Since a phenotype could not be observed in plants containing p*UBI*:*ZmM26* or p*UBI*:amiR-*ZmM26*, these plants/lines were later taken together as a control group (red color code). This plant material was probably closer related to the material of p*UBI*:*ZmMADS1* plants compared with our own HiII plant material, because it experienced the same transformation procedure. The average leaf number of this control group, which is called control hereafter, is 17.8 (± 1.59). This is significantly ($p \leq 0.05$) lower than the leaf number of the

overexpressing group 1 of *ZmMADS1* (19.1 (± 1.66)) and significantly higher ($p \leq 0.01$) than the highly overexpressing group 3 (15.0 (± 1.12)).

The time point of reaching developmental stage VT in days after emergence (DAE) was also observed as a characteristic trait for flowering time (*Table 10*). VT was reached when all tassel branches were fully visible, extended outwards and not held together by the upper leaves. The control group reached this stage 63.1 (± 5.28) DAE. The p*Ubi*:*MADS1* group 1 reached VT 66.7 (± 4.45) DAE, group 2 62.6 (± 11.53) DAE and group 3 56.7 (± 2.05). For group 3 this is significantly ($p \leq 0.01$) earlier compared with the control group (*Table 10*).

Table 10. **Flowering time in p*UBI*:*MADS1* plants.** Flowering time is given in days after emergence of plants until reaching VT, anthesis and R1 (silking). The height to the lowest branch of the tassels is given in cm. p*UBI*:*MADS1* group 1 plants have a log2 relative expression of *MADS1* ≤ 3.3, group 2 3.3 < log2 relative expression < 6.6 and group 3 log2 relative expression > 6.6. Mean values ± standard deviation are indicated, numbers of plants (n) is in parenthesis. Asterisks indicate highly significant differences ($p \leq 0.01$) to the control plants.

	Days to VT	Days to anthesis	Days to R1	Height in cm
p*UBI*:*MADS1* group 1	66.7 ± 4.45 (n = 9)	68.7 ± 4.55 (n = 9) *	79.3 ± 10.39 (n = 9)	243.2 ± 16.70 (n = 9) *
p*UBI*:*MADS1* group 2	62.6 ± 11.53 (n = 12)	66.2 ± 5.27 (n = 12)	77.2 ± 8.28 (n = 11)	221.3 ± 13.21 (n = 12)
p*UBI*:*MADS1* group 3	56.7 ± 2.05 (n = 7) *	57.7 ± 2.31 (n = 7) *	62.9 ± 4.91 (n = 8) *	160.6 ± 47.71 (n = 8) *
Control	63.1 ± 5.28 (n = 59)	64.3 ± 4.73 (n = 57)	78,7.7 ± 9.96 (n = 48)	224.7 ± 18.89 (n = 58)

The time to anthesis in DAE, *i. e*. flowering time of the male flower was analyzed in the transgenic lines as well (*Table 10*). A few plants of the control group and the p*UBI*:*MADS1* plants did not produce anthers at all. However, this cannot be assigned as a clear phenotype, because this phenomenon could be observed occasionally also for HiII A and HiII B plants in our greenhouse, indicating that this might be due to genetic background or suboptimal growth conditions. Therefore, these plants were excluded from this part of the analyses. Anthesis was observed in the control group 64.3 (± 4.73) DAE. The tassel of p*UBI*:*MADS1* group 1 started flowering after 68.7 (±4.55) days, group 2 after 66.2 (± 5.27) days and the third group after 57.7 (± 2.31) days. The three groups differed significantly ($p \leq 0.01$) from each other, while only group 2 did not differ significantly from the control group (*Table 10*). The time to anthesis correlated with the overexpression of *ZmMADS1* in all observed overexpressing plants with a correlation coefficient of -0.63.

The time to flower of the female flower was also determined in DAE (*Table 10*). Again, some plants are missing in the analyses, because on the first sight no cob was visible at these plants. The rest of the plants reached stage R1 in the control group at 78.7 (± 9.96) DAE, in the p*Ubi*:*MADS1* group 1 at 79.3 (± 10.39) DAE, in group 2 at 77.2 (± 8.28) DAE and in group 3 at 62.9 (± 4.91) DAE. The three *ZmMADS1* overexpressing groups differed again significantly ($p \leq 0.01$) from each other, but only group 3 differed also significantly from the control group (*Table 10*). The time to silking correlates with the overexpression of *ZmMADS1* with a correlation coefficient of -0.57.

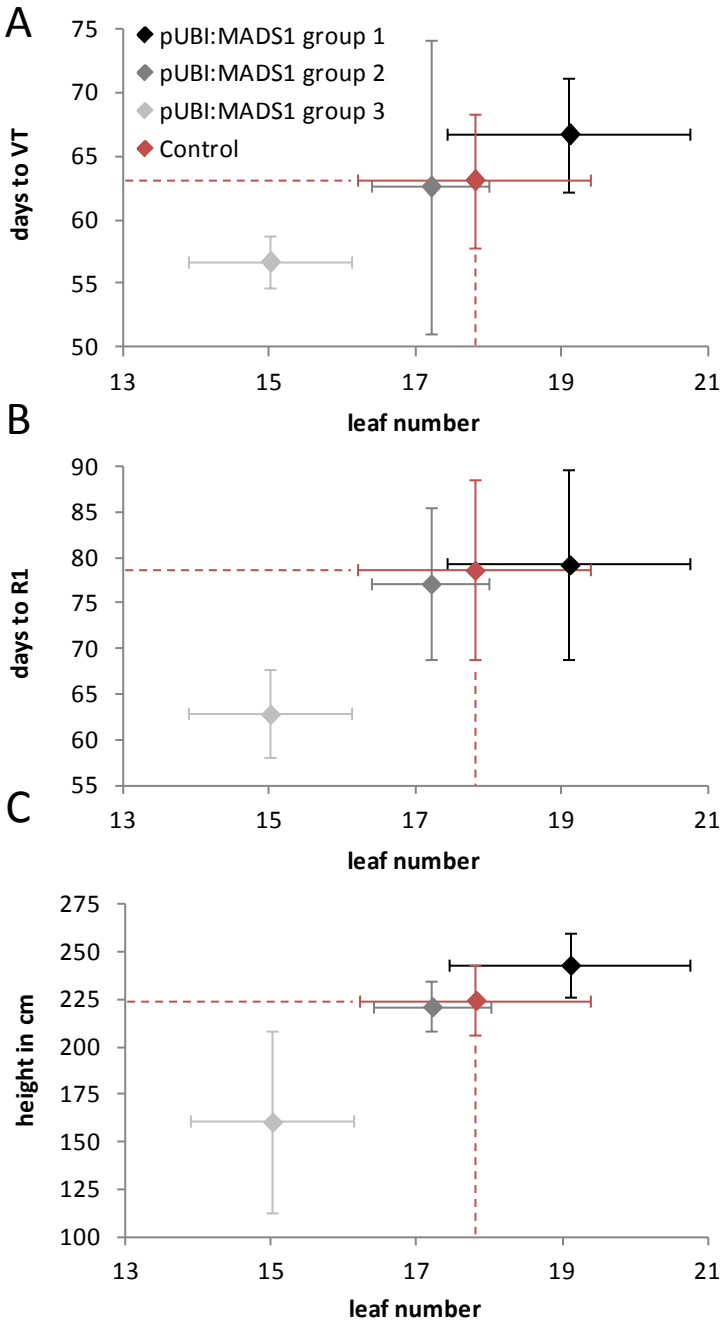

***Figure 26*. Correlations between leaf number and (A) time to reach VT (B) time to reach R1 and (C) plant height of *ZmMADS1* overexpression plants.** *ZmMADS1* overexpressing group 1 is shown in black, group 2 in dark grey, group 3 in light grey and the control group in red. The mean and the standard deviation of the total leaf number is indicated on the x – axis and mean and the standard deviation of one of the three above mentioned traits on the y – axis. The mean value of the control group is projected as dashed lines to the axis.

As a vegetative attribute plant height was measured from the growing substrate to the lowest branch of the tassel (*Table 10*). The control group grew 224.7 (± 18.89) cm high. The p*Ubi*:*MADS1* group 1 overexpressing plants reached a height of 243.2 (± 16.70) cm, group 2 plants 221.3 (± 13.21) cm and group 3 plants reached 160.6 (± 47.71) cm high. Again, all three groups differed significantly ($p \leq 0.01$) from each other and only group 2 plants did not differ significantly from the control group (*Table 10*). Plant height of all *ZmMADS1* overexpressing plants correlated with a correlation coefficient of -0.73 with the expression level of *ZmMADS1*.

Since the expression level of *ZmMADS1* correlated with leaf number (*Figure 25 B*) and with the traits days to VT, days to anthesis, days to R1, and plant height (*Table 10*), also a correlation of leaf number and days to VT, days to R1 and plant height could be detected (*Figure 26 A - C*).

In summary, *ZmMADS1* overexpression leads to an early flowering phenotype as illustrated by a reduced leaf number, a smaller plant height and shorter period to male and female flowering of transgenic maize lines compared to control plants. These data show that MADS1 represents a positive regulator of flowering time in maize.

6. DISCUSSION

The regulation of flowering time is a very complex mechanism: various endogenous and environmental signals are synchronized to induce flowering time at the right time to guarantee maximal reproductive success. Flowering time regulation is very well investigated in the long day (LD) model plant Arabidopsis and the short day (SD) plant rice, but little is known about these mechanisms in maize, which is generally considered as a day neutral (DN) plant species. Maize is however the most important crop since it is needed both for animal and human nutrition as well as an alternative energy resource. Maize yield largely depends on environmental conditions such as the length of the vegetation period and light intensity. The possibility to regulate the time of flowering and thus plant maturity can be one alternative to increase and sustain yield at unfavorable conditions. The aim of this work was to identify novel flowering time regulatory genes in maize leaves using comparative transcriptomics to study and eventually influence this trait.

6.1. COMPARATIVE TRANSCRIPTOMIC ANALYSES IDENTIFIED *ZMMADS1* AND *ZMM26* AS PUTATIVE FLOWERING TIME REGULATORS

The transcriptome data set showed that the concept of sampling time points and the selection of analyzed maize lines was very well chosen. Several possible flowering time regulatory genes were found in these analyses. These genes either have been shown already to play a role in flowering time in maize, or respective homologs from other species are important in flowering time regulation. *ZCN8,* for example, was found as an up-regulated putative candidate gene for the pair B77 and E2558W. The *FT* homolog *ZCN8* is a positive regulator of flowering time in maize (Danilevskaya *et al*., 2008a; Lazakis *et al*., 2011; Meng *et al*., 2011). Additionally to *ZCN8, ZmM19* appeared on the list as putative candidate for this pair. It has been shown by Wingen *et al*. (2012) that a mutation in the promoter of this gene leads to ectopic expression of *ZmM19* in glumes of pod corn (*Tunicate* maize) and thus to the development of leaf-like structures surrounding the kernels. *ZmM19* is a homolog of *SVP*, a negative regulator of flowering time in Arabidopsis (Hartmann *et al*., 2000). In the list of the pair 4F-240 BX 16 and 4F-350 CN 2 the flowering time regulator *ZmRelated to AP2.7*

(*ZmRAP2.7*) was found to be down-regulated. *ZmRAP2.7* encodes an AP2-like transcription factor, which represses flowering and was identified as a *cis*-regulatory downstream target of the major flowering time QTL *Vegetative to generative transition1* (*Vgt1*) (Salvi *et al*., 2007). *ZmRAP2.7* is orthologous to *RAP2.7*/*TOE1*, a transcription factor that regulates flowering time in Arabidopsis (Aukerman and Sakai, 2003; Okamuro *et al*., 1997). Also *ZCN21*, a gene family member of the phosphatidylethanolamine-binding protein (PEBP) FT-like II class candidate flowering time regulators (Danilevskaya *et al*., 2008a) was identified. However, a distinct function has not yet been described for *ZCN21*, because a transcript of this gene had not been detected before (Danilevskaya *et al*., 2008a).

The strongest proof that the transcriptome analyses resulted in putative flowering time regulatory genes is given by the nature of the candidates that were chosen for further investigations, because they showed the expected expression profile for a flowering activator in all four investigated maize lines. The expression of *ZmMADS1* (*MADS1* from maize), a homolog of the Arabidopsis key floral inductive pathway integrator *SOC1* (Borner *et al*., 2000; Lee *et al*., 2000; Moon *et al*., 2005; Samach *et al*. 2000; Yoo *et al*., 2005) and the flowering time regulators *SOC1*/*MADS50* (Lee *et al*., 2004) and *MADS56* (Ryu *et al*., 2009) from rice, is up-regulated at the time point of the floral transition similar to the expression pattern of *SOC1*/*MADS50* in whole shoots (Tadege *et al*. 2003) and *SOC1* in the shoot apical meristem (Lee *et al.*, 2000; Samach *et al*. 2000). In phylogenetic analyses *ZmMADS1* clusters in a clade with *OsMADS50* within the *SOC1*-like genes. The second candidates *ZmM26* and *ZmM19* are both homologs of the negative flowering time regulator *SVP* from Arabidopsis. *OsMADS22*, *OsMADS47* and *OsMADS55* are also homologs of *ZmM26* and *ZmM19*. Ectopic expression of *OsMADS22* was shown to alter meristem indeterminacy in rice spikelets (Sentoku *et al*., 2005) and leads to abnormal flower formation after expression in Arabidopsis (Lee *et al*., 2012). Overexpression of *OsMADS47* and *OsMADS55* in Arabidopsis leads to abnormal flower formation as well (*Fornara et al., 2008;* Lee *et al*., 2012), but in case of *OsMADS55* additionally to a delay in flowering induction (Lee *et al*., 2012). From these three MADS-box genes from rice, only *OsMADS55* is able to rescue the Arabidopsis *svp* early flowering phenotype (*Fornara et al., 2008;* Lee *et al*., 2012). *TaVRT-2*, a wheat homolog of *ZmM26*, is thought to repress floral transition in wheat (Kane *et al*., 2005). It has been shown for *HvBM1* and *HvBM10* that overexpression of these two genes leads to inhibitions of floral development and floral reversions in barley and also in Arabidopsis, where it leads

to floral reversion phenotypes (Trevaskis *et al.*, 2007). The expression level of the *SVP*-like genes in wheat leaves stays nearly constant and is decreasing over time in the shot apex (Trevaskis *et al.*, 2007). In rice leaves the expression level of *OsMADS47* decreases, while the level of *OsMADS55* increases and the one of *OsMADS22* stays constant (Lee *et al*., 2008a). As shown in this work, the expression level of *ZmM26* increased until the flowering meristem was determined. The comparison of overexpression phenotypes and the expression profiles indicate that the function of *SVP*-like genes is very diverse in maize, rice and barley, and only partly related to the function of *SVP* in Arabidopsis. *ZmM26*, *OsMADS22* and *BM10* are grouping to the same clade of *SVP*-like genes. This could be an example for divergent evolution.

ZmMADS1 and *ZmM26* both encode Type II MADS-box transcription factors of the MIKC^C group. MIKC^C group MADS-box genes are involved in diverse functions, but especially control reproduction in flowering plants. Amongst others, they are involved in determination of flowering time, like *AtSOC1* (Lee *et al.*, 2000; Samach *et al*. 2000), *AtSVP* (Hartmann *et al*., 2000), *AtAGL24* (Michaels *et al*., 2003; Liu *et al*., 2008; Yu *et al*., 2002) and *AtFLC* (Amasino, 2004; Searle *et al.*, 2006). MIKC^C group MADS-box genes are also playing important roles in the specification of floral meristem identity, like *AtAP1* (Irish & Sussex, 1990; Mandel *et al*., 1992; Weigel *et al*., 1992), *AtFUL* (Ferrandiz *et al*., 2000) and *AtSEP3* (Pelaz *et al*., 2000), floral organ identity, like *AtAP1* (Irish & Sussex, 1990; Mandel *et al*., 1992; Weigel *et al*., 1992), *AtSEP1* to *3* (Pelaz *et al*., 2000), and *AtAGAMOUS* (*AtAG*) (Bowman *et al*., 1989; Mizukami & Ma, 1992), and fruit formation, like *AtFUL* (Gu *et al*., 1998), *AtSHATTERPROOF1* (*AtSHP1*) and *AtSHP2* (Liljegren *et al*., 2000).

All these lines of evidence for a successful initial experiment justify proceeding with the objective of the identification and characterization of novel flowering time regulators in maize.

6.2. *ZMMADS1* RESCUES THE ARABIDOPSIS *SOC1-2* FLOWERING TIME PHENOTYPE

The indication that *ZmMADS1* is a flowering time regulatory gene is given by the fact that ectopic expression of *ZmMADS1* is able to induce early flowering in *Arabidopsis thaliana* under LD and SD conditions. Additionally ZmMADS1 is also able to rescue the late flowering phenotype of the Arabidopsis *soc1-2* mutant. Induction of early flowering by *ZmMADS1*

seems to be dosage dependent, because flowering time phenotypes varied in strength, as it has been reported for *AtSOC1* itself (Borner *et al*., 2000). To clarify whether the distinct rescue phenotypes are indeed dosage dependent, the expression level of *ZmMADS1* in these lines needs to be examined in future experiments.

Overexpression of *AtSOC1* in Arabidopsis leads to flowering after only 4-5 rosette leaves formed in the most severe lines (Borner *et al*., 2000). Such extreme events were also observed in the T0 generation of ectopically expressed *ZmMADS1* driven by the *CaMV35S* promoter in both wild-type and *soc1-2* background (data not shown). These extreme events came along with sterility, caused by elongated pistils, which prevented self-pollination. Similarly, this sterility phenotype has also been observed for overexpression of *AtSOC1* (Borner *et al*., 2000) and *OsSOC1*/*OsMADS50* (Tadege *et al*., 2003). Due to the sterility phenotypes, these lines could not be included in further flowering time analyses, for which the T1 generation was used. Consequently, the mean values regarding flowering time were rather overestimated and the strength of the phenotype likely underestimated, respectively.

6.3. CELLULAR AND SUBCELLULAR LOCALIZATION

Immunolocalization experiments revealed that the ZmMADS1 protein might be present in high amounts in the bundle sheath cells surrounding the vasculature in the leaves, but also in lower concentration in other tissues. For *SOC1* mRNA it has been reported, that it is present in most tissues of the mature Arabidopsis plant (Borner *et al*., 2000; Lee *et al*., 2000; Samach *et al*. 2000). In p*SOC1*:*GUS* studies this expression pattern has been confirmed, with the strongest GUS staining in the SAM and RAM region and in major veins (Hepworth *et al*., 2002; Immink *et al*., 2012; Michaels *et al*., 2005; Yoo *et al*., 2005). Protein localization cannot always easily be compared to mRNA localization, but mRNA localization often shows a similar expression pattern and at least provides a hint, where the protein can be found, too. Additionally, it is difficult to compare mRNA and protein localization in an eudicot C3-leaf with the localization in a grass C4-leaf with its peculiar architecture, especially the existence of bundle sheath surrounding the vasculature. It has been shown that the rice *FT* homologs, *HD3a* and *RFT1*, are downstream targets of rice *SOC1* homologs *OsMADS50* and *OsMADS56* (Komiya *et al.*, 2009; Lee *et al*., 2004; Ryu *et al*., 2009). Reporter fusion proteins of RFT1 and HD3a are found in the vascular tissue of rice leaf blades (Komiya *et al*., 2008; Tamaki *et al*.,

2007), similar to the mRNA of the maize *FT* homolog *ZCN8* (Meng *et al*., 2011). It has been shown further that it is sufficient to induce flowering in rice, when *HD3a* is expressed in cells near the phloem (Tamaki *et al*., 2007). If *ZmMADS1* has the same function of activating floral transition in the leaf, like *OSMADS50* and *OsMADS56*, this could be regulated in the bundle sheath cells. It is thus conceivable that either ZmMADS1 moves from the bundle sheath cells into the vasculature and activates *ZCN8* expression directly, or this happens indirectly by the activation of other genes, like in rice where *OSMADS50* and *OsMADS56* activate *EHD1*, which in turn activates *HD3a* and *RFT1* (Doi *et al*., 2004). Since it was not possible to exclude that the signals are derived from cross reactions of the immune serum with other proteins, transgenic maize lines driving the expressing of *GUS* or a *MADS1-GFP* fusion protein under control of the endogenous *ZmMADS1* promoter could be used to analyze its localization during floral transition in more detail.

In case of ZmM26 a clear statement cannot be given, because it seems that there is no specific antibody in the crude antiserum able to detect the ZmM26 protein. A recombinant protein will be needed to investigate whether the peptide antibody is able to recognize the entire ZmM26 protein. The peptide, which was used for immunization, can be detected by the crude antiserum, as well as by a purified antiserum. Another possibility is that the protein amount of ZmM26 in leaf tissues is below the detection limit for fluorophore-based immunohistochemistry. Also here a transgenic approach using a ZmM26 protein reporter fusion under control of the endogenous *ZmM26* promoter would be very helpful to overcome this problem.

ZmMADS1-GFP fusion protein was shown to be localized to the nucleus when expressed in Arabidopsis or tobacco leaf epidermis cells. The fluorescence signal of the overexpressed fusion protein appeared in a dotted pattern within the nucleus. A similar nuclear localization pattern was observed when the MADS-box protein *FBP9* fused to *YFP* was overexpressed in petunia leaf protoplasts (Immink *et al.*, 2002). Nuclear localization in general is in agreement with findings for other MADS-box genes. For AtSOC1, for example, it has been shown using bimolecular fluorescence complementation (BiFC) that it interacts in the nucleus with SAP18 (Liu *et al*., 2009). OsMADS50 and OsMADS56 are nuclear localized as well (Ryu *et al*., 2009). Also rice SVP-like proteins OsMADS22, OsMADS47 and OsMADS55 localize to the nucleus of onion epidermal cells and rice protoplasts (Lee *et al*., 2008b). MADS-domain proteins are expected to be located in the nucleus because several nuclear localization signals (NLS) have

been reported in the MADS-domain (Gauthier-Rouviere *et al*., 1995; Immink *et al*., 2002; McGonigle *et al*., 1996). In 6,668 MADS domain proteins the most prominent NLS is a KR[K/R]X_4KK motif at position 22 to 30 (Gramzow & Theissen, 2010). This motif can also be found at the described position in ZmMADS1 and ZmM26 in all analyzed genotypes.

6.4. ZMMADS1 PROTEIN ABUNDANCE MIGHT BE REGULATED BY DAY TIME

Protein abundance of ZmMADS1 could be regulated by day time. In western blot analyzes it was not possible to detect protein bands of the size corresponding to the calculated molecular weight of the ZmMADS1 monomer (26.4 kDa). Since the protein extract was made from whole leaves, which contains several tissues, and the ZmMADS1 protein might be mainly in vascular tissues, it is possible that ZmMADS1 was diluted too strongly, that it was not possible to detect ZmMADS1 in the western blot. However, a signal with an apparent molecular weight of approximately 90 kDa was detectable. This band was fluctuating in intensity over the day in a continuous way over a period of two days, with the maximum at 4 hours after dawn. A second strong band at the height of 55 kDa was constantly visible. Most likely, the 55 kDa band represents the large subunit of RuBisCo. Possibly, the fluctuating band might be a higher-order complex containing ZmMADS1. Generally, protein complexes should not occur under denaturing conditions. It is thought that the interaction of MADS-box proteins is mainly mediated by hydrophobic and some charged amino acid residues of the K domain of MIKC-type of MADS-box proteins (reviewed by Kaufmann *et al*., 2005) and that the formation of higher-order complexes is only possible when two CArG-boxes are present at a promoter (reviewed by de Folter & Angenent, 2006). It could be possible, however, that there was still DNA in the protein extract as a DNase-treatment was not performed, promoting the formation of higher-order complexes. Nevertheless, it has already been shown for FLC, that it is possible to detect monomers of MADS-box proteins of the correct size using western blots. However, these studies were performed using overexpressing Arabidopsis lines (Helliwell *et al*., 2006). So far, the presence of ZmMADS1 could not be confirmed. A positive control in form of a recombinant ZmMADS1 protein would help to show that the peptide antibody is able to specifically detect the ZmMADS1 protein. Until now only the peptide, which was used for immunization, could be used as a positive control and the peptide was indeed detected by the antiserum. The

putative complex could be purified from the protein extract using the antiserum coupled to a sepharose column, afterwards digested with trypsin and mass spectrometrically analyzed using matrix-assisted laser desorption/ionization. So it would be possible to confirm whether ZmMADS1 is present in this complex. This approach may also help to identify putative interaction partners.

6.5. *ZMM26* IS NOT INVOLVED IN LD-DEPENDENT FLOWERING TIME REGULATION

It was not possible to identify a response of *ZmM26* expression to length of day or day time in the lines 4F-249 BX 16, 4F-350 CN 2, B77 or E2558W. It is possible, that *ZmM26* is not involved in photoperiodic flowering time regulation, similar to the *SVP*-like genes *OsMADS22*, *OsMADS47* and *OsMADS55* in rice (Duan *et al*., 2006; Lee *et al*., 2008a) that rather play a role in the brassinosteroid response. Although the influence of brassinosteroid signals on flowering time in Arabidopsis is discussed (reviewed by Li *et al*., 2010) and *OsMADS55* is able to rescue the *svp* mutant flowering time phenotype in Arabidopsis (*Fornara et al., 2008;* Lee *et al*., 2012), a role in flowering time regulation in rice has not been shown for *OsMADS22*, *OsMADS47* and *OsMADS55*. However, overexpression of *OsMADS55* leads to the formation of abnormal florets (Lee *et al*., 2008a). Also the three barley *SVP*-like genes *BM1*, *BM10* and *HvVRT2* are not involved in the regulation of the time point of floral transition. Instead, overexpression of *BM1* or *BM10* leads to an inhibition of floral development and to floral reversions (Trevaskis *et al*., 2007). From these three *SVP*-like genes it has been further shown, that they are not diurnal expressed (Trevaskis *et al*., 2007). It might thus be that ZmM26 plays a role in one of the pathways of flowering time regulation, but not in the four maize genotypes investigated during this work, which do not respond to this pathway. However, the photoperiodic pathway can be excluded here since all four genotypes react to changes in day length by the reduction of leaf number.

In contrast to the results of *ZmM26*, the expression analyses of the second investigated maize *SVP*-like gene *ZmM19* showed that this transcript is regulated by day time, albeit this seems to occur in a photoperiod-independent manner. To clarify this hypothesis, the expression pattern should be analyzed in 8 h light / 16 h dark SD condition, instead of a 12 h light / 12 h dark SD condition like in this work to see a potentially stronger effect. It was difficult to recognize a difference in the expression of *ZmM19* by changing the day length

just by four hours particularly since the expression maximum of *ZmM19* was observed shortly before the end of the day and seems to be influenced by natural variations. Further clarification about the role of *ZmM19* in flowering time regulation will require transgenic approaches or complementation assays in Arabidopsis.

Transgenic maize lines with different expression levels of *ZmM26* did not show a significant phenotype suggesting that *ZmM26* is not a flowering time regulator. However, the amiRNA construct might also be not functional and the differences in the expression level might be caused by variations among plants. Down-regulation of *ZmM26* expression in *ZmM26* overexpressing lines can be explained by the phenomenon called co-suppression, which was first described by Napoli *et al*. (1990) and finally led to the discovery of RNA interference (Fire *et al*., 1998). However, down-regulation of *ZmM26* does not lead to a change in flowering time. During this work no analyses were done investigating a putative involvement in the brassinosteroid response that was reported to play a role for the rice *SVP*-like genes *OsMADS22*, *OsMADS47* and *OsMADS55* (Duan *et al*. 2006; Lee *et al*., 2008). This should be considered in future experiments, which should also involve all maize *SVP*-like genes. Taken together, the expression analyses and functional studies performed in this work suggest that *ZmM26* is not involved in flowering time regulation in maize.

6.6. EXPRESSION OF *ZMMADS1* IS INFLUENCED BY DAY LENGTH

The regulation of the ZmMADS1 protein by day time or length could not be finally clarified, but the regulation of the *ZmMADS1* transcript was obvious. Expression of *ZmMADS1* was diurnally regulated in leaves in LD and SD conditions. Expression maximum was at dawn both under SD and LD conditions. Remarkably, the difference between maximum and minimum was higher in SD condition indicating a more prominent role for flowering under SD condition in maize. *OsMADS50* and *OsMADS56* are also diurnally regulated with a peak at dawn (Ryu *et al*., 2009). Here only a 14 h light / 10 h dark period representing LD condition was analyzed. In addition to the expression pattern, its levels are also comparable. In rice a 4-fold difference for *OSMADS56* and an 8-fold difference for *OsMADS50* was reported (Ryu *et al*., 2009). In the maize lines used here, the differences were in the same range with 3- to 9-fold in LD and 6- to 16-fold in SD condition. Since the day lengths used in the rice and in this maize experiment are not identical, the experiments

cannot be directly compared. Nevertheless, this is another indication that *ZmMADS1* could have a similar role compared with *OsMADS50* and *OsMADS56*.

The other two *SOC1*-like genes in maize, *ZmMADS56* and a not further characterized gene with the identifier GRMZM2G070034 do not respond to day length or time. This could have two reasons, either this is a genotypic effect, like shown for the expression of *ZCN8*, where a dirurnal regulation is only detectable in some genotypes (Meng *et al*., 2011), or both of these genes do not act antagonistically to *ZmMADS1* in flowering time regulation like rice *OsMADS50* and *OsMADS56* do. In future experiments the capability of these genes to complement Arabidopsis *soc1* mutants should be studied as well as overexpression and down-regulation approaches directly in maize.

6.7. *ZMMADS1* OVEREXPRESSION RESULTS IN CHANGES OF FLOWERING TIME IN A DOSAGE DEPENDENT MANNER

To interpret different flowering time phenotypes, which were observed in *ZmMADS1* overexpressing maize plants, it was planned to compare these with transgenic maize plants expressing a *ZmMADS1*-RNAi construct. Unfortunately, transformation of maize with the latter construct was not successful. This could be due to some smaller differences in handling during the transformation process compared to the original transformation procedure published by Frame *et al*. (2002). Possibly, a different combination of vector and Agrobacterium strain could also have caused a problem. In this work the pTF101.1 vector was used (Paz *et al.*, 2004) together with the *Agrobacterium tumefaciens* strain LB4404, while the Plant Transformation Facility at the Iowa State University uses this vector and the strain EHA101. Plant material used for transformation could also have a large impact on transformation success and efficiency. Originally, immature HiII F2 hybrid embryos are used for transformation, while in this work F1 hybrids were used for the transformation procedure. According publicly available information, HiII A and B are both partially inbred lines selected from a cross between A188 and B73 (Armstrong et al., 1991). Due to self-propagation of the plant material, the material used in this work became inbred lines, which could be counterproductive. It could also be possible that the plant material was stressed by environmental factors during growth in the greenhouse resulting in unsuccessful

transformation. After all, it should also be taken into account that *ZmMADS1* could play an important role during plant regeneration, and that the absence of *ZmMADS1* disrupts plant regeneration. The last hypothesis could be tested and studied whether the expression level of *ZmMADS1* is reduced in putative transgenic calli. In future experiments this problem could be circumvented if the RNAi construct is driven by an inducible promoter, which can be activated later during plant growth.

Overexpressing of *ZmMADS1* in maize showed that flowering time changed depending on the extent of overexpression. When overexpression was less than 10-fold, flowering time was delayed, considering leaf number and the time until anthesis, indicating that *ZmMADS1* represses flowering time. When *ZmMADS1* was overexpressed between 10-fold and 100-fold, a slight difference in flowering time could be discovered. Based on these finding one could interpret that *ZmMADS1* is not a flowering time regulator. However, if *ZmMADS1* was overexpressed more than 100-fold, flowering time, leaf number, days to VT, days to anthesis and days to R1, were reduced drastically. The effect was not as strong as for *OsMADS50*, where a flowering callus has been observed (Lee *et al*., 2004). But in maize flowering time is thought to be controlled by small additive QTLs with few genetically or environmental interactions (Buckler *et al*., 2009) and therefore changes in the expression of a single gene would not be expected to have a huge impact on flowering time.

So far the strongest flowering time regulator in maize is *ZmID1* (Colasanti *et al.,* 1998). In the field, *id1* mutants produce about 18 leaves more compared with control plants (Danilevskaya *et al*., 2008b). The phenotype of EMS-mutagenesis derived *zmdlf1* mutants is slightly weaker with a delay in flowering by about 10 to 14 days and 5 to 8 additional leaves, depending on the mutant allele and the genetic background (Muszynski *et al*., 2006). Flowering after *ZmRAP2.7* overexpression was delayed in the T0 generation by 1 to more than 4 weeks and these plants contained 2 to 5 additional leaves (Salvi *et al*., 2007). *ZmRAP2.7* RNAi plants showed about 5 leaves less compared to control plants (Salvi *et al*., 2007). Plants overexpressing *ZmM4* flowered in the field on average 5 days earlier and had 2 leaves less than non-transgenic control plants (Hi-Type II maize) (Danilevskaya *et al*., 2008b). The ectopic overexpression of *ZCN8* in the SAM leads to the production of 1-2 fewer leaves compared to non-transgenic control plants (Meng *et al*., 2011). Also *gigz1a /zmgi1 Mutator* insertion lines show a reduced leaf number by 1 or 2 leaves depending on the strength of the mutant allele (Bendix *et al*., 2013). Comparing these phenotypes with the *ZmMADS1*

overexpressing phenotype, a reduction of the time to anthesis of 7 days and a reduction in leaf number by 3 indicates a rather strong flowering time phenotype for maize. In comparison, the effect of *ZmMADS1* on flowering time seems not as strong as *ZmID1*, *ZmDLF1* and *ZmRAP2.7*, but stronger than *ZmM4, GIGZ1a*/*ZmGI1* and *ZCN8*. Since the phenotypic data of *ZmMADS1* overexpressing plants are collected in LD condition, it would now be interesting to study, if the phenotype becomes even more pronounced in SD condition and whether *ZmMADS1* is a regulator in a short day dependent flowering time regulatory pathway.

A major open question remains: Why is flowering time delayed if *ZmMADS1* is just slightly overexpressed? The answer may be that *ZmMADS1* represses a more prominent long day dependent flowering activation pathway and acts itself as an activator of a less prominent perhaps short day dependent flowering activation pathway (*Figure 1*). A slight overexpression of *ZmMADS1* thus would increase the inhibitory effect and the less prominent *ZmMADS1* pathway needs to take over the flowering activation, which would reduce, for example, leaf number. With a dosage depend flowering activation by *ZmMADS1*, flowering time would become comparable to wild type levels. However, when *ZmMADS1* overexpression is much stronger finally flowering time is reduced (*Figure 27*).

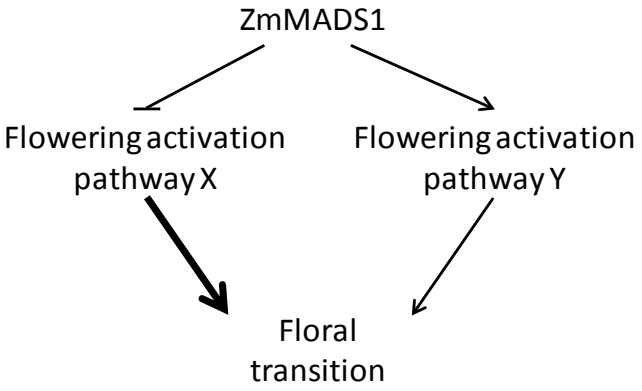

Figure 27. **Working model for ZmMADS1 function in long day dependent flowering time regulation.** Arrows indicate positive regulation, T bars indicate negative regulation. Thickness of the arrows is proportional to the influence on regulating the floral transition. *ZmMADS1* is a positive regulator in pathway Y, while it is influencing pathway X negatively. The main regulation of LD dependent flowering is performed by pathway X, so that ZmMADS1 and pathway Y are playing a minor role. A strong increase in the concentration of ZmMADS1 leads to a stronger repression of pathway X and a more pronounced flowering time regulation of pathway Y.

6.8. OUTLOOK

6.8.1. THE FUTURE FOR ZMMADS1 RESEARCH

The further characterization of *ZmMADS1* will be an interesting and challenging work. The main goal should be to integrate *ZmMADS1* in the flowering time regulatory network of maize. This could be done by first analyzing *ZmMADS1* overexpressing plants regarding a function in SD dependent flowering time activation and to compare this with the LD results obtained in this work. Crosses of *ZmMADS1* overexpressing plants with other flowering time maize mutants, especially *id1* and *gi1*, can give first indications in which pathway *ZmMADS1* is active. This information could be supported by expression analyses of known flowering time regulatory genes like *ZmGI1*, *ZCN8* and *ZmID1* in *ZmMADS1* overexpressing plants.

A *ZmMADS1* knock down phenotype should be analyzed to further confirm its function in flowering time regulation. Therefore, transformation of the RNAi construct against *ZmMADS1* has to be repeated. To confirm immunolocalization data and to use these plants for immunoprecipitation assays and identification of interacting proteins, transgenic plants could be generated expressing a translational fusion of *ZmMADS1* with either *GFP* or *GUS* driven by the *ZmMADS1* promoter. When the information about interaction partner is gained, chromatin immunoprecipitation (ChIP) assays could be performed to identify downstream targets of *ZmMADS1*. Antibodies against recombinant ZmMADS1 would be the best tool to confirm the data of the protein accumulation analysis in the day course experiments. Such antibodies could also be used to confirm the immunolocalization studies and ChIP experiments. Moreover, immunolocalization data could be compared to *in situ* hybridization assays to analyze if there are local differences in transcription and translation.

The analysis of upstream regulation of *ZmMADS1* is also a very interesting topic for further research. This work could be started with the analysis of the promoter sequence by screening for common sequence motifs *in silico*. This could then be followed by a yeast one-hybrid screen to identify transcriptional regulators binding at *cis*-elements in the *ZmMADS1* promoter region.

6.8.2. OUTLOOK FOR FUTURE STUDIES ABOUT THE MAIZE *SVP*-LIKE GENES

Since the analyses made for the *SVP*-like gene *ZmM26* did not reveal a function in flowering time in maize it would be very interesting now to investigate the actual function of

ZmM26 and the other maize *SVP*-like genes *ZmM19*, *ZmM21* and *ZmMADS47*. At least *ZmM19* should be included in future research studies, because the oligo on the microarray (OptiV1S21916), which detected *ZmM26* as a putative candidate, is also able to detect *ZmM19* with a sequence identity of 100%. It would be reasonable to start with complementation assays using the Arabidopsis *svp* mutant, even if such experiments were not successful for the rice *SVP*-like genes and their function in rice. However, these experiments would provide a hint, which of the four genes could have the most important role during flowering time. Additional complementation studies could be performed in Arabidopsis mutants, which are disturbed in their brassinosteroid response. After identifying the most interesting candidate, transgenic maize plant overexpressing and down-regulating the respective gene would show if there is a function in maize. It could then also be elucidated whether there is a function related to the regulation of flowering time, like in Arabidopsis, or if there is a function related to the brassinosteroid response, like in rice, or if there is a completely different function.

7. BIBLIOGRAPHY

Abe M, Kobayashi Y, Yamamoto S, Daimon Y, Yamaguchi A, Ikeda Y, Ichinoki H, Notaguchi M, Goto K, Araki T (2005) FD, a bZIP protein mediating signals from the floral pathway integrator FT at the shoot apex. *Science* **309:** 1052-1056

Abendroth LJ, R.W. Elmore, M.J. Boyer, S.K. Marley (2011) Corn growth and development. PMR 1009. *Iowa State University Extension, Ames, Iowa*

Amasino R (2004) Vernalization, competence, and the epigenetic memory of winter. *The Plant Cell* **16:** 2553-2559

Armstrong CL, Green CE, Philipps RL (1991) Development and availability of germplasm with high Type II culture formation response. *MNL* **65:** 92-93

Aukerman MJ, Sakai H (2003) Regulation of flowering time and floral organ identity by a microRNA and its *APETALA2*-like target genes. *The Plant Cell* **15:** 2730-2741

Bartetzko V, Sonnewald S, Vogel F, Hartner K, Stadler R, Hammes UZ, Bornke F (2009) The *Xanthomonas campestris* pv. *vesicatoria* type III effector protein XopJ inhibits protein secretion: evidence for interference with cell wall-associated defense responses. *Molecular Plant-Microbe Interactions* **22:** 655-664

Bendix C, Mendoza JM, Stanley DN, Meeley R, Harmon FG (2013) The circadian clock-associated gene *gigantea1* affects maize developmental transitions. *Plant Cell and Environment* **36:** 1379-1390

Borner R, Kampmann G, Chandler J, Gleissner R, Wisman E, Apel K, Melzer S (2000) A MADS domain gene involved in the transition to flowering in Arabidopsis. *The Plant Journal* **24:** 591-599

Bowman JL, Smyth DR, Meyerowitz EM (1989) Genes directing flower development in Arabidopsis. *The Plant Cell* **1:** 37-52

Bradford MM (1976) A rapid and sensitive method for the quantitation of microgram quantities of protein utilizing the principle of protein-dye binding. *Analytical Biochemistry* **72:** 248-254

Buckler ES, Holland JB, Bradbury PJ, Acharya CB, Brown PJ, Browne C, Ersoz E, Flint-Garcia S, Garcia A, Glaubitz JC, Goodman MM, Harjes C, Guill K, Kroon DE, Larsson S, Lepak NK, Li H, Mitchell SE, Pressoir G, Peiffer JA, Rosas MO, Rocheford TR, Cinta Romay M, Romero S, Salvo S, Sanchez Villeda H, da Silva HS, Sun Q, Tian F, Upadyayula N, Ware D, Yates H, Yu J, Zhang Z, Kresovich S, McMullen MD (2009) The genetic architecture of maize flowering time. *Science* **325:** 714-718

Chailakhyan MK (1936) New facts in support of the hormonal theory of plant development. *Proceedings of the USSR Academy of Sciences* **13:** 79-83

Christensen AH, Sharrock RA, Quail PH (1992) Maize polyubiquitin genes: structure, thermal perturbation of expression and transcript splicing, and promoter activity following transfer to protoplasts by electroporation. *Plant Molecular Biology* **18:** 675-689

Clough SJ, Bent AF (1998) Floral dip: a simplified method for Agrobacterium-mediated transformation of *Arabidopsis thaliana*. *The Plant Journal* **16:** 735-743

Colasanti J, Coneva V (2009) Mechanisms of floral induction in grasses: something borrowed, something new. *Plant Physiology* **149:** 56-62

Colasanti J, Tremblay R, Wong AYM, Coneva V, Kozaki A, Mable BK (2006) The maize *INDETERMINATE1* flowering time regulator defines a highly conserved zinc finger protein family in higher plants. *BMC Genomics* **7:** 17

Colasanti J, Yuan Z, Sundaresan V (1998) The *indeterminate* gene encodes a zinc finger protein and regulates a leaf-generated signal required for the transition to flowering in maize. *Cell* **93:** 593-603

Corbesier L, Vincent C, Jang SH, Fornara F, Fan QZ, Searle I, Giakountis A, Farrona S, Gissot L, Turnbull C, Coupland G (2007) FT protein movement contributes to long-distance signaling in floral induction of Arabidopsis. *Science* **316:** 1030-1033

Danilevskaya ON, Meng X, Hou ZL, Ananiev EV, Simmons CR (2008) A genomic and expression compendium of the expanded *PEBP* gene family from maize. *Plant Physiology* **146:** 250-264

Danilevskaya ON, Meng X, Selinger DA, Deschamps S, Hermon P, Vansant G, Gupta R, Ananiev EV, Muszynski MG (2008) Involvement of the MADS-Box gene *ZMM4* in floral induction and inflorescence development in maize. *Plant Physiology* **147:** 2054-2069

de Folter S, Angenent GC (2006) *trans* meets *cis* in MADS science. *Trends in Plant Science* **11:** 224-231

Doi K, Izawa T, Fuse T, Yamanouchi U, Kubo T, Shimatani Z, Yano M, Yoshimura A (2004) *Ehd1*, a B-type response regulator in rice, confers short-day promotion of flowering and controls *FT*-like gene expression independently of *Hd1*. *Genes & Development* **18:** 926-936

Dong ZS, Danilevskaya O, Abadie T, Messina C, Coles N, Cooper M (2012) A gene regulatory network model for floral transition of the shoot apex in maize and its dynamic modeling. *PLoS One* **7 (8):** e43450. doi:10.1371/journal.pone.0043450

Duan K, Li L, Hu P, Xu SP, Xu ZH, Xue HW (2006) A brassinolide-suppressed rice MADS-box transcription factor, OsMDP1, has a negative regulatory role in BR signaling. *The Plant Journal* **47:** 519-531

Edwards K, Johnstone C, Thompson C (1991) A simple and rapid method for the preparation of plant genomic DNA for PCR analysis. *Nucleic Acids Research* **19:** 1349-1349

Emerson RA (1924) Control of flowering in teosite. *Journal of Heredity* **15:** 41-48

Ferrandiz C, Gu Q, Martienssen R, Yanofsky MF (2000) Redundant regulation of meristem identity and plant architecture by *FRUITFULL*, *APETALA1* and *CAULIFLOWER*. *Development* **127:** 725-734

Fire A, Xu SQ, Montgomery MK, Kostas SA, Driver SE, Mello CC (1998) Potent and specific genetic interference by double-stranded RNA in *Caenorhabditis elegans*. *Nature* **391:** 806-811

Fornara F, Gregis V, Pelucchi N, Colombo L, Kater M (2008) The rice *StMADS11*-like genes *OsMADS22* and *OsMADS47* cause floral reversions in Arabidopsis without complementing the *svp* and *agl24* mutants. *Journal of Experimental Botany* **59:** 2181-2190

Fowler S, Lee K, Onouchi H, Samach A, Richardson K, Coupland G, Putterill J (1999) *GIGANTEA*: a circadian clock-controlled gene that regulates photoperiodic flowering in Arabidopsis and encodes a protein with several possible membrane-spanning domains. *The EMBO Journal* **18:** 4679-4688

Frame BR, Shou HX, Chikwamba RK, Zhang ZY, Xiang CB, Fonger TM, Pegg SEK, Li BC, Nettleton DS, Pei DQ, Wang K (2002) *Agrobacterium tumefaciens*-mediated transformation of maize embryos using a standard binary vector system. *Plant Physiology* **129:** 13-22

Gauthierrouviere C, Vandromme M, Lautredou N, Cai QQ, Girard F, Fernandez A, Lamb N (1995) The serum response factor nuclear-localization signal: general implications for cyclic-AMP-dependent protein-kinase activity in control of nuclear translocation. *Molecular and Cellular Biology* **15:** 433-444

Gouy M, Guindon S, Gascuel O (2010) SeaView Version 4: A multiplatform graphical user interface for sequence alignment and phylogenetic tree building. *Molecular Biology and Evolution* **27:** 221-224

Gramzow L, Theissen G (2010) A hitchhiker's guide to the MADS world of plants. *Genome Biology* **11:** 214

Gu Q, Ferrandiz C, Yanofsky MF, Martienssen R (1998) The *FRUITFULL* MADS-box gene mediates cell differentiation during Arabidopsis fruit development. *Development* **125:** 1509-1517

Hartmann U, Hohmann S, Nettesheim K, Wisman E, Saedler H, Huijser P (2000) Molecular cloning of *SVP*: a negative regulator of the floral transition in Arabidopsis. *The Plant Journal* **21:** 351-360

Hepworth SR, Valverde F, Ravenscroft D, Mouradov A, Coupland G (2002) Antagonistic regulation of flowering-time gene *SOC1* by *CONSTANS* and *FLC* via separate promoter motifs. *The EMBO Journal* **21:** 4327-4337

Heuer S, Hansen S, Bantin J, Brettschneider R, Kranz E, Lorz H, Dresselhaus T (2001) The maize MADS box gene *ZmMADS3* affects node number and spikelet development and is co-expressed with *ZmMADS1* during flower development, in egg cells, and early embryogenesis. *Plant Physiology* **127:** 33-45

Hofgen R, Willmitzer L (1988) Storage of competent cells for Agrobacterium transformation. *Nucleic Acids Research* **16:** 9877-9877

Immink RGH, Gadella TWJ, Ferrario S, Busscher M, Angenent GC (2002) Analysis of MADS box protein-protein interactions in living plant cells. *Proceedings of the National Academy of Sciences of the United States of America* **99:** 2416-2421

Immink RGH, Pose D, Ferrario S, Ott F, Kaufmann K, Valentim FL, de Folter S, van der Wal F, van Dijk ADJ, Schmid M, Angenent GC (2012) Characterization of SOC1's central role in flowering by the identification of its upstream and downstream regulators. *Plant Physiology* **160:** 433-449

Inoue H, Nojima H, Okayama H (1990) High efficiency transformation of *Escherichia coli* with plasmids. *Gene* **96:** 23-28

Irish EE, Nelson TM (1991) Identification of multiple stages in the conversion of maize meristems from vegetative to floral development. *Development* **112:** 891-898

Irish VF, Sussex IM (1990) Function of the *apetala-1* gene during Arabidopsis floral development. *The Plant Cell* **2:** 741-753

Itoh H, Nonoue Y, Yano M, Izawa T (2010) A pair of floral regulators sets critical day length for *Hd3a* florigen expression in rice. *Nature Genetics* **42:** 635-U115

Jaeger KE, Wigge PA (2007) FT protein acts as a long-range signal in Arabidopsis. *Current Biology* **17:** 1050-1054

Jung C, Muller AE (2009) Flowering time control and applications in plant breeding. *Trends in Plant Science* **14:** 563-573

Jung JH, Ju Y, Seo PJ, Lee JH, Park CM (2012) The SOC1-SPL module integrates photoperiod and gibberellic acid signals to control flowering time in Arabidopsis. *The Plant Journal* **69:** 577-588

Kane NA, Danyluk J, Tardif G, Ouellet F, Laliberte JF, Limin AE, Fowler DB, Sarhan F (2005) *TaVRT-2*, a member of the *StMADS-11* clade of flowering repressors, is regulated by vernalization and photoperiod in wheat. *Plant Physiology* **138:** 2354-2363

Kardailsky I, Shukla VK, Ahn JH, Dagenais N, Christensen SK, Nguyen JT, Chory J, Harrison MJ, Weigel D (1999) Activation tagging of the floral inducer *FT*. *Science* **286:** 1962-1965

Karimi M, Depicker A, Hilson P (2007) Recombinational cloning with plant gateway vectors. *Plant Physiology* **145:** 1144-1154

Kaufmann K, Melzer R, Theissen G (2005) MIKC-type MADS-domain proteins: structural modularity, protein interactions and network evolution in land plants. *Gene* **347:** 183-198

Knott JE (1934) Effect of a localized photo-period on spinach. *Proceedings of the American Society for Horticultural Science* **31:** 152-154

Kobayashi Y, Kaya H, Goto K, Iwabuchi M, Araki T (1999) A pair of related genes with antagonistic roles in mediating flowering signals. *Science* **286:** 1960-1962

Komiya R, Ikegami A, Tamaki S, Yokoi S, Shimamoto K (2008) *Hd3a* and *RFT1* are essential for flowering in rice. *Development* **135:** 767-774

Komiya R, Yokoi S, Shimamoto K (2009) A gene network for long-day flowering activates *RFT1* encoding a mobile flowering signal in rice. *Development* **136:** 3443-3450

Krohn NG, Lausser A, Juranic M, Dresselhaus T (2012) Egg cell signaling by the secreted peptide ZmEAL1 controls antipodal cell fate. *Developmental Cell* **23:** 219-225

Lazakis CM, Coneva V, Colasanti J (2011) *ZCN8* encodes a potential orthologue of Arabidopsis *FT* florigen that integrates both endogenous and photoperiod flowering signals in maize. *Journal of Experimental Botany* **62:** 4833-4842

Lee H, Suh SS, Park E, Cho E, Ahn JH, Kim SG, Lee JS, Kwon YM, Lee I (2000) The AGAMOUS-LIKE 20 MADS domain protein integrates floral inductive pathways in Arabidopsis. *Genes & Development* **14:** 2366-2376

Lee J, Lee I (2010) Regulation and function of SOC1, a flowering pathway integrator. *Journal of Experimental Botany* **61:** 2247-2254

Lee JH, Park SH, Ahn JH (2012) Functional conservation and diversification between rice OsMADS22/OsMADS55 and Arabidopsis SVP proteins. *Plant Science* **185:** 97-104

Lee S, Choi SC, An G (2008) Rice SVP-group MADS-box proteins, OsMADS22 and OsMADS55, are negative regulators of brassinosteroid responses. *The Plant Journal* **54:** 93-105

Lee S, Jeong D-H, An G (2008) A possible working mechanism for rice SVP-group MADS-box proteins as negative regulators of brassinosteroid responses. *Plant Signaling & Behavior* **3:** 471-474

Lee SY, Kim J, Han JJ, Han MJ, An GH (2004) Functional analyses of the flowering time gene *OsMADS50*, the putative *SUPPRESSOR OF OVEREXPRESSION OF CO 1*/*AGAMOUS-LIKE 20* (*SOC1*/*AGL20*) ortholog in rice. *The Plant Journal* **38:** 754-764

Li D, Liu C, Shen L, Wu Y, Chen H, Robertson M, Helliwell CA, Ito T, Meyerowitz E, Yu H (2008) A repressor complex governs the integration of flowering signals in Arabidopsis. *Developmental Cell* **15:** 110-120

Li JH, Li YH, Chen SY, An LZ (2010) Involvement of brassinosteroid signals in the floral-induction network of Arabidopsis. *Journal of Experimental Botany* **61:** 4221-4230

Liljegren SJ, Ditta GS, Eshed HY, Savidge B, Bowman JL, Yanofsky MF (2000) *SHATTERPROOF* MADS-box genes control seed dispersal in Arabidopsis. *Nature* **404:** 766-770

Liu C, Chen H, Er HL, Soo HM, Kumar PP, Han J-H, Liou YC, Yu H (2008) Direct interaction of *AGL24* and *SOC1* integrates flowering signals in Arabidopsis. *Development* **135:** 1481-1491

Liu C, Xi WY, Shen LS, Tan CP, Yu H (2009) Regulation of floral patterning by flowering time genes. *Developmental Cell* **16:** 711-722

Livak KJ, Schmittgen TD (2001) Analysis of relative gene expression data using real-time quantitative PCR and the $2^{-\Delta\Delta C_T}$ method. *Methods* **25:** 402-408

Logemann J, Schell J, Willmitzer L (1987) Improved method for the isolation of RNA from plant tissues. *Analytical Biochemistry* **163:** 16-20

Mandel MA, Gustafsonbrown C, Savidge B, Yanofsky MF (1992) Molecular characterization of the Arabidopsis floral homeotic gene *APETALA1*. *Nature* **360:** 273-277

Matsubara K, Yamanouchi U, Wang ZX, Minobe Y, Izawa T, Yano M (2008) *Ehd2*, a rice ortholog of the maize *INDETERMINATE1* gene, promotes flowering by up-regulating *Ehd1*. *Plant Physiology* **148:** 1425-1435

McDaniel CN, Hsu FC (1976) Position-dependent development of tobacco meristems. *Nature* **259:** 563-565

McGonigle B (2012) Down-regulation of gene expression using artificial microRNAs. *E. .I du Pont de Nemours and Company*

McGonigle B, Bouhidel K, Irish VF (1996) Nuclear localization of the Arabidopsis *APETALA3* and *PISTILLATA* homeotic gene products depends on their simultaneous expression. *Genes & Development* **10:** 1812-1821

McSteen P, Laudencia-Chingcuanco D, Colasanti J (2000) A floret by any other name: control of meristem identity in maize. *Trends in Plant Science* **5:** 61-66

Meng X, Muszynski MG, Danilevskaya ON (2011) The *FT*-like *ZCN8* gene functions as a floral activator and is involved in photoperiod sensitivity in maize. *The Plant Cell* **23:** 942-960

Michaels SD, Ditta G, Gustafson-Brown C, Pelaz S, Yanofsky M, Amasino RM (2003) *AGL24* acts as a promoter of flowering in Arabidopsis and is positively regulated by vernalization. *The Plant Journal* **33:** 867-874

Michaels SD, Himelblau E, Kim SY, Schomburg FM, Amasino RM (2005) Integration of flowering signals in winter-annual Arabidopsis. *Plant Physiology* **137:** 149-156

Miller TA, Muslin EH, Dorweiler JE (2008) A maize *CONSTANS*-like gene, *conz1*, exhibits distinct diurnal expression patterns in varied photoperiods. *Planta* **227:** 1377-1388

Mizukami Y, Ma H (1992) Ectopic expression of the floral homeotic gene *AGAMOUS* in transgenic Arabidopsis plants alters floral organ identity. *Cell* **71:** 119-131

Moon J, Lee H, Kim M, Lee I (2005) Analysis of flowering pathway integrators in Arabidopsis. *Plant and Cell Physiology* **46:** 292-299

Moon J, Suh SS, Lee H, Choi KR, Hong CB, Paek NC, Kim SG, Lee I (2003) The *SOC1* MADS-box gene integrates vernalization and gibberellin signals for flowering in Arabidopsis. *The Plant Journal* **35:** 613-623

Muszynski MG, Dam T, li BL, Shirbroun DM, Hou Z, Bruggemann E, Archibald R, Ananiev EV, Danilevskaya ON (2006) *Delayed flowering1* encodes a basic leucine zipper protein that mediates floral inductive signals at the shoot apex in maize. *Plant Physiology* **142:** 1523-1536

Napoli C, Lemieux C, Jorgensen R (1990) Introduction of a chimeric chalcone synthase gene into petunia results in reversible co-suppression of homologous genes *in trans*. *The Plant Cell* **2:** 279-289

Neuffer MG, Coe EH, Wessler SR (1997) Mutants of maize, Second edition. *Cold Spring Harbor Laboratory Press, Cold Spring Habor, NY*

Okamuro JK, Caster B, Villarroel R, VanMontagu M, Jofuku KD (1997) The AP2 domain of *APETALA2* defines a large new family of DNA binding proteins in Arabidopsis. *Proceedings of the National Academy of Sciences of the United States of America* **94:** 7076-7081

Onouchi H, Igeno MI, Perilleux C, Graves K, Coupland G (2000) Mutagenesis of plants overexpressing *CONSTANS* demonstrates novel interactions among Arabidopsis flowering-time genes. *The Plant Cell* **12:** 885-900

Parenicova L, de Folter S, Kieffer M, Horner DS, Favalli C, Busscher J, Cook HE, Ingram RM, Kater MM, Davies B, Angenent GC, Colombo L (2003) Molecular and phylogenetic analyses of the complete MADS-box transcription factor family in Arabidopsis: New openings to the MADS world. *The Plant Cell* **15:** 1538-1551

Park DH, Somers DE, Kim YS, Choy YH, Lim HK, Soh MS, Kim HJ, Kay SA, Nam HG (1999) Control of circadian rhythms and photoperiodic flowering by the Arabidopsis *GIGANTEA* gene. *Science* **285:** 1579-1582

Park SJ, Kim SL, Lee S, Je BI, Piao HL, Park SH, Kim CM, Ryu CH, Xuan YH, Colasanti J, An G, Han CD (2008) Rice *Indeterminate 1* (*OsId1*) is necessary for the expression of *Ehd1* (*Early heading date 1*) regardless of photoperiod. *The Plant Journal* **56:** 1018-1029

Parker JMR, Guo D, Hodges RS (1986) New hydrophilicity scale derived from high-performance liquid chromatography peptide retention data: correlation of predicted surface residues with antigenicity and x-ray-derived accessible sites. *Biochemistry* **25:** 5425-5432

Paz MM, Shou HX, Guo ZB, Zhang ZY, Banerjee AK, Wang K (2004) Assessment of conditions affecting Agrobacterium-mediated soybean transformation using the cotyledonary node explant. *Euphytica* **136:** 167-179

Pelaz S, Ditta GS, Baumann E, Wisman E, Yanofsky MF (2000) B and C floral organ identity functions require *SEPALLATA* MADS-box genes. *Nature* **405:** 200-203

Pick TR, Brautigam A, Schluter U, Denton AK, Colmsee C, Scholz U, Fahnenstich H, Pieruschka R, Rascher U, Sonnewald U, Weber APM (2011) Systems analysis of a maize leaf developmental gradient redefines the current C4 model and provides candidates for regulation. *The Plant Cell* **23:** 4208-4220

Porri A, Torti S, Romera-Branchat M, Coupland G (2012) Spatially distinct regulatory roles for gibberellins in the promotion of flowering of Arabidopsis under long photoperiods. *Development* **139:** 2198-2209

Putterill J, Robson F, Lee K, Simon R, Coupland G (1995) The *CONSTANS* gene of Arabidopsis promotes flowering and encodes a protein showing similarities to zinc finger. *Cell* **80:** 847-857

Ryu CH, Lee S, Cho LH, Kim SL, Lee YS, Choi SC, Jeong HJ, Yi J, Park SJ, Han CD, An G (2009) *OsMADS50* and *OsMADS56* function antagonistically in regulating long day (LD)-dependent flowering in rice. *Plant Cell and Environment* **32:** 1412-1427

Sachs J (1865) Wirkung des Lichtes auf die Blütenbildung unter Vermittlung der Laubblätter. *Botanische Zeitung* **23:** 117-121; 125-131; 133-139

Salvi S, Sponza G, Morgante M, Tomes D, Niu X, Fengler KA, Meeley R, Ananiev EV, Svitashev S, Bruggemann E, Li B, Hainey CF, Radovic S, Zaina G, Rafalski JA, Tingey SV, Miao GH, Phillips RL, Tuberosa R (2007) Conserved noncoding genomic sequences associated with a flowering-time quantitative trait locus m maize. *Proceedings of the National Academy of Sciences of the United States of America* **104:** 11376-11381

Samach A, Onouchi H, Gold SE, Ditta GS, Schwarz-Sommer Z, Yanofsky MF, Coupland G (2000) Distinct roles of CONSTANS target genes in reproductive development of Arabidopsis. *Science* **288:** 1613-1616

Sambrook J, Fritsch EF, Maniatis T (1989) Molecular cloning: a laboratory manual. 1 2 and 3. *Cold Spring Harbor Laboratory Press: Cold Spring Harbor, New York, USA*.

Schwarz S, Grande AV, Bujdoso N, Saedler H, Huijser P (2008) The microRNA regulated SBP-box genes *SPL9* and *SPL15* control shoot maturation in Arabidopsis. *Plant Molecular Biology* **67:** 183-195

Searle I, He YH, Turck F, Vincent C, Fornara F, Krober S, Amasino RA, Coupland G (2006) The transcription factor FLC confers a flowering response to vernalization by repressing meristem competence and systemic signaling in Arabidopsis. *Genes & Development* **20:** 898-912

Sentoku N, Kato H, Kitano H, Imai R (2005) *OsMADS22*, an *STMADS11*-like MADS-box gene of rice, is expressed in non-vegetative tissues and its ectopic expression induces spikelet meristem indeterminacy. *Molecular Genetics and Genomics* **273:** 1-9

Singleton WR (1946) Inheritance of indeterminate growth in maize. *Journal of Heredity* **37:** 61-64

Strable J, Borsuk L, Nettleton D, Schnable PS, Irish EE (2008) Microarray analysis of vegetative phase change in maize. *The Plant Journal* **56:** 1045-1057

Suarez-Lopez P, Wheatley K, Robson F, Onouchi H, Valverde F, Coupland G (2001) *CONSTANS* mediates between the circadian clock and the control of flowering in Arabidopsis. *Nature* **410:** 1116-1120

Tadege M, Sheldon CC, Helliwell CA, Upadhyaya NM, Dennis ES, Peacock WJ (2003) Reciprocal control of flowering time by *OsSOC1* in transgenic Arabidopsis and by *FLC* in transgenic rice. *Plant Biotechnology Journal* **1:** 361-369

Tamaki S, Matsuo S, Wong HL, Yokoi S, Shimamoto K (2007) Hd3a protein is a mobile flowering signal in rice. *Science* **316:** 1033-1036

Taoka K, Ohki I, Tsuji H, Furuita K, Hayashi K, Yanase T, Yamaguchi M, Nakashima C, Purwestri YA, Tamaki S, Ogaki Y, Shimada C, Nakagawa A, Kojima C, Shimamoto K (2011) 14-3-3 proteins act as intracellular receptors for rice Hd3a florigen. *Nature* **476:** 332-U397

Towbin H, Staehelin T, Gordon J (1979) Electrophoretic transfer of proteins from polyacrylamide gels to nitrocellulose sheets: procedure and some applications. *Proceedings of the National Academy of Sciences of the United States of America* **76:** 4350-4354

Trevaskis B, Tadege M, Hemming MN, Peacock WJ, Dennis ES, Sheldon C (2007) *Short Vegetative Phase*-like MADS-box genes inhibit floral meristem identity in barley. *Plant Physiology* **143:** 225-235

Tsuji H, Taoka K, Shimamoto K (2011) Regulation of flowering in rice: two florigen genes, a complex gene network, and natural variation. *Current Opinion in Plant Biology* **14:** 45-52

Turnbull C (2011) Long-distance regulation of flowering time. *Journal of Experimental Botany* **62:** 4399-4413

Wang JW, Czech B, Weigel D (2009) miR156-regulated SPL transcription factors define an endogenous flowering pathway in *Arabidopsis thaliana*. *Cell* **138:** 738-749

Weigel D, Alvarez J, Smyth DR, Yanofsky MF, Meyerowitz EM (1992) *LEAFY* controls floral meristem identity in Arabidopsis. *Cell* **69:** 843-859

Wigge PA, Kim MC, Jaeger KE, Busch W, Schmid M, Lohmann JU, Weigel D (2005) Integration of spatial and temporal information during floral induction in Arabidopsis. *Science* **309:** 1056-1059

Wilson RN, Heckman JW, Somerville CR (1992) Gibberellin is required for flowering in *Arabidopsis thaliana* under short days. *Plant Physiology* **100:** 403-408

Wingen LU, Muenster T, Faigl W, Deleu W, Sommer H, Saedler H, Theissen G (2012) Molecular genetic basis of pod corn (*Tunicate* maize). *Proceedings of the National Academy of Sciences of the United States of America* **109:** 7115-7120

Wong AYM, Colasanti J (2007) Maize floral regulator protein INDETERMINATE1 is localized to developing leaves and is not altered by light or the sink/source transition. *Journal of Experimental Botany* **58:** 403-414

Wu G, Poethig RS (2006) Temporal regulation of shoot development in *Arabidopsis thaliana* by *miR156* and its target *SPL3. Development* **133:** 3539-3547

Yano M, Katayose Y, Ashikari M, Yamanouchi U, Monna L, Fuse T, Baba T, Yamamoto K, Umehara Y, Nagamura Y, Sasaki T (2000) *Hd1*, a major photoperiod sensitivity quantitative trait locus in rice, is closely related to the arabidopsis flowering time gene *CONSTANS*. *The Plant Cell 12:* 2473-2483

Yoo SK, Chung KS, Kim J, Lee JH, Hong SM, Yoo SJ, Yoo SY, Lee JS, Ahn JH (2005) *CONSTANS* activates *SUPPRESSOR OF OVEREXPRESSION OF CONSTANS 1* through *FLOWERING LOCUS T* to promote flowering in Arabidopsis. *Plant Physiology* **139:** 770-778

Yu H, Xu YF, Tan EL, Kumar PP (2002) AGAMOUS-LIKE 24, a dosage-dependent mediator of the flowering signals. *Proceedings of the National Academy of Sciences of the United States of America* **99:** 16336-16341

Zhang LF, Chia JM, Kumari S, Stein JC, Liu ZJ, Narechania A, Maher CA, Guill K, McMullen MD, Ware D (2009) A genome-wide characterization of microRNA genes in maize. *PLoS Genetics* **5 (11):** e1000716.doi:10.1371/journal.pgen.1000716

8. APPENDIX

8.1. MICROARRAY OLIGOS

***Table 11*. Microarray oligos of flowering time candidates.** The OPTIMAS identifier and the respective microarray oligo of all flowering time candidates of the maize pairs 4F-350 CN 2 / 4F-240 BX 16 and E2558W / B77 in alphabetical order are listed.

OPTIMAS identifier	Sequence 5' -> 3'
P_OptiV1C00462	TACAGCAAGATCCTCAAAGATCTCAAGAAAGAGTTCTGCTGCAATGGTACAGTGGTCCAG
P_OptiV1C01178	TACAAGGCCAAGAAGTACAAGGACTACCAGCACTGCAAGATCAACAAGCTCCCCATGTAA
P_OptiV1C01437	ATCCGTTTCACTACTGCCCCGCTGTTCTGGATCGGGAGACGTGTGTGCTCTCAGTTCTCA
P_OptiV1C01853	TGGTACAATAGGAGATGGAAAAATACGAGGGAAGAAGAGGATTCCTTTCCCAAATCAGGC
P_OptiV1C01938	ATTCTTGTTCCTCCAATCCATCGCTTTCTTCATCGTCGGCATTGGCTATGTCGGAACATT
P_OptiV1C02818	AGACGATCAAGGAGGCGCTCCCCGCTGACATGTGGAGCCTCGAGATGAAGAAAGCCTGGG
P_OptiV1C03164	AAATTTGTTGGTAGAGCTGAAGCCCTTGGACGTGGATTCTGGGTTGGAGTGCAATATGAT
P_OptiV1C03183	ATTACTTCAAGGCTGCACTGCAGTTTGTCGTCAACCCTGGAAAATTTGGTTTTAGCACGG
P_OptiV1C04175	CAGGCTCTCGCGCTCAGGCTGCACCTGGGGAAGCTCGCTGTTGCTGCACACTCTTCTTGA
P_OptiV1C05995	TCCATTGAAGAACTGCATAATCTGGAGGTTAAACTGGCGAAGAGCCTTCACGTCATCAGA
P_OptiV1C05996	TAACCTGATTTGTCATCCTTGTGGCTTCATGATGCGATGTTGCGCTTGTACCGTTTGCTA
P_OptiV1C06259	AACGAAGCTGACCAGGAGCTTCCGCTACGAGGACTACAGCACCAGGCGAGTCTTCCTGCG
P_OptiV1C06771	TACATATTTCAACTGTCAAAGGGAAGGTGGATCCGGCGGAAGAAGGTTTAGGGAAGAGTA
P_OptiV1C08761	AGTCTTGATCGATGGGAAGGACGTCAAGAAGCTTAAGCTCAAGTGTCTCAGGAAACACAT
P_OptiV1C09078	TGATGATGGCTGCCTTGTGTTGCATGGAAGTGAAAAAACAAGATGGTCTGTGTTGATCTG
P_OptiV1C09461	ATCCTCCGACTTTGGGTTGTTAAGGCATTTCAGAAACGAGGATCTGAAGCAAGTGCTGAA
P_OptiV1C10423	GGATCAGGGTCCTGATGCTGACGCTTTCGACGGAGAGGTTTCTGAAGATTCAGAGGGAGG
P_OptiV1C10635	AATGAACATGATTCCTGGATTCCATTCTTCGTCCACTAGCGGTTGCAATGACAGTGGCTT
P_OptiV1C11740	TCACCATGGTGGGGTATGGTGCCGAATCCGGTGGCCGCAAATACTGGATCGTCAAGAACT
P_OptiV1C11764	AACAGCTCCGTGTTTGAGCCCGGACAGACTTCTTCTCATCAGCTGCACGACAGAATATGA
P_OptiV1C13062	GACATTTTCCACATGATACTACACTCAGTCTGGTTTAGCAGGGTGAACCAGATCCGTTAG
P_OptiV1C17237	CAAAAGGAAACTTTTGGGTGAGAGGTTGGAAGACTGCTCCATTGAAGAGCTGCACAGTTT
P_OptiV1N35188	TAACATTCAGAATATGTATCCTGTTGCTCTTCCGTTCCCCTTTCTAAAATAAGGTATCAA
P_OptiV1N35942	GCCCATTTTTAGGTGGGTCCCTAAACAACAATATTCTGCAAAATATACATGTATACCTTA
P_OptiV1N37090	ATGCACCAACACGGCTGAACATCGTGTATTTGGGGTACCTCTCCTCTGAATATATGCTAA
P_OptiV1N40004	TGTGCATGTGTCTGGCTTTTGAAAGGTGTACCTCGTCATTTATGGACTTATATGTATGTA
P_OptiV1N40037	CAGCTGTGTCGTCTGCGTAGAACGTTGTATGTGTTTCATCAACATTTTAATATACAATAT
P_OptiV1S17892	GCATACGACATCGTGGTGGACAAGCTCATCCAGCAGAACTCCAAGTACCTGATGATGTGA
P_OptiV1S18200	CTGTCCACCGGCGGGTCGTTGGACAAGGGTATCCAAGAATTCGTCGCCGCTATACTGTGA
P_OptiV1S18426	ACTGGTGGTTCTTCGACCAGTTCAGGACCTCCATGATCAAGATGAGCCAGCTCAGGGGAC
P_OptiV1S18863	TCACAAACCATGAGATGAGTGCATCAGGAGATCTCCACAGGAGGCCTGCAGGGGCTGTTC
P_OptiV1S18918	AGCCTCGCCAACAGCGTCAAGAGCGTCAACATGGGCACCGTCGCCACCATCCCCGGCAAG
P_OptiV1S19217	TTCATCACCAAGTTCTACGAGACTCTCCGCCTACAGCAGGCCGACGCCACGCCTGACAAC
P_OptiV1S19635	ACAAGGCAGCCACCTACTTGTACATGCAGGAGGTGTGGGCAGTGAGGAGGAGGCCGACGA
P_OptiV1S20394	GGCAATGTTGAGCCGGTGCCGGCCAAGGCCAACGAGGCGGCGCCATCGGAGGCTTGCTAG
P_OptiV1S21266	ATTACTGCATTTGAGAAGCAGCACAAGCGGAGACTTGCATACAGCATTTCATTCTACTAA
P_OptiV1S21916	ACAAAGGATCAACAATTCTTGGAACAGATCAATGACCTCGAACGTAAGTGGAGATCCTTT
P_OptiV1S21916	ACAAAGGATCAACAATTCTTGGAACAGATCAATGACCTCGAACGTAAGTGGAGATCCTTT

P_OptiV1S24287	TCTAAGGGATCTGTATCCTTATGACTGTGCGTACAAGATGGCCATGCTAGCAAAACAGTG
P_OptiV1S24539	TCGCCGTCCTCTGGGAAATGGTGTTCCGTGGAACTGACACCGTCGCCGTGCTGATGGAGT
P_OptiV1S24670	CCCTTCACAATCATCAACGAAATGATCATTTTCACCACGGGGCTCTCCTCCTTAGCTTAG
P_OptiV1S26447	AGTACTTGCACTGGATGGTGACTGACATCCCCGCATCAACTGACAATACACACGGCCGTG
P_OptiV1S26715	GATGATTCTGAAAATCAAGACATACAAATTCTACCAAGACTACTCTGGTCTAAGCCATAA
P_OptiV1S26761	GCACTCATCGTCCATATCGGCGATCAGATCGAGGCAAGCGACCTACGTAGCATCTTTTTT
P_OptiV1S28227	CGAGCAGAGTGCTTCAAGGGAGGCGTCTTCATCACATGCAACTACTATGCCACGGACCTC
P_OptiV1S29412	ATGGTCATGCTCATAACCACAGTCATGCTCACCCTGGTGATGATCATTATATGGAGAACG
P_OptiV1S29722	AGCGTCAGCGACGTCATGTTCTACTCGGTGACCAACACGCCCAGAGCCTCTTCCGTGACC
P_OptiV1S29802	TATGAGAAGGAGAAGCAACTTTACTCTGGTGGCTCCGGTCAGAGCCAACGTGCCGGTGAG
P_OptiV1S30318	TTCTTCGATTTCAAGAACGATAACGACATGAGCTTCGTCTACGCGGAGGTTGACACATTC
P_OptiV1S31605	TTTATCCGACTCGGGACGCATTATTTGTACCACAACAAAACACGTGTTACACTATTGTAA
P_OptiV1S32916	TGCAGCGGAGTTCCAGGTCCAGCGCGCGAGCGACGACGCGCGGTGGGGAGCGGCGCTCCG
P_OptiV1S33653	CATTCTGGGAGTTCACAGGATAATGATGATGGTTCGGATGTCTCTCTAAAATTAGGGTGA

8.2. PROTEIN IDENTIFIERS OF THE ALIGNMENTS

8.2.1. ZMMADS1 AND HOMOLOGS

ZmMADS1	GRMZM2G171365
ZmMADS56	GRMZM2G026223
GRMZM2G070034	
OsMADS56	LOC_Os10g39130
OsMADS50	LOC_Os03g03070
TaAGL7	gb|ABF57947.1|
TaWM21B	emb|CAM59066.1|
TaWM1B	emb|CAM59040.1|
TaAGL38	gb|ABF57938.1|
TaAGL20	gb|ABF57922.1|
TaWM21A	dbj|BAF56968.1|
TaAGL21	gb|ABF57923.1|
TaWM1A	emb|CAM59039.1|
HvSOC	dbj|BAK00484.1|
AtSOC1	AT2G45660

8.2.2. ZMM26 AND HOMOLOGS

ZmM26	GRMZM2G046885
ZmM19	GRMZM2G370777
ZmMADS47	GRMZM2G059102
ZmM21	GRMZM5G814279
OsMADS22	LOC_Os02g52340
OsMADS55	LOC_Os06g11330
OsMADS47	LOC_Os03g08754
TaAGL11	gb|ABF57916.1|
TaWM22A	emb|CAM59067.1|

TaWM22B	emb|CAM59068.1|
TaWM24B	emb|CAM59070.1|
TaWM24A	emb|CAM59069.1|
TaAGL36	gb|ABF57936.1|
TaVRT-2	gb|AAY43789.1|
TaWM28B	emb|CAM59075.1|
TaWM28A	emb|CAM59074.1|
TaAGL13	gb|ABF57917.1|
TaMADS10	gb|ABL11476.1|
HvBM10	gb|ABM21529.1|
HvVRT-2	gb|ABB13345.1|
HvBM1-2	emb|CAB97350.1|
HvBM1	emb|CAB97349.1|
AtSVP	AT2G22540
AtAGL24	AT4G24540

8.3. QRT-PCR PRIMERS

***Table 12*. Primers used for transcription analyses.** The gene, the orientation of the primer, the primer sequence, the annealing temperature in °C and the product size on gDNA and cDNA templates in bp are indicated.

Gene	orientation	Primer sequence (5' -> 3')	$T_{Annealing}$ °C	Product gDNA	Product cDNA
GAP-DH	Forward	AGGGTCCACTCAAGGGTATCAT	61,5	244 bp	133 bp
	Reverse	ACGAGCTTGACGAAGTGGTC			
MADS1	Forward	ACGTGGAGGACGGTCACCGG	62	124 bp	124 bp
	Reverse	GACCTGACCGCCACTGCAGC			
MADS56	Forward	TGCAAGCCAAGCCCAAGCCA	59	163 bp	163 bp
	Reverse	TGAGCAGGCCGGAGCAGCTA			
GRMZM2 G070034	Forward	GACCCTGCTCCAAGACAACA	60	359 bp	174 bp
	Reverse	TCCCTGCCGGGTAATCCTAT			
ZmM26	Forward	GGCAGATGAGAGGTGAAGA	58	3285 bp	387 bp
	Reverse	GACAAGGAGCCTCATTTCCTG			
ZmM19	Forward	TGATCTGGGTGGAGCTGCGG	61,5	358 bp	358 bp
	Reverse	CTACGCTCAGGTTGTATGCAGACTC			
GIGZ1a	Forward	AGCCCGTCCTACCGGTGCC	64	193 bp	193 bp
	Reverse	TTGGAAGCCGATGTCAGATCCAGGA			

8.4. CLONING PRIMERS

Table 13. **Primers used for cloning.** If a restriction site was introduced, the name of the enyzme was included in the primer name and restriction sites are marked in italics. pENTR indicates introduction of the sequence motif CACC (italic) at the very 5'-end of the primer sequence for pENTR/D-TOPO cloning. '-f' indicates forward primer, '-r' indicates reverse primer, '-s-' indicates sense orientation, '-a-' indicates antisense orientation of the product.

Primer	**Sequence (5' -> 3')**	**Construct**
M5RNAi-s-BSRGI	GACACA*TGTACA*AAGCAGAAGGAGATGAGTCT	p*Ubi*:*MADS1*-RNAi
M5RNAi-s-MluI	GACACA*ACGCGT*TCTCCACGTCCATCCCGTCG	p*Ubi*:*MADS1*-RNAi
M5RNAi-a-BamHI	GACACA*GGATCC*TCTCCACGTCCATCCCGTCG	p*Ubi*:*MADS1*-RNAi
M5RNAi-a-EcoRI	GACACA*GAATTC*AAGCAGAAGGAGATGAGTCT	p*Ubi*:*MADS1*-RNAi
amiM26-s (Primer 1)	TCTTAACTTTAGAGATACGTCCCCATCATGCATGCAGC AG	p*Ubi*:amiR-*Zmm26*
amiM26-a (Primer 2)	TGGGGACGTATCTCTAAAGTTAAGATGGCAGGGAGG GCCA	p*Ubi*:amiR-*Zmm26*
amiM26*-s (Primer 3)	GGGGAACGTATCTCTTAAGTTATAATTGCAGAGAGAG ACC	p*Ubi*:amiR-*Zmm26*
amiM26*-a (Primer 4)	TTATAACTTAAGAGATACGTTCCCCCTCTTGCTTGCTT GG	p*Ubi*:amiR-*Zmm26*
amiR-ZmM26-f	AAGCAGGCTGAGCTCGTCCC	p*Ubi*:amiR-*Zmm26*
amiR-ZmM26-r	AGCTGGGTTCCGGATGGGC	p*Ubi*:amiR-*Zmm26*
CDS MADS1 5' pENTR	*CACC*ATGGTGCGGGGCAAGACGCAGATG	p*Ubi*:*MADS1* p*35S*:*MADS1*(-*GFP*) p*SOC1*:*MADS1*(-*GFP*)
CDS MADS1 3'	CTAGCCTGACCTGACCGCCACTG	p*Ubi*:*MADS1*
CDS MADS1 3' degenBamHI	*GGATCM*GCCTGACCTGACCGCCACTG	p*35S*:*MADS1*(-*GFP*) p*SOC1*:*MADS1*(-*GFP*)
CDS Zmm26 5' pENTR	*CACC*ATGGCGAGGGAGAGGCGGGAG	p*Ubi*:*ZmM26*
CDS Zmm26 3'	TTACTTCCATGCAACGCAAGGCAGCCCTAA	p*Ubi*:*ZmM26*
pUbi-XmaI-f	GACACA*CCCGGG*AGTGCAGCGTGACCCGGTCG	p*Ubi*:*MADS1* (pTF101.1) p*Ubi*:*ZmM26* (pTF101.1) p*Ubi*:amiR-*ZmM26* (pTF101.1)
NOSt-BamHI-r	GACACA*GGATCC*CGATCTAGTAACATAGATGA	p*Ubi*:*MADS1* (pTF101.1) p*Ubi*:*ZmM26* (pTF101.1) p*Ubi*:amiR-*ZmM26* (pTF101.1)
M5RNAi1-XmaI-f	GACACA*CCCGGG*CTGCAGTGCAGCGTGACCCG	p*Ubi*:*MADS1*-RNAi (pTF101.1)
M5RNAi1-HindIII-r	GACACA*AAGCTT*TAAATTGAACGGAGAATATT	p*Ubi*:*MADS1*-RNAi (pTF101.1)

8.5. VECTOR MAPS

8.5.1. MAIZE TRANSFORMATION VECTORS AND CLONING INTERMEDIATES

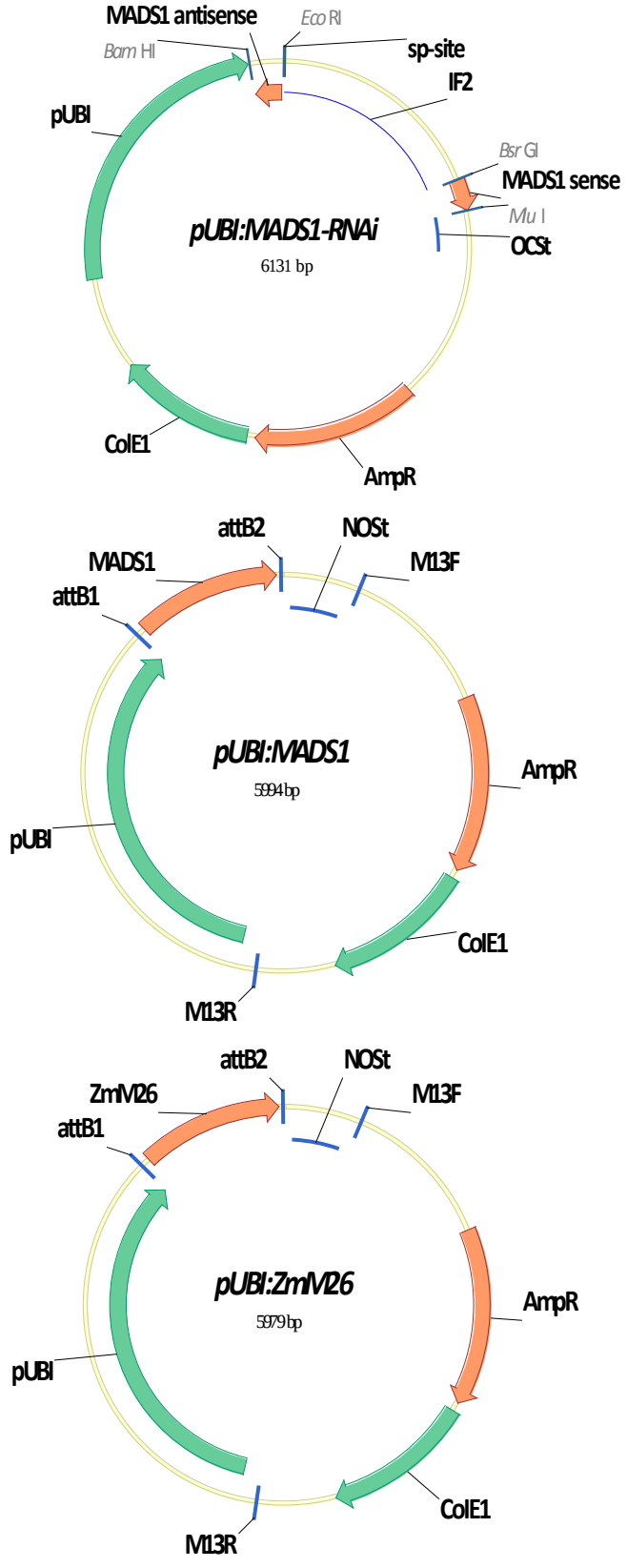

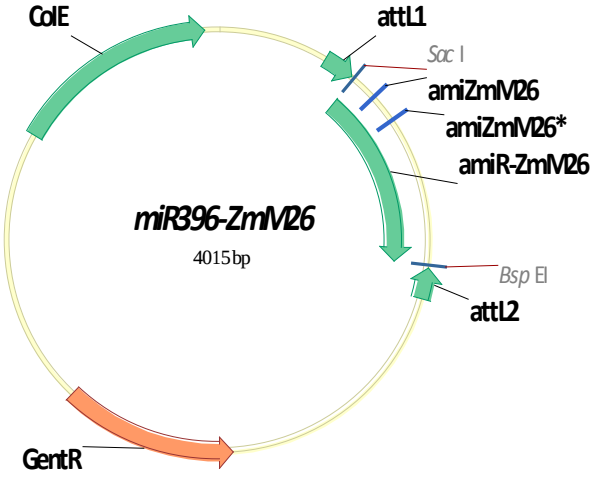
ColE
attL1
Soc I
amiZmMI26
amiZmMI26*
amiR-ZmMI26
miR396-ZmMI26
4015 bp
Bsp EI
attL2
GentR

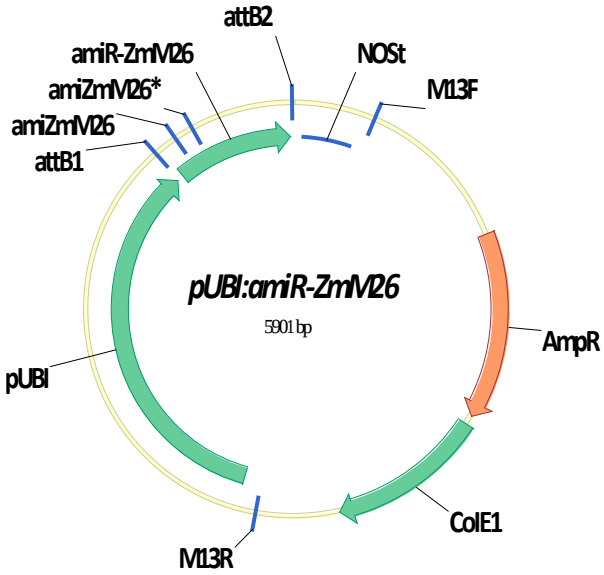
attB2
amiR-ZmMI26
NOSt
amiZmMI26*
M13F
amiZmMI26
attB1
pUBI:amiR-ZmMI26
5901 bp
AmpR
pUBI
ColE1
M13R

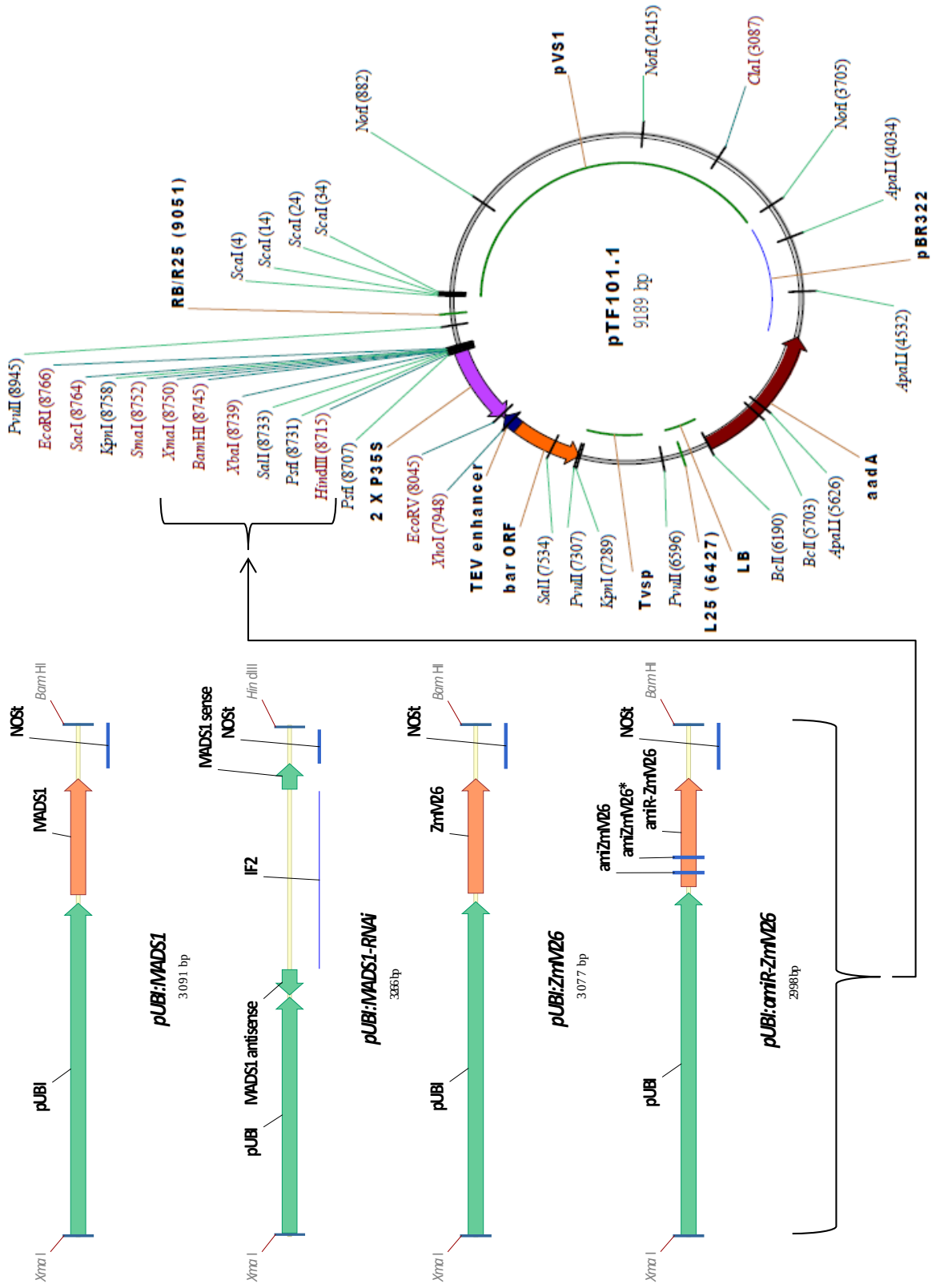
pTF101.1
9189 bp
RB/R25 (9051)
2 X P35S
TEV enhancer
bar ORF
Tvsp
L25 (6427)
LB
aadA
pBR322
pVS1
pUBI:MADS1
3091 bp
pUBI:MADS1-RNAi
3361bp
pUBI:ZmM26
3077 bp
pUBI:amiR-ZmM26
2998bp
pUBI
MADS1
NOSt
MADS1 sense
MADS1 antisense
IF2
ZmM26
amiZmM26
amiZmM26*
amiR-ZmM26
Xma I
BamHI
HindIII

8.5.2. ARABIDOPSIS TRANSFORMATION VECTORS AND CLONING INTERMEDIATES

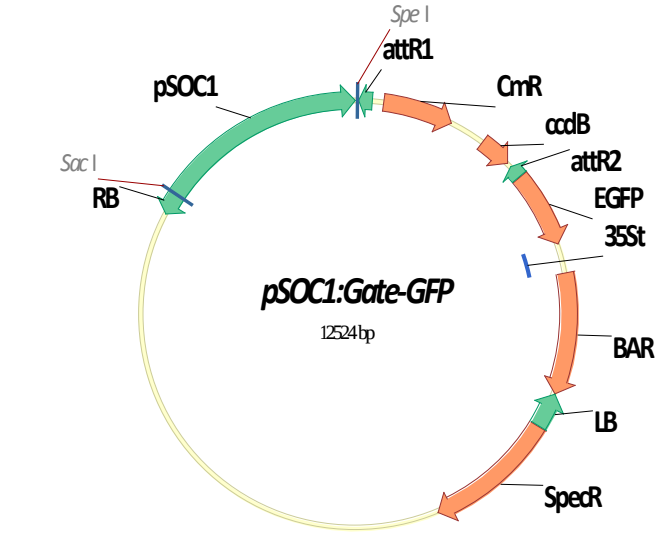

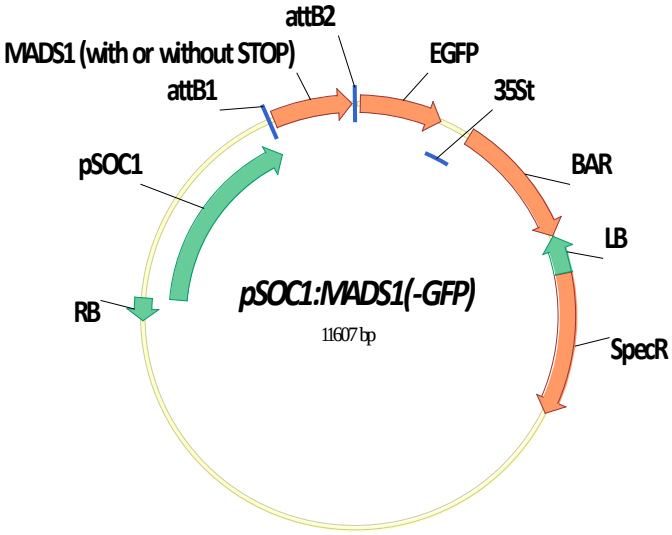

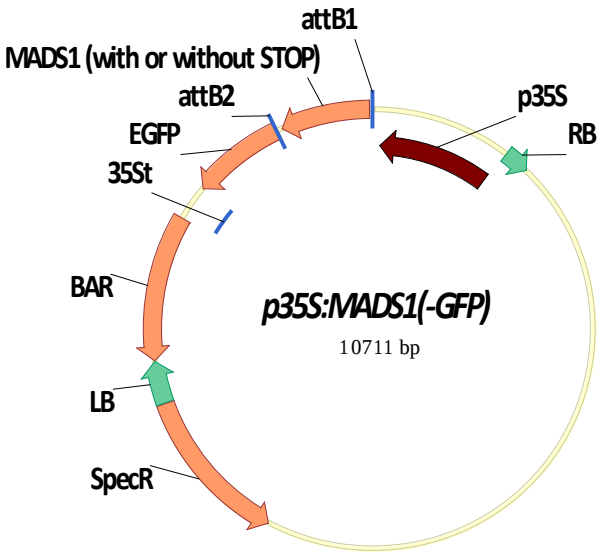

9. ACKNOWLEDGMENT

I am deeply grateful to Prof. Dr. Thomas Dresselhaus for giving me the opportunity to do my PhD in his lab. I would like to thank him for scientific discussions, advice and last but not least for the correction of this thesis.

I am very thankful to my supervisor Dr. Manfred Gahrtz for sharing his extensive knowledge, scientific discussions and for his guidance at the beginning of my PhD.

I would like to thank my external RIGel mentor Prof. Dr. Uwe Sonnewald for his advice and motivating word, as well as for being part of my examination committee as second PhD assessor.

I would like to thank Dr. Urte Schlüter for the hybridization of the microarrays and for help with and the introduction into the analyses of microarray data.

I am deeply thankful to Dr. Svenja Rademacher for the introduction into qRT-PCR, which was the mostly used method during this work, for fruitful discussions, inspirations, good suggestions and for reading this thesis critically. And now I give my special thanks to my wife Svenja Alter for motivations, support and trust. You are my bridge over troubled water.

I thank Dr. Andrea Bleckmann for introduction into confocal microscopy.

I am thankful to Prof. Dr. Claus Schwechheimer for providing the Arabidopsis *soc1*-2 mutant seeds.

I am obliged to Vroni for any administrative help and the greenhouse team, Günther and Uschi, for their indefatigable dedication for successful plant growth.

I would like to thank all colleagues of the department of Cell Biology and Plant Biochemistry. Special thanks go to all present and past members of the maize lab, for their help and most of all for the good times we had together, especially on silly Friday. A very special thanks goes out to everyone, who joint me doing ‘PAUSE’ and during drinking refreshing ‘Dachbier’.

Last but not least, I would like to give a special thanks to my parents Ulrike and Günter for their continuous support, love and for keeping me grounded. Besides them, I would like to thank also my brother Olaf and my sister Kathi helping me to become the person I am, so that I could go through all of this.